Thesis

Kidney injury in cholestasis and advanced stage liver disease

Submitted by

Dr[in]. med. univ.

Elisabeth TATSCHER

for the degree of Doctor of Medical Science

(Dr. scient. med.)

at the

Medical University of Graz,

Department of Internal Medicine,

Division of Gastroenterology and Hepatology

under the supervision of

Univ. Prof. Dr. med. univ. Peter Fickert

April 2023, Graz

Statutory Declaration and Disclosures

I hereby declare that this thesis is my own original work and that I have fully acknowledged by name all of those individuals and organisations that have contributed to the research for this thesis (for further details see "Acknowledgements"). Due acknowledgement has been made in the text to all other material used. Throughout this thesis and in all related publications I followed the "Standards of Good Scientific Practice and Ombuds Committee at the Medical University of Graz".

Parts of this thesis have been published in Fickert P*, Krones E* et al. Hepatology. 2013; Krones E et al. J Hepatol. 2017; Krones, E et al. Dig Dis. 2015 and Krones E et al. Biochim Biophys Acta. 2018 (*for details please see "Notification"*).

This work was supported by the following institutions:

- "The Role of Autophagy in Cholemic Nephropathy" Start-Project, Medical University of Graz (to Elisabeth Tatscher, formerly Krones)
- Mobilitätsstipendium (Travel Grant) für Frauen, Gender Unit, Medical University of Graz (to Elisabeth Tatscher, formerly Krones)
- Böhringer Ingelheim Fonds Travel Grant (to Elisabeth Tatscher, formerly Krones)
- Grant support (P25911-B19) from the Austrian Science Foundation (to the main supervisorPeter Fickert)

Please also note, that the surname of the doctoral student changed from "Krones" to "Tatscher" due to marriage in 2019.

Graz, April 5th, 2023

Acknowledgements

First, my sincere thank goes to the main supervisor of this thesis, Professor Peter Fickert, my mentor since the beginning of my clinical and scientific career. He developed the idea of this project and helped with the design of the experiments and the related publications. He taught me many different aspects of molecular hepatology and scientific working and inspired me to become a hepatologist.

Further, I would like to acknowledge my co-supervisors Professor Alexander R. Rosenkranz and Doz. Cord Langner, Assoz. Prof. Kathrin Eller and Ass. Prof. Alexander H. Kirsch from the Department of Nephrology at the Medical University of Graz, Prof. Tobias B. Huber and Prof. Florian Grahammer and their former team in Freiburg, Prof. Hanns-Ulrich Marschall and his team (i.e. Annika Wahlström and Marcus Stahlmann) at Gothenburg University, Prof. Michael Trauner and Dr. Emina Halilbasic from the Medical University of Vienna, Marion J. Pollheimer from the Department of Pathology at the Medical University of Graz, Tarek Moustafa and Prof Helmut Denk for their important contribution to this work. I thank Andrea Thüringer, Judith Gumhold, Dagmar Silbert, Andrea Deutschmann, Dietmar Glänzer, Bianca Frauscher, and Katharina Kinslechner for excellent technical assistance. I also like to acknowledge all other co-authors of the two original articles (Fickert P*, Krones E* et al. Hepatology. 2013 and Krones E et al. J Hepatol. 2017) this thesis is based on, including Min Yang, Hartmut Jaeschke, Geurt Stokman, Rebecca G. Wells, Gosta Eggertsen and Carsten A. Wagner (for Fickert P*, Krones E* et al. Hepatology. 2013) and Karin Wagner (for Krones E et al. J Hepatol. 2017); however, data from these collaborations have not been included in this thesis.

Doctoral student Elisabeth Tatscher received funding from the Medical University of Graz (Start-Project, Medical University of Graz and Mobilitätsstipendium (Travel Grant) für Frauen, Gender Unit, Medical University of Graz) and a travel grant from the Böhringer Ingelheim Fonds.

Finally, I want to express my deepest gratitude to my husband Florian, my son Anton, my daughter Sophia, my parents, friends and colleagues for their love and support.

Notification

The current doctoral thesis is based on the publication of two original papers and two reviews, which have been published in *Hepatology (Wiley)*, *Journal of Hepatology (Elsevier)*, *Digestive Diseases (Karger)* and a special issue of *Biochimica et Biophysica Acta (Elsevier),* respectively. The published manuscripts were drafted by the doctoral candidate, Elisabeth Tatscher (formerly Krones). Therefore, significant parts of the thesis are similar to the following published manuscripts:

- Fickert P*, Krones E*, Pollheimer MJ, Thueringer A, Moustafa T, Silbert D, Halilbasic E, Yang M, Jaeschke H, Stokman G, Wells RG, Eller K, Rosenkranz AR, Eggertsen G, Langner C, Denk H, Wagner CA, Trauner M. ***(*P.F. and E.K. contributed equally to this paper)*** Bile Acids Trigger Cholemic Nephropathy in Common Bile-Duct-ligated Mice. Hepatology. 2013 Dec;58(6):2056-69.

- Krones E, Eller K, Pollheimer MJ, Racedo S, Kirsch AH, Frauscher B, Wahlström A, Ståhlman M, Trauner M, Grahammer F, Huber TB, Wagner K, Rosenkranz AR, Marschall HU, Fickert P. NorUrsodeoxycholic Acid Ameliorates Cholemic Nephropathy in Bile Duct Ligated Mice. J Hepatol. 2017 Jul;67(1):110-119.

- Krones, E; Wagner, M; Eller, K; Rosenkranz, AR; Trauner, M; Fickert, P. Bile acid-induced Cholemic Nephropathy. (Review) Dig Dis. 2015;33(3):367-75. doi: 10.1159/000371689.

- Krones E, Pollheimer MJ, Rosenkranz AR, Fickert P. Cholemic Nephropathy – A Clinical Consequence of Altered Bile Acid Metabolism? Biochim Biophys Acta. 2018 Apr;1864(4 Pt B):1356-1366. doi: 10.1016/j.bbadis.2017.08.028.

All contributing authors have explicitly agreed to the use of the data from the original manuscripts in this thesis. Permissions to reproduce content, figures and tables have been obtained from the respective publishers of the journals.

Table of Contents

List of Figures

List of Tables

List of Abbreviations

ABCB4	ATP binding cassette subfamily B member 4
ACLD	advanced chronic liver disease
ACLF	acute on chronic liver failure
AD	acute decompensation
AIH	autoimmune hepatitis
AKI	acute kidney injury
ALT	alanine aminotransferase
AP	alkaline phosphatase
AQP2	aquaporine 2
ASBT	apical sodium-dependent bile acid transporter
ASH	alcoholic steatohepatitis
ATN	acute tubular necrosis
BMWF	Bundesministerium für Bildung, Wissenschaft und Forschung (Austrian Federal Ministry of Education, Science and Research)
BW	body weight
C3	complement component 3
C4	complement component 3
CA	cholic acid
CBDL	common bile duct ligation
CCC	cholangiocellular carcinoma
CDCA	chenodeoxycholic acid
CKD	chronic kidney disease
CLIF-C	chronic liver failure
CLIF-SOFA	chronic liver failure-sequential organ failure assessment
Colα1(I)	collagen α1(I)
CRP	c-reactive protein
CTP	Child-Turcotte-Pugh
Ctrl	control
CysC	cystatin C
d	days
DDC	3,5-diethoxycarbonyl-1,4-dihydrocollidine
DILI	drug induced liver injury

EDTA	ethylenediaminetetraacetic acid
e.g.	Latin: Exempli Gratia, for example
eGFR	estimated glomerular filtration rate
FENa	fractional excretion of filtered sodium
FVB/N	friend virus B NIH Jackson
FXR	farnesoid X receptor
GC	granular casts
GCDCA	glycochenodeoxycholic acid
GFR	glomerular filtration rate
GlcA	glucuronic acid
HCl	hydrogen chloride
HCV	hepatitis C virus
H&E	hematoxylin and eosin
HEPES	4-(2-hydroxyethyl)-1-piperazineethanesulfonic acid
HLH	hemophagocytic lympho-histiocytosis
HO-1	heme oxygenase 1
HPF	high power field
HRP	horseradish peroxidase
hrs	hours
HRS	hepatorenal syndrome
ICA	International Club of Ascites
IgA	immunoglobuline A
IL-18	interleukin-18
i.p.	intraperitoneal
I/R	ischemia/reperfusion
KIM-1	kidney injury molecule-1
LCA	lithocholic acid
Lcn2	lipocalin-2
L-FABP	liver type fatty acid-binding protein
LPS	lipopolysaccharide
MCA	muricholic acid
Mcp-1	monocyte chemo attractant protein-1
MDCK	Madin-Darby canine kidney
Mdr2	multidrug related protein 2

MDRD	modification of diet in renal disease
MELD	model of end stage liver disease
mGFR	measured glomerular filtration rate
MODY	maturity-onset diabetes of the young
N/A	not applicable
NaCl	sodium chloride
NaOH	sodium hydroxide
NASH	nonalcoholic fatty liver disease
NGAL	neutrophil-gelatinase associated lipocalin
NKCC2	Na+-K+-2Cl- cotransporter
*nor*UDCA	*nor*Ursodeoxycholic acid
n.s	not significant
NSAIDs	non-steroidal anti-inflammatory drugs
OST	organic solute transporter
PAMPs	pathogen-associated molecular patterns
PAS	periodic acid–Schiff
PBC	primary biliary cholangitis
PBS	phosphate buffered saline
PCR	polymerase chain reaction
PSC	primary sclerosing cholangitis
RAAS	renin–angiotensin–aldosterone system
RBCs	red blood cells
RNA	ribonucleic acid
ROS	reactive oxygen species
RRT	renal replacement therapy
RTEC	renal tubular epithelial cells
sCr	serum creatinine
SDS page	sodium dodecyl sulphate polyacrylamide gel
SFOG	acid fuchsine–orange G
SIRS	systemic inflammatory response syndrome
SOP	sham operation
SPSS	Statistical Package for the Social Sciences
SR	sirius red
Tβ-MCA	tauro-β-muricholic Acid

TCA	taurocholic acid
Tgf-β1	transforming growth factor-β1
TLR4	toll-like receptor 4
UDCA	ursodeoxycholic acid
(u)NGAL	urinary neutrophil-gelatinase associated lipocalin
UPLC-MS	ultra-performance liquid chromatography–tandem mass spectrometry
UUL	unilateral ureter ligation
Vcam-1	vascular cell adhesion molecule 1
w	weeks
WB	western blot
WST-1	water soluble tetrazolinium
WT	wildtype

Abstract

Kidney function is a major prognostic factor in patients with liver disease. Acute kidney injury (AKI) commonly occurs in patients with cirrhosis and may be related to prerenal causes such as fluid loss, intrinsic causes, or, although rare, postrenal causes. The commonly known hepatorenal syndrome-type AKI (HRS-AKI) represents a functional and potentially reversible form of progressive renal failure in the absence of identifiable causes. However, there is increasing evidence for structural renal changes at least in a subgroup of patients with liver diseases. Besides bacterial infections, fluid loss, and use of nephrotoxic drugs AKI in liver disease may be triggered by tubular toxicity of cholephiles. The latter became known as cholemic nephropathy, an increasingly recognized condition in patients with cholestasis describing impairment of renal function together with typical histological changes. These findings question the traditional concepts of predominant functional renal failure in liver disease, especially in the specific group of patients with cholestasis. The underlying pathophysiologic mechanisms of cholemic nephropathy are not entirely understood and clear diagnostic criteria and treatment options are still missing. The aim of this thesis was to explore the pathophysiologic mechanisms and possible therapeutic strategies of cholemic nephropathy. By modelling cholemic nephropathy in long-term common bile duct ligation (CBDL) in mice, a well-established mouse model for obstructive cholestasis with accumulation and alternative renal excretion of potentially nephrotoxic cholephiles such as bile acids, it was shown, that renal excreted bile acids might represent the culprits in pathogenesis of cholemic nephropathy. The fact that CBDL mice with a more hydrophilic and therefore less toxic bile acid pool (e.g. by genetic or dietary modulation of the bile acid composition) were protected, strongly argue for urinary excreted bile acids as causative factor for the characteristic morphological changes that can be found in cholemic nephropathy. These results may pave the way for novel strategies of prevention and treatment in the difficult to manage group of patients with advanced (cholestatic) liver diseases and concomitant impairment of renal function.

Zusammenfassung

Ein akutes Nierenversagen (acute kidney injury, AKI) tritt bei etwa 20% aller hospitalisierten Patient*innen mit Leberzirrhose auf und stellt eine oft lebensbedrohliche und prognostisch schwerwiegende Komplikation dar. Ursachen und Differentialdiagnosen des akuten Nierenversagens bei Leberzirrhose umfassen prärenale Ursachen (z.B. Flüssigkeitsverlust), strukturelle Schädigungen der Niere selbst, sowie in seltenen Fällen Ursachen im Bereich der ableitenden Harnwege (postrenales AKI). Die Ursachen des akuten Nierenversagens bei Leberzirrhose beinhalten das als funktionell und potentiell reversibel betrachtete hepatorenale Syndrom (HRS-AKI), dessen klinische Charakteristika und Differentialdiagnose komplex und schwierig sind und den Ausschluss struktureller Nierenschädigungen umfassen. Im Gegensatz dazu mehren sich die Hinweise dafür, dass Patient*innen mit fortgeschrittenen Lebererkrankungen oftmals strukturelle Nierenschäden aufweisen. Häufig findet sich hier der Begriff „cholämische Nephropathie“ oder „cholämische Nephrose“. Dieser Begriff charakterisiert eine mit typischen strukturellen Veränderungen des Nierengewebes einhergehende Form der Nierenfunktionseinschränkung bei Cholestase. Das primäre Ziel dieser Dissertation war die Klärung der Entstehungsmechanismen der cholämischen Nephropathie um darauf aufbauend neue Therapiekonzepte zu entwickeln. Die im Zuge dieser Dissertation generierten tierexperimentellen Daten weisen auf eine zentrale pathogenetische Bedeutung renal ausgeschiedener Gallensäuren für die Entstehung struktureller Schädigungen im Bereich der Niere hin. Zudem konnte durch eine experimentelle Modulation der Gallensäurezusammensetzung (genetisch oder dietätisch) eine deutliche Verbesserung bzw. Verhinderung der gallensäure-induzierten Nierenschädigung im Tiermodell erreicht werden. Diese Erkenntnisse können im Sinne eines translationellen Ansatzes wichtige diagnostische und therapeutische Implikationen für die Humanmedizin nach sich ziehen.

1 INTRODUCTION

1.1 The prognostic importance of kidney function in liver disease

The inclusion of serum creatinine (sCr) in various scores and prognosis models such as (I) the Model of End Stage Liver Disease (MELD) Score, which stratifies severity of end-stage liver disease and is currently used for priorization for liver transplantation [1], (II) the CLIF-C Acute-on-Chronic Liver Failure (ACLF) score and the CLIF-C Acute Decompensation (AD) score, predicting mortality in patients with ACLF and decompensated cirrhosis [2, 3] and (III) the Lille Model for Alcoholic Hepatitis (ASH) predicting mortality in ASH patients that not respond to steroid therapy [4] underlines the important prognostic role of kidney function in liver disease.

1.2 Acute kidney injury in cirrhosis and advanced chronic liver disease (ACLD)

Renal dysfunction commonly (up to 49%) occurs in patients with cirrhosis and portal hypertension (ascites) and advanced chronic liver disease (ACLD) [5-8]. Acute kidney injury (AKI), defined by a significant reduction in glomerular filtration rate (GFR) over a short time period, is a common and challenging complication in patients with (chronic) liver disease since it significantly impairs morbidity and mortality [9-13]. AKI in cirrhosis may be divided into 3 groups: (I) Volume-responsive prerenal azotemia (i.e. decreased renal perfusion pressure due to fluid loss through overdose of diuretics, gastrointestinal bleeding, lactulose-induced diarrhea, infections with fever or large volume paracentesis without albumin replacement; 15-45%), (II) intrinsic causes (i.e. glomerular disease, acute tubular necrosis, ATN), and (III) postrenal causes (i.e. obstructive uropathy), representing less than 1% of cases [14]. For decades, AKI in cirrhosis/ACLD was synonymous with hepatorenal syndrome (HRS) type 1, now known as the hepatorenal syndrome type of AKI (HRS-AKI) [8]. Since 1996, when the diagnostic criteria for HRS were defined, several refinements of diagnostic criteria were published. The latest originate from 2015 and are mainly based on definitions for AKI by the nephrologist's community [8, 15]. AKI in

cirrhosis/ACLD is currently defined according to the International Club of Ascites (ICA) criteria [15]. As such, AKI in cirrhosis/ACLD is defined as an acute increase in serum creatinine of ≥0.3 mg/dL within 48 hours or by ≥50% from a stable baseline serum creatinine (sCr) within 3 months (presumed to have developed within the past 7 days when no prior SCr values are available) [15]. Compared to former, rather stringent criteria based on absolute sCr, the threshold of sCr ≥1.5 mg/dL to diagnose AKI was abandoned, since milder degrees of AKI in cirrhosis had often remained underdiagnosed. AKI in cirrhosis can be classified in 3 stages according to severity [15]. As such, stage 1 AKI is defined by rather small changes in sCr, while stages 2 and 3 AKI are defined by a two-fold and three-fold increase in sCr, respectively (Table 1).

Definition and staging of AKI according to the ICA criteria	
Definition of AKI	Increase in sCr ≥0.3 mg/dL ≤ 48 hours or increase by ≥50% from baseline
ICA-AKI Stage 1	Increase in sCr ≥0.3 mg/dl or Increase in sCr by ≥50% - 100% from baseline
ICA-AKI Stage 2	Increase in sCr by ≥100% - 200% from baseline
ICA-AKI Stage 3	Increase in sCr by ≥200% from baseline or Increase in sCr to ≥4 mg/dL with an acute increase by ≥0.3 mg/dL or need for renal replacement therapy (RRT)

Table 1. Definition and staging of AKI according to the ICA criteria.
Modified after Angeli et al., Diagnosis and management of acute kidney injury in patients with cirrhosis: revised consensus recommendations of the International Club of Ascites, 2015 [15]. AKI, acute kidney injury; ICA, International Club of Ascites; sCr, serum creatinine.

As a distinct entity of prerenal AKI in cirrhosis, HRS-AKI, formerly known as HRS type 1 as already stated earlier, defines as potentially reversible deterioration of renal function in the absence of identifiable causes [15, 16]. HRS-AKI can either develop spontaneously or, similar to other forms of prerenal AKI, triggered by a precipitating event such as aggressive diuretic treatment, large-volume paracentesis without albumin replacement, gastrointestinal bleeding, diarrhea, or (bacterial) infections [17]. But in contrast to other forms of prerenal AKI, renal function in HRS-AKI does not improve by withdrawal of diuretics and volume expansion. HRS-AKI (former type 1 HRS) is defined as ≥ stage 2

AKI that is diagnosed after other causes of kidney injury have been ruled out [18]. The specific diagnostic criteria for diagnosis of HRS-AKI are summarized in Table 2.

Diagnostic criteria of HRS-AKI (former type 1 HRS)
• Diagnosis of cirrhosis and ascites • Diagnosis of AKI according to ICA-AKI criteria (AKI stage 2 or 3) • No response after 2 consecutive days of diuretic withdrawal and plasma volume expansion with 1g albumin per kg body weight • Absence of shock • No current or recent use of nephrotoxic drugs (e.g. NSAIDs, contrast media) • No evidence of structural kidney injury (proteinuria >500mg/day, >50 RBCs per high power field, parenchymal damage in renal ultrasonography)

Table 2. Definition of HRS-AKI according to ICA criteria.
Modified after Angeli et al., Diagnosis and management of acute kidney injury in patients with cirrhosis: revised consensus recommendations of the International Club of Ascites, 2015 [15]. HRS, hepatorenal syndrome; sCr, serum creatinine; NSAIDs, non-steroidal anti-inflammatory drugs; RBCs, red blood cells.

Formerly named type 2 HRS, characterized by a stable or slowly progressive impairment in renal function in decompensated liver cirrhosis with refractory ascites has been classified as a form of chronic kidney disease (CKD) in patients with cirrhosis (HRS-CKD) [16, 19] and is also classified as HRS-non-AKI (HRS-(N)AKI) [8, 20]. Diagnosis of type 2 HRS/HRS-CKD in clinical practice remains challenging, as it – similar to HRS-AKI - still remains a diagnosis by exclusion and – as already mentioned above - patients with cirrhosis often present with several other potential causes for CKD. Although being more favorable when compared to HRS-AKI, prognosis in type 2 HRS/ HRS-CKD is poor and recurrence rates are high [21].

1.3 Pitfalls in the diagnosis of AKI and HRS

An accurate evaluation of renal function is of utmost importance but often difficult to achieve in patients with cirrhosis and/or acute-on-chronic liver failure. SCr, an easily measurable and widely available marker of excretory renal function, is known to overestimate GFR in cirrhosis (malnutrition, decreased formation due to muscle wasting,

increased tubular secretion, dilution due to increased volume of distribution) [22-25]. SCr-based equations to determine GFR thus frequently overestimate renal function in patients with liver cirrhosis [23, 25, 26]. In cirrhosis, GFR estimates using cystatin C (CysC), a low molecular weight protein of the cystatin superfamily of cysteine protease inhibitors [27] that has been considered a more sensitive indicator of renal function than sCr, have been shown to be superior in predicting renal function compared to Cr-based equations [23, 25, 28-32]. Serum CysC is independent of muscle mass, age and sex and its measurement is not influenced by serum bilirubin, inflammation or malignancy [23, 25, 27, 33]. However, low serum albumin levels, elevated white blood cell count, and elevated c-reactive protein (CRP) levels, abnormalities that are frequently present in cirrhotic patients, may impair the reliability of CysC-based equations [34]. In summary, sCr-based equations have been considered inaccurate to assess renal function in cirrhosis. CysC-based equations showed a better performance than Cr-based ones and seemed to be less influenced by Child-Turcotte-Pugh (CTP) score, but rather trend to underestimate GFR in cirrhosis [28, 31].

1.4 AKI biomarkers in liver disease

Not only because of different treatment strategies and outcome, early identification of the AKI phenotype (i.e. differential diagnosis between prerenal azotemia, HRS-AKI and ATN-AKI) is crucial in patients with cirrhosis. Since prerenal AKI cases can usually be successfully reversed by plasma volume expansion, the most challenging issue is to differentiate between functional HRS-AKI and intrinsic ATN-AKI [20] Diagnostic markers that are conventionally used to distinguish between the different AKI phenotypes such as fractional excretion of filtered sodium (FENa) or urea and determination of proteinuria, is not specific and poorly sensitive in cirrhosis. Kidney biopsy is technically difficult to obtain and inherits some relevant risks in cirrhotic patients (e.g. bleeding). SCr and CysC-based eGFR equations as the currently available non-invasive tools to assess renal function in cirrhosis are inaccurate and the clearance of exogenous markers as the gold standard is time consuming and costly and might be biased by changes of volume distribution due to ascites [35]. Also, sCr is a marker of kidney filtration, not kidney injury, and can thus not distinguish between functional and structural AKI phenotypes. There is urgent need for other biomarkers in order to correctly identify the cause of impaired renal

function in ACLD/cirrhosis [35]. Biomarkers of tubular injury are highly suggestive of structural injury when appearing along with an acute drop in GFR [20, 35]. Of all available biomarkers studied so far, urinary interleukin-18 (IL-18), a proinflammatory cytokine which is released into urine following tubular injury, kidney injury molecule-1 (KIM-1), a transmembrane protein which is upregulated in proximal tubular injury, liver type fatty acid-binding protein (L-FABP), a small protein expressed in the proximal tubule and neutrophil gelatinase-associated lipocalin (NGAL) seem to be the most promising ones [20, 35-39]. All those urinary biomarkers have been shown to be significantly higher in ATN-AKI than in in prerenal AKI, with NGAL being also helpful in distinguishing ATN-AKI from HRS-AKI [40-42], however, none of them could accurately distinguish between prerenal AKI and HRS-AKI [20, 43]. NGAL, a 25kDa protein, produced by many organs including kidney, lung and stomach, has been the most extensively studied urinary biomarker in kidney injury [35, 44-48]. In experimental models, NGAL expression was shown to increase very rapidly (within 2 hrs) after ischemic or toxic insults of the kidney [46, 47]. These results of NGAL being able to distinguish between ATN-AKI and HRS-AKI have to be in parts interpreted with caution, since they were obtained without histological confirmation of ATN [35]. NGAL levels may also increase due to sepsis or liver injury [49, 50]. Mechanisms leading to urinary excretion of urinary biomarkers include protein release due to cell damage, protein release due to recruitment of inflammatory cells (IL-18), diminished tubular reabsorption of proteins (e.g. beta-2 microglobulin), and upregulation of tubular proteins secondary to tubular injury (NGAL, KIM-1 L-FABP, CysC) [35]. Increased serum levels of beta-2 microglobulin, a small molecule present in all nucleated cells which is freely filtered and reabsorbed in proximal tubules, are found as GFR declines, however, several other conditions such as inflammation, autoimmune disease and malignancy might lead to an increase of this protein which limits its reliability in cirrhotic patients [51, 52]. Overall, the use of biomarkers might be helpful in early detection of impaired renal function and differentiation between the different phenotypes of AKI in ACLD/cirrhosis (differentiation between ATN-AKI and HRS-AKI would be of utmost clinical importance); however, their measurement underlies potential biases and further studies are needed [53].

	Source	Rationale	Origin
Biomarkers			
NGAL	Urine Serum	Proximal tubular ischemia leads to upregulation	Proximal tubule, distal tubule, leucocytes
KIM-1	Urine	Proximal tubular ischemia leads to shedding of ectodomain into urine	Proximal tubule
IL-18	Serum Urine	Upregulation in ischemic injury and tubular inflammation	Monocytes, dendritic cells, macrophages, epithelial cells of the proximal tubule
L-FABP	Urine	Translocation from cytosol to tubular lumen during ischemia	Proximal tubule, liver, intestine
Urine microscopy			
Microscopy of centrifuged urine	Urine	Correlation with kidney histology	

Table 3. Potential biomarkers for structural kidney alterations in liver disease.
Adapted from Siew et al, J Am Soc Nephrol 2011 [54]. IL-18, interleukin 18; KIM-1, kidney injury molecule-1; L-FABP, liver type fatty acid binding protein, NGAL, neutrophil gelatinase associated lipocalin.

1.5 Pathophysiology of AKI in cirrhosis/ACLD – functional, structural or both?

The current pathophysiologic concept of HRS-AKI development includes splanchnic vasodilatation with subsequent activation of vasoconstrictors and related renal circulatory abnormalities in the absence of alternative identifiable causes [55-58]. Progressive splanchnic and systemic arterial vasodilatation in cirrhosis, caused by overproduction of various vasoactive substances like nitric oxide, carbon monoxide and endocannabinoids, is the principal driver of HRS-AKI pathogenesis [8, 14, 57, 59, 60], since it causes a reduction in effective arterial blood volume and mean arterial pressure, which in turn leads to of various vasoconstrictor systems such as the renin–angiotensin–aldosterone system (RAAS), the sympathetic nervous system, and increased release of vasopressin in order to maintain hemodynamic stability [8, 60]. Due to effective hypovolemia, the autoregulatory mechanisms of the kidney to maintain renal perfusion get overwhelmed resulting in renal

vasoconstriction and a decline of renal function [59]. Besides the traditional concept of hemodynamic abnormalities, other factors, including structural alterations via ischemia and/or inflammation [19] and nephrotoxins may contribute to AKI development in cirrhosis.

Also, the vasodilatation theory in HRS-AKI pathogenesis has been challenged by a theory of systemic inflammatory multiorgan disease [61]. Results of the CANONIC study, a large observational study which was performed in order to develop a definition of ACLF able to identify cirrhotics with a high short-term mortality risk, showed that AKI was associated at first with systemic inflammation and not that much with cardiocirculatory dysfunction [13]. Systemic inflammatory response syndrome (SIRS) and sepsis, commonly observed triggers of AKI in cirrhosis, were hypothesized to lead to renal redistribution of blood flow out of the cortex resulting in ischemia of the corticomedullary junction with subsequent tubular injury [61, 62]. Translocation of bacteria and bacterial products (pathogen-associated molecular patterns (PAMPs)) from the gut due to increased intestinal permeability related to portal hypertension is frequently associated with SIRS [61]. The main pattern recognition receptor studied in that context is toll-like receptor 4 (TLR4) which has been found to be overexpressed in tubular epithelial cells of an experimental model of cirrhosis secondary to an inflammatory insult and in urine and kidney tissue patients with cirrhosis and AKI as well as in a subset of HRS-AKI patients [63, 64]. Also, some of these PAMPs contribute to the splanchnic and systemic arterial vasodilatation due to vasoactive properties [8].

In addition, underlying chronic kidney disease (CKD) secondary to comorbidities that are frequently present in cirrhosis (i.e. arterial hypertension, diabetes, overweight or glomerulonephritis associated with viral hepatitis) may prone to AKI development [35].

Although current diagnostic criteria for HRS-AKI include the exclusion of parenchymal renal disease (i.e. proteinuria < 0,5 g/d, < 50 red cells/HPF, no evidence for structural renal disease upon renal ultrasound) [55] (Table 2), several clinical studies report on structural kidney injury at least in a subgroup of patients with end-stage liver diseases. As such, structural abnormalities including vascular and tubular epithelial injury upon renal histology in patients with advanced stage liver disease and (acute) kidney injury without proteinuria and hematuria have been reported [65-67]. The clinical importance and then

notion, that AKI in cirrhosis is not only a hemodynamic problem is underpinned by the fact that 61% of patients do not adequately respond to vasoactive therapy [68].

These findings question the traditional concepts of a purely functional renal failure in liver diseases, especially in jaundiced patients. AKI or renal dysfunction in patients with liver cirrhosis is becoming more and more evident to represent a mixed bag of heterogeneous conditions. To ignore the contribution of morphological/structural renal changes, that may especially occur in cholestatic or advanced stage liver disease associated with jaundice (such as advanced liver cirrhosis or ACLF), would lead to an incomplete representation of the whole spectrum of renal alterations that may occur in the setting of acute or chronic liver disease.

1.6 The kidney in cholestasis

Bile acids are sterol-derived molecules that exhibit numerous physiological functions in lipid, protein and glucose metabolism and innate immunity [69]. Not only the liver but also the small intestine and the kidney are involved in bile acid transport and regulation [69]. After secretion into the small intestine, bile acids undergo nearly complete reuptake in the terminal ileum and return back into the portal circulation and finally to the liver where they are resecreted into bile [70-72]. Around 10-50% (depending on the bile acid species) of the reabsorbed bile acids escape hepatic extraction and reenter peripheral circulation [72]. Bile acids present in the blood plasma that are not protein bound are subjected to glomerular filtration (around 100 µmol per day under physiological conditions) [72]. Due to the fact that the filtered bile acids are nearly completely reabsorbed in the proximal tubules of the nephron by a sodium-dependent mechanism, the amount of urinary excreted bile acids under physiologic conditions is small (around 1-2 µmol per day) [72-75]. Similar to the enterocyte in the ileum, the proximal tubule epithelium expresses the apical sodium-dependent bile acid transporter (ASBT) on the apical surface [76, 77], and organic solute transporters (OST)α-OSTβ on the basolateral membrane for absorption of bile acids from the tubule lumen and basolateral export into the systemic circulation [78].
Cholestasis, an impairment of bile formation and/or flow on either the level of hepatocytes (e.g. sepsis-induced cholestasis, drug-induced cholestasis) or cholangiocytes (e.g.

sclerosing cholangitis, intra- and/or extrahepatic bile duct obstructions) results in interruption of the enterohepatic circulation of bile acids [70]. This is characterized by systemic accumulation of bile acids and bilirubin, which might be of toxic potential. [79, 80]. Hepatocytes in cholestatic liver diseases (e.g. obstructive jaundice or autoimmune cholestatic liver diseases such as primary biliary cholangitis or primary biliary cirrhosis) and respective animal models (e.g. common bile duct ligated (CBDL) or bile acid-fed rodents) limit increased intracellular levels of bile acids and bilirubin via induction of alternative excretory routes (i.e. basolateral hepatocellular export) and renal elimination [71, 80-87].

Despite beneficial hepatic and systemic effects of alternative excretion of potentially toxic cholephiles this might cause kidney injury [88].

However, little is known whether cholestasis associated with increased urinary excretion of potentially cytotoxic cholephiles such as bile acids or bilirubin may be causally linked to AKI in jaundiced patients due to cholestatic or end-stage liver diseases.

1.7 Historical notes of renal failure in jaundice

The clinical association between obstructive jaundice and AKI is well-known and was already described in 1899 by Quincke and Nothnagel during autopsy examinations of jaundiced patients with kidney injury/disease and in 1911 by P. Clairmont and H. v. Haberer entitled “Mitteilung über Anurie nach Gallensteinoperationen” (“communication about anuria following gallstone surgery”) [53, 89-92]. The morphological and histological description of the kidney alterations in jaundice by Quincke and Nothnagel included diffuse staining of the kidney cortex with bilirubin, tubular accumulation of pigment, intraluminal yellow, green or brownish tubular casts, diffuse swelling of tubular epithelial cells and necrosis [53]. In 1922 Haessler et al. postulated a causal link between jaundice and kidney injury after analyzing urine sediments of jaundiced humans and dogs [53]. From a clinical perspective, especially surgeons fear perioperative AKI in patients with (obstructive) jaundice who undergo invasive diagnostic and therapeutic procedures due to high postoperative morbidity and mortality [53, 93, 94].

In the pediatric literature, cholestatic liver diseases associated with progressive tubulointerstitial nephropathy (including early onset of tubulointerstitial nephritis, tubular atrophy, dilatation of tubules, and interstitial and periglomerular fibrosis along with clinical and biochemical signs of cholestasis) have been reported as a distinct entity [95-100]. Cholestatic liver diseases have also been linked to tubulointerstitial nephropathies such as Fanconi Syndrome [95, 97, 100-105]. Obstructive jaundice was additionally shown to cause partially reversible proximal tubular dysfunction [106].

1.8 Cholemic nephropathy

The specific morphological kidney alterations due to cholestasis became known as *cholemic nephropathy* [107-111]. This "umbrella term" describes impairment of renal function in jaundice together with a characteristic histomorphological appearance that includes tubular epithelial damage (predominantly at the level of distal nephron segments) and intraluminal (bile) cast formation. Up to now, a high number of synonyms appears in medical literature. These include icteric nephrosis/nephropathy, jaundice-related nephropathy, bile cast nephropathy, and bile acid nephropathy [107, 108, 110-113]. Until 2000, the term cholemic nephropathy has almost disappeared from modern medical literature but experienced a kind of renaissance triggered by a considerable number of case reports and clinical studies [113]. As such, cholemic nephropathy has been described in different clinical scenarios including drug-induced (cholestatic) liver injury, fulminant acute hepatitis, ASH, and advanced stage liver disease [107, 112-139] (Table 4).

Besides this increasing number of clinical cases and older studies on cholemic nephropathy which were published between 1920 and 1970 [108, 110, 111, 140, 141], animal experiments focusing on the pathogenesis of renal injury in cholestasis were performed. Mainly rats and dogs were used for these experimental approaches [108, 141-145]. The proposed mechanistic concepts included oxidative stress, which was hypothesized to be induced by urinary excreted bilirubin that subsequently leads to damage of tubular cell membranes [146]. Other proposed triggers include portal venous and systemic endotoxemia due to increased translocation from the gut, increased production and/or expression of vasoactive mediators such as endothelin or thromboxane, direct tubular

effects of bile and volume depletion [142, 143, 146-155]. Bilirubin, however, has even been found to exhibit antioxidative and therefore renoprotective properties in experimental settings [156-159].

1.8.1 Definition and characteristics of cholemic nephropathy

The term “cholemic nephropathy” denotes (acute) kidney injury in patients with (obstructive) jaundice along with characteristic histological alterations such as tubular epithelial injury (mainly directed towards distal nephron segments) and subsequent intraluminal cast formation [107, 113]. The currently existing different terms for the same clinical condition (i.e. bile cast nephropathy or icteric nephrosis) result from description of the characteristic morphology (i.e. bile casts) on the one hand and possible triggers – such as it is the case for the term “bile acid nephropathy” - on the other hand [53, 112, 113]. The term cholemic nephropathy seems to be advantageous, since it neither restricts to a specific histology nor to a specific etiopathogenesis, however, both have not been entirely clarified so far [53]. Regarding the macroscopic features of cholemic kidneys, the cortex and medulla are yellowish in the beginning and turn to green after formalin fixation since this processing leads to conversion of bilirubin to biliverdin [113]. Since the bilirubin concentration is highest at the level of distal nephron segments, the green color is especially accentuated in the area of the medullar pyramids [113]. All histological kidney alterations in jaundice reported so far were reported to be predominantly present in tubules and especially distal nephron segments (e.g., collecting ducts) [113]. The characteristically observed intraluminal casts consisting of exfoliated epithelial cells could be easily identified and confirmed by histochemical Hall (or Fouchet) or periodic-acid Schiff (PAS) staining of kidney sections [113]. Besides intraluminal casts and tubular epithelial injury, the presence of mononuclear inflammatory cells in the vasa recta has been reported [113]. The evidence for glomerular alterations in obstructive jaundice is scarce and limited to a low number of reports on mesangial C3, glomerular C4d and IgA deposition and hyperplasia of the parietal layer of Bowman’s capsule [108, 116, 160].

1.8.2 Clinical studies on cholemic nephropathy

As already stated earlier, the clinical phenomenon of kidney injury in obstructive jaundice has been known for years and has been described in several case reports and experimental studies. Uslu et al. reported on acute tubular necrosis and venous dilatation upon renal biopsies in 20 consecutive patients with short-term obstructive cholestasis (mean duration of biliary obstruction 15 ± 1,4 days, mean total bilirubin 10.1 ± 1.0 mg/dL). Those were found despite normal mean arterial pressure, perioperative volume expansion and almost normal excretory renal function measured by conventionally used biochemical parameters (preoperative serum creatinine 0.97 ± 0.1 mg/dL, mean GFR 81.9 ± 0.4 ml/min) [116]. However, no correlation between the severity of jaundice (total serum bilirubin levels) and the presence/severity of the renal alterations was observed [116]. In 2013, very interesting results of an autopsy study (41 autopsy cases and 3 patients with kidney biopsies) were published by van Slambrouck *et al* [113]. In this study, they found bile casts in distal nephron segments of jaundiced patients with cirrhosis (e.g., alcoholic liver disease, alcohol-associated hepatitis, hepatitis C, non-alcoholic steatohepatitis (NASH), cryptogenic cirrhosis), cholestasis (e.g., obstructive jaundice, primary sclerosing cholangitis (PSC), cholangitis lenta) and acute liver dysfunction [e.g., fulminant autoimmune hepatitis (AIH)]. In contrast to the previously described study by Uslu *et al.,* were no correlation between the presence of renal alterations and the severity of jaundice was described, the presence of bile casts in the van Slambrouck *et al.* study significantly correlated with total and direct bilirubin levels [113]. Interestingly, 13 of the 44 patients were clinically classified as HRS-AKI, however, the majority of these (11 out of 13, 85%) had bile casts detected upon kidney histology. Bile casts were present in all patients with alcoholic liver disease but only in 40% of the cases with obstructive jaundice. Based on their findings, the authors hypothesized that bile casts contribute to kidney injury by direct bile and bilirubin toxicity and tubular obstruction analogous to other forms of cast nephropathy such as myeloma or myoglobin-associated cast nephropathy [113]. Of interest, two included patients with jaundice due to hemolysis (with accumulation of indirect/unconjugated bilirubin) did not show bile casts upon kidney histology [113]. As a resonance to the paper by van Slambrouk *et al.,* a high number of reports on similar cases has been published since 2000 [112, 118-123, 125-139, 161, 162]. These are summarized in Table 4.

Author	Year	(n)	Etiology	Bili (mg/dl)	Diagnosis	Histology	Outcome
Bal *et al.* [124]	2000	3	Subacute liver failure	20 ± 10,2	Biopsy (post-mortem)	Mesangial proliferation and thickening, basement membrane thickening, presence of hyaline, granular and bile casts	N/A
Kiewe *et al.* [115]	2004	1	Hodgkin's lymphoma with liver involvement	11.7	Biopsy	Multiple intratubular greenish bile casts	Improvement along with restoration of cholestasis
Betjes *et al.* [107]	2006	2	Obstructive jaundice AIH	36.2 33.2	Biopsy	bilirubin pigment in the tubules tubular cell necrosis	Improvement of renal function along with decrease of bilirubin, or death
Uslu *et al.* [116]	2010	20	Obstructive jaundice	10.1 ± 1.0	Biopsy	Dilatation of peritubular venules, acute tubular necrosis	Recovery of renal function in all patients after biliary drainage
Bredewold *et al.* [117]	2011	1	Jaundice due to mono-nucleosis infectiosa	36.1	Biopsy	Acute tubular necrosis, bile casts	Recovery
van Slambrouck *et al.* [113]	2013	24	Obstructive cholestasis	24.9	Autopsy Biopsy	Bile casts with involvement of distal nephron segments	N/A
Rafat et al. [118]	2013	1	Jaundice due to CCC	30	Biopsy	Bile thrombi in dilated tubules Bile granules in cytoplasm of tubular	Patient died due to CCC

						epithelial cells	
Luciano *et al.* [112]	2014	1	Cholestatic jaundice related to ingestion of anabolic steroids	47.9	Urine micro-scopy Biopsy	Granular casts and heavily pigmented renal tubular epithelial cell casts upon urine microscopy Dilated tubules containing heavily pigmented granular casts upon histology	Serum creatinine levels remained mildly elevated
van der Wijngaart *et al.* [119]	2014	1	Obstructive jaundice (gallstones)	39.6	Biopsy	Bile casts, reactive changes of tubular epithelial cells	Improve-ment of kidney function after biliary drainage and RRT
Jain *et al.* [120]	2015	1	Jaundice following wedge resection of liver	42.5	Urine microscopy Biopsy	Bile casts and leucine crystals upon urine microscopy Intratubular bile casts upon kidney biopsy	N/A
Sequeira *et al*. [121]	2015	1	ASH	23.1	Biopsy	Acute tubular injury, bile casts	RRT
Tabatabaee *et al.* [122]	2015	2	Cholestatic DILI	50	Biopsy	Acute tubular epithelial cell damage, bile cast deposition	Improve-ment of serum creatinine along with decrease of bilirubin
Patel *et al.* [123]	2016	1	DILI	19.3	Biopsy	Pigmented bilirubin casts and droplets in proximal	Combined liver and kidney transplant

						and distal tubules, tubular atrophy and interstitial fibrosis	
Sens *et al.* [124]	2016	1	Cholestasis in a patient with MODY type 5	20.1	Biopsy	Bile casts, marked tubular necrosis	Improve-ment of serum creatinine along with decrease of bilirubin
Werner *et al*. [125]	2016	1	Jaundice due to CCC	N/A	Biopsy	Dilated tubules, bile casts	Resolution of renal function after restoration of cholestasis
Alkhunaizi *et al.* [126]	2016	1	Cholestatic DILI	44	Biopsy	Bile casts within distal tubular lumina, filamentous bile inclusions within tubular cells, signs of acute tubular injury	Improve-ment of serum creatinine along with decrease of bilirubin
Alnasrallah *et al.* [127]	2016	1	DILI	51.5	Biopsy	Dilated tubules, bile casts, tubular epithelial injury	Decline of serum creatinine after improveme nt of jaundice
Mohapatra *et al.* [128]	2016	20	Severe falciparum malaria complicated with jaundice	26.5 ± 4.1	Urine micro-scopy Biopsy	Bile-stained casts upon urine microscopy Numerous tubular casts, acute tubular Necrosis but maintained glomerular	Recovery time of renal dysfunction 15.1 ± 6.5 days

						architecture upon kidney histology	
Leclerc *et al.* [129]	2016	1	DILI	30.9	Biopsy	Brown casts clogging the tubular lumen, brown deposits in the cytoplasm of tubular epithelial cells	Improve-ment of kidney function after normali-zation of bilirubin and RRT
Foshat *et al.* [163]	2017	52	Cirrhosis (HCV)	10.4 ± 12.0	Autopsy	Hall-stain positive bile casts	N/A
Aniort *et al.* [130]	2017	1	Obstructive cholestasis (gallstones)	32.6	Biopsy	Intralumina l green casts, tubular injury	Complete recovery following removal of the bile duct obstruction
Sood *et al*. [131]	2017	1	Acute liver failure	30.9	Biopsy	bile casts, tubular epithelial injury	N/A
Nayak *et al.* [132]	2018	1	Hepatitis E	33.9	Biopsy	Tubular injury, bile casts	Recovery
Ravi *et al.* [133]	2018	1	Acute hepatitis A	N/A	Biopsy	Bile casts	Recovery after RRT
Torrealba *et al.* [164]	2018	2	ASH Wilson's disease	37.8 43.2	Biopsy	Granular casts, bile casts, tubular necrosis	Patients died
Bräsen *et al.* [134]	2019	8	Liver diseases of various etiologies (acute and chronic)	45.8 ± 18	Biopsy	Bile casts, loss of AQP2 in collecting ducts	3 recovered, 5 RRT
Mukherjee *et al.* [135]	2019	1	ACLF	26.5–41.7	Autopsy	bile casts, focal necrosis and desquamati on tubular epithelium	Patient died
Chango	2020	1	Hemophago-	52.7	Biopsy	Bile casts,	Patient died

Azanza *et al.* [136]			cytic lympho-histiocytosis with liver failure			tubular injury	due to HLH and liver failure
Priyaa *et al.* [137]	2021	14	Hepatic failure (various etiologies)	N/A	Biopsy (post-mortem)	Tubular injury, bile casts, glomeruli unremarkable	N/A
Al Awadhi *et al.* [138]	2021	1	DILI	31.27	Biopsy	Bile casts, tubular atrophy, interstitial fibrosis	Improve-ment of kidney function after RRT
Maiwall *et al.* [139]	2022	42	ACLF	30.78 ± 12.25	Biopsy (post-mortem)	Bile casts in distal (and proximal) tubules, bilirubin crystals upon urine microscopy	N/A

Table 4. Common clinical features in 20 case reports/case series on cholemic nephropathy since 2000.
ACLF, acute-on-chronic liver failure; AIH, autoimmune hepatitis; AQP2. Aquaporin 2; ASH, alcoholic steatohepatitis; CCC, cholangiocellular carcinoma DILI, drug-induced liver injury; HCV, hepatitis C virus; N/A, not applicable, MODY, Maturity Onset Diabetes of the Youth; RRT, renal replacement therapy. Adapted/updated from Krones E et al, Biochim Biophys Acta Mol Basis Dis. 2018;1864(4 Pt B):1356-1366 [53] with permission of Elsevier. Table drafted by Elisabeth Tatscher.

A clinical case series published by Bräsen and Mederacke et al. in 2019 identified 79 patients with liver disease and impaired renal function (AKI in 57%, CKD in 43%) of whom 8 were diagnosed with cholemic nephropathy (presenting as AKI). Those with cholemic nephropathy had higher serum bilirubin levels and a high prevalence of abnormalities upon urinalysis, underlining the importance of this simple diagnostic method in the workup of AKI in ACLD/cirrhosis [134, 165]. In a large prospective cohort of ACLF patients, cholemic nephropathy was identified as the predominant cause for AKI 3 (33 out of 61 post-mortem renal biopsies, 54%). Interestingly, 22 out of these 33 (66.7%) patients were initially diagnosed as HRS-AKI. Also, Terlipressin response rates were poor in this cohort [139].

These obvious clinical associations strongly argue for a key pathogenetic role of cholephilic molecules such as bile acids; although the underlying mechanisms and the causative link between potentially toxic and alternatively urinary excreted cholephiles on one hand and the structural renal alterations in cholemic nephropathy on the other remains unclear and not well defined. Consequently, animal models with combined cholestatic and/or end-stage liver disease together with specific *in vitro* approaches should be supportive for mechanistic studies regarding the pathobiology of cholemic nephropathy.

1.9 Animal Models for sclerosing cholangitis and biliary fibrosis

Well characterized animal models allowing time course studies are indispensable to investigate complex diseases and biological processes involving multiple organ systems such as kidney injury in cholestatic liver diseases. In contrast to rats, the biliary physiology of mice closer resembles the human condition (e.g. presence of a gall bladder). Studying mice also has the advantage of multiple available knock-out technology in this species [166]. Multidrug resistance 2 (Mdr2, Abcb4) gene knockout mice spontaneously develop key features of human sclerosing cholangitis such as onion-skin-like periductal fibrosis, strictures and dilatations of bile ducts [167-169]. Long-term CBDL in mice was shown to be associated with chronic cholestasis, biliary cirrhosis and ascites formation [170]. Feeding the porphyrinogenic substance 3,5- dietoxycarbonyl-1,4-dihydrochollidine (DDC) leads to development of sclerosing cholangitis and pronounced biliary fibrosis within weeks [167, 171]. Another example of chemically-induced cholestatic liver disease is the lithocholic acid (LCA)-fed mouse model which shows segmental bile duct obstruction, destructive cholangitis and periductal fibrosis [172]. There is an increasing number of well-characterized mouse models for chronic cholestatic liver disease with certain biochemical (i.e. increased serum bile acid and alkaline phosphatase levels) as well as histopathological characteristics of chronic progressive liver diseases (i.e. ductular reaction/proliferation and porto-portal bridging, chicken wire fibrosis) [166]. However, it remains undefined whether these models are associated with impaired renal function or renal pathology since this has not been systematically studied so far. Detailed morphological and longitudinal studies in regard to kidney injury in these models would be

mandatory for future comprehensive mechanistic studies on the important pathobiology of cholemic nephropathy.

1.10 Hypothesis

Overwhelming alternative urinary excretion of potentially toxic cholephilic molecules in cholestatic liver diseases leads to cholemic nephropathy.

1.11 Aims

The aims of this this thesis were 1) to establish and characterize a mouse model of combined cholestatic liver and kidney disease enabling detailed time-course studies in cholemic nephropathy and 2) to identify potential triggers and mediators with a specific focus on bile acids, and 3) to embody novel strategies to prevent and treat kidney injury in cholestatic liver diseases with the aid of specific gene knock-out mice and dietary interventions.

This information will help to gain novel mechanistic insights into the complex pathophysiology and characterize novel ways of prevention and treatment for cholemic nephropathy.

2 METHODS

2.1 Animal experiments.

Protocols on animal experiments were approved by the Federal Ministry of Education, Science and Research of the Republic of Austria (BMWF-66.010/0045-II/10b/2010, BMWF-66.010/0012-II/3b/2014, BMWF-66.010/0011-WF/V/3b/2015). All animal experiments (except from Mdr2 knock-out ($Mdr2^{-/-}$) mice, FVB/N background) were performed in 8-10-weeks-old male C57BL/6 mice with a body weight ranging between 25 and 30 g. The mice were kept with a 12:12 hour light:dark cycle and permitted *ad libitum* consumption of water and food. Experimental designs are summarized in Table 5. Each animal experiment was performed in groups of (4)5-10 mice.

Background	Genetic Background	Intervention	Duration	Diet
C57BL/6	WT	CBDL	3 days	Chow
C57BL/6	WT	SOP	3 days	Chow
C57BL/6	WT	CBDL	7 days	Chow
C57BL/6	WT	SOP	7 days	Chow
C57BL/6	WT	CBDL	3 weeks	Chow
C57BL/6	WT	SOP	3 weeks	Chow
C57BL/6	WT	CBDL	6 weeks	Chow
C57BL/6	WT	CBDL	8 weeks	Chow
C57BL/6	WT	SOP	8 weeks	Chow
C57BL/6	$FXR^{+/+}$	CBDL	3 days	Chow
C57BL/6	$FXR^{+/+}$	SOP	3 days	Chow
C57BL/6	$FXR^{-/-}$	CBDL	3 days	Chow
C57BL/6	$FXR^{-/-}$	SOP	3 days	Chow
C57BL/6	$FXR^{+/+}$	CBDL	8 weeks	Chow
C57BL/6	$FXR^{+/+}$	SOP	8 weeks	Chow
C57BL/6	$FXR^{-/-}$	CBDL	8 weeks	Chow
C57BL/6	$FXR^{-/-}$	SOP	8 weeks	Chow
C57BL/6	$FXR^{+/+}$	UUL	2 weeks	Chow
C57BL/6	$FXR^{-/-}$	UUL	2 weeks	Chow
C57BL/6	WT	CBDL	3 days	Chow
C57BL/6	WT	CBDL	3 days	*nor*UDCA 0,5%
FVB/N	$Mdr2^{-/-}$	-	4 weeks	Chow
FVB/N	$Mdr2^{+/+}$	-	4 weeks	Chow

C57BL/6	WT	-	4 weeks	DDC 0.1%
C57BL/6	WT	-	8 weeks	DDC 0.1%
C57BL/6	WT	CBDL	8 weeks	Chow
C57BL/6	WT	CBDL	8 weeks	*nor*UDCA 0,125% *for Prevention*
C57BL/6	WT	CBDL	8 weeks	*nor*UDCA 0,125% *for Rescue*
C57BL/6	WT	I/R 30 min	18 hrs	*nor*UDCA 0,125%
C57BL/6	WT	I/R 30 min	18 hrs	Chow
C57BL/6	WT	I/R 30 min	48 hrs	*nor*UDCA 0,125%
C57BL/6	WT	I/R 30 min	48 hrs	Chow
C57BL/6	WT	UUL	2 weeks	*nor*UDCA 0,125%
C57BL/6	WT	UUL	2 weeks	Chow
C57BL/6	WT	LPS	12 hrs	*nor*UDCA 0,5%
C57BL/6	WT	LPS	12 hrs	Chow

Table 5. Overview on animal experiments.
CBDL, common bile duct ligation; DDC; 3,5-diethoxycarbonyl-1,4-dihydrocollidine; I/R, ischemia/reperfusion; LPS, lipopolysaccharide; Mdr2, multidrug related protein 2; *nor*UDCA, *nor*Ursodeoxycholic acid; SOP, sham operation; UUL, unilateral ureter ligation; WT, wildtype.

2.1.1 Genetically modified mouse strains.

$Mdr2^{-/-}$ mice (FVB/N background, Jackson Laboratory, Bar Harbor, ME) representing a well-characterized genetic mouse model of sclerosing cholangitis [167-169] were screened for the presence of kidney alterations. $Mdr2^{-/-}$ mice were harvested at 4 months of age. The effects of CBDL were also compared in Farnesoid X receptor (FXR) knock-out mice ($FXR^{-/-}$; congenic C57/BL6) and respective wild type (WT) controls as outlined in Fickert P, Krones E et al, Hepatology. 2013;58(6):2056-69 [100].

2.1.2 Description of experimental procedures.

For all surgical procedures the animals were subjected to general anesthesia (isoflurane, Abbott, induction with 4%, maintenance with 2%) and peri- and postoperative analgesia

[Metamizol (Novalgin®, Sanofi-Aventis, Vienna, Austria) 500mg/100 ml via drinking water, Fentanyl (Hexal AG, Holzkirchen, Germany)5µg/kg subcutaneously]. During anesthesia mice were kept on a heating plate. At the end of either experiment, mice were sacrificed by decapitation under general anesthesia (isoflurane, Abbott).

2.1.3 Common bile duct ligation (CBDL), Cholecystectomy and sham operation (SOP).

After midline incision of the abdomen, the common bile duct was identified and ligated as close as possible to the liver hilum. Also, the gallbladder was removed after ligation of the cystic duct (cholecystectomy). For sham operation (SOP), mice underwent the same procedure, but without bile duct ligation and cholecystectomy. In order to study different time points, mice were harvested 3 days, 7 days, as well as 3, 6, and 8 weeks following CBDL or SOP.

2.1.4 Unilateral ureter ligation (UUL).

This model for non-cholestatic tubulointerstitial kidney fibrosis was chosen in order to mimic obstructive postrenal kidney injury. UUL was performed in WT and $FXR^{-/-}$ mice. After midline abdominal incision and preparation of the kidneys, double-ligation of the left ureter was performed and mice were harvested after 7 days. The right kidney was used as an internal control in each animal.

2.1.5 3,5-diethoxycarbonyl-1,4-dihydrocollidine (DDC) intoxication.

To induce sclerosing cholangitis C57BL/6 mice were fed a 0.1% DDC-supplemented diet for 4 and 8 weeks [171].

2.1.6 *nor*Ursodeoxycholic acid (*nor*UDCA) feeding - The therapeutic efficacy of *nor*UDCA was studied in 3 days and long-term (8 weeks) CBDL.

Bile acids represent an established treatment option for cholestatic liver disease such as PBC. During the last decades biochemically modified bile acid derivatives were developed and studied in various conditions [173, 174]. As such, *nor*ursodeoxycholic acid (*nor*UDCA), side-chain shortened derivative of UDCA, has clinically been investigated in a phase III clinical trial in patients with PSC and is currently (2022/23) tested in a phase II clinical trial in patients with primary biliary cholangitis (PBC) [175-178]. In mouse models of cholestasis, *nor*UDCA was shown to increase bicarbonate-dependent bile flow and to induce alternative eliminatory routes for potentially (hepato)toxic bile acids [178]. Consequently, *nor*UDCA represents an attractive compound to be studied in cholemic nephropathy, especially in the setting of advanced (cholestatic) liver disease. To unravel *nor*UDCA's therapeutic potential and mechanism(s) of action in the kidney, longitudinal studies in the CBDL mouse model (but also other nephropathy mouse models, see below) were performed. *Nor*UDCA was obtained as a generous gift from Dr. Falk Pharmaceuticals.

To study its effects in 3 days CBDL mice, *nor*UDCA-enriched diets (0,5%) were started 5-7 days prior to CBDL and given until harvesting. The therapeutic efficacy in long-term CBDL was investigated using two different experimental setups: *norUDCA for Prevention* and *norUDCA for Rescue*. *NorUDCA for Prevention (5 vs. 5 mice)*: To study whether *nor*UDCA prevents cholemic nephropathy in long-term CBDL, *nor*UDCA-enriched diets (0.125% w/v, corresponding to 200 mg/kg/day for a mouse of 25 g body weight eating about 4g daily) or a standard mouse diet (Sniff, Soest, Germany) were started 5 days before CBDL was performed and were given until harvesting after 8 weeks of CBDL. *NorUDCA for Rescue (5 vs. 5 mice)*: To study whether *nor*UDCA treatment is able to ameliorate/rescue the cholemic kidney phenotype in CBDL, *nor*UDCA-enriched diets (0.125% w/v) or a standard chow was started 3 days after CBDL was performed and was administered until harvesting after 8 weeks of CBDL. The time point to start the diet at day 3 after CBDL was chosen since serum bile acids were previously shown to peak at that time point. Also, the first histological collecting duct lesions were observed 3 days after CBDL [100].

2.1.7 Unilateral ureter ligation (UUL) and ischemia/reperfusion (I/R) injury in *nor*UDCA-fed mice.

To study whether a bile acid derivative (i.e. *nor*UDCA) could improve kidney injury in other nephropathy models, mice were fed *nor*UDCA-enriched diets and then (i) subjected to ischemia/reperfusion (I/R) injury or (ii) to UUL. These experiments were performed in collaboration with the Renal Division in Freiburg (University Hospital Freiburg; Freiburg, Germany) after approval by the Committee on Research Animal Care Freiburg. For either studies, mice were pre-fed for 5 days with normal or 0.125% *nor*UDCA chows (n = 6 vs. 6 mice). For surgery, mice were anesthetized using isoflurane (induction with 4%, maintenance with 2%) and given 0.05 mg/kg Buprenorphine s.c. (Temgesic®, Essex Pharma, Munich, Germany). During anesthesia mice were kept on a self-regulating heating plate with a rectal temperature probe in place. For I/R injury experiments, the left renal artery was clamped for 30 minutes following a left back incision. After visual control of reperfusion, the abdomen was closed using absorbable suture. Every mouse was given 40µl/g BW 0.9% NaCl solution i.p. and drinking water containing 500mg/100 ml Metamizol (Novalgin®, Sanofi, Hoechst, Germany). Kidneys were harvested at 18h (3 vs. 3 mice) and 48h (3 vs. 3 mice). For UUL, at day 5 after pre-feeding of 0.125% *nor*UDCA (n=4) or chow (n=2), mice were subjected to a ligation of the left ureter as described above. Tissues were harvested 2 weeks thereafter. Diets in each experimental setting were continued until harvesting.

2.1.8 LPS-induced acute kidney injury.

To study whether *nor*UDCA could ameliorate kidney injury in a model of using lipopolysaccharide (LPS), chow- and *nor*UDCA-fed mice were injected LPS (5µg/kg BW) or vehicle (NaCl 0.9%) in their peritoneum (4 groups; chow/vehicle, chow/LPS, *nor*UDCA/vehicle, *nor*UDCA/LPS; 5 mice per group). Similar to the upper described I/R and UUL experiments, diets (0.5% *nor*UDCA or chow) were started 5 days prior to intraperitoneal LPS/vehicle injection and continued until harvesting. The mice were sacrificed 12 h after LPS challenge. Urine, blood and kidney tissues were collected for determination of urinary NGAL levels, serum urea levels, mRNA levels (macrophage marker F4/80; vascular cell adhesion molecule-1, Vcam-1; monocyte chemo attractant

protein-1, Mcp-1; lipocalin 2, Lcn2 (i.e. NGAL); Kim-1, and immunohistochemistry (Vcam-1).

2.2 Serum Biochemical Analysis.

Throughout all experimental settings, blood was taken at time of harvesting by decapitation and centrifuged (4500 rpm) at room temperature for 20 minutes. All serum samples were then stored at -80°C. Analyses for alanine aminotransferase (ALT), alkaline phosphatase (AP), total serum bile acids, and urea were performed using a Cobas 501® analyser (Roche Diagnostics, Mannheim, Germany).

2.3 Urine Sampling.

Some experimental groups were kept in metabolic cages for collection of urine prior to harvesting (for 6 to a maximum of 12 hours). *Nor*UDCA-fed mice were housed in metabolic cages one day prior to CBDL, 3 days following CBDL and one day before harvesting. Urinary output was determined 5 days after diets were started (one day prior to CBDL) and 3 days following CBDL (pooled urine samples of 4 vs. 4 mice; 2 mice per metabolic cage).

2.4 Cytologic urinalysis

Urine cytology was used to screen for tubular epithelial injury. At time of harvesting urine was sampled via bladder puncture. At least 1.5 ml of urine was necessary for automatic flow cytometry (Sysmex UF 1000®) and subsequent Papanicolao staining of urine sediments. Urine samples were analyzed for presence and number of renal tubular epithelial cells (RTEC) and granular casts (GC).

2.5 Histology.

For histomorphological analysis using conventional light microscopy, tissues were first fixed for 24h using a 3.7% neutral buffered formaldehyde solution, embedded in paraffin, then 2 µm thick sections were cut and stained with Haematoxylin and Eosin (H&E), periodic acid–Schiff (PAS), Sirius Red (SR), and acid fuchsine–Orange G (SFOG).

2.6 Immunohistochemistry

Immunohistochemistry was performed either on acetone-fixed (-20°C for 10 min) cryosections (1.5µm thick) (for Vcam-1) or on microwave-treated (EDTA Sodium buffer pH 8.0) or 0.1% Protease XXIV-treated paraffin sections (2µm thick) [for the macrophage marker F4/80, the collecting duct marker aquaporine 2, AQP2 and the Na+-K+-2Cl-cotransporter, NKCC2 (SLC12A1), located at the apical membrane of epithelial cells of the thick ascending limb of Henle] of kidney tissue. Antibodies used were the purified rat anti-mouse CD106 (Vcam-1) antibody (dilution 1:100; BD Pharmingen^{TM}, 550547), rat anti mouse F4/80 (dilution 1:50; AbD Serotec, MCA497GA), rabbit anti-AQP2 (dilution 1:1000; Abcam plc, ab85876) and rabbit anti-SLC12A1 antibody (dilution 1:100, Sigma, AV41388). For detection of primary antibodies the appropriate secondary antibodies were used and binding was visualized using β-amino-9-ethyl-carbazole (Dako AEC + High Sensitivity Substrate Chromogen Ready-to-Use, Dako Denmark A/S, Glostrup, Denmark, K3461).

2.7 Immunofluorescence

For immunofluorescence microscopy including double labeling for the basement membrane protein laminin and the collecting duct transporter AQP2, formaldehyde-methanol-acetone-fixed cryosections of kidney tissue were used (3µm thick). For apoptosis marker active caspase 3 and the proliferation marker Ki67 paraffinized kidney sections were used. Antibodies used were rabbit anti-laminin (dilution 1:200; Abcam plc, ab11575), rabbit anti-AQP2 (dilution, 1:500; Abcam plc, ab85876) or goat anti-AQP2 (dilution

1:500; Abcam plc, ab105171), rabbit anti-active caspase-3 (dilution 1:100; R&D Systems, AF835) and rabbit anti-Ki-67 (dilution 1:100, Thermo Scientific, RM-9106-S0). For detection of primary antibodies the appropriate secondary fluorophore-conjugated secondary antibodies were used and for visualization of the cell nucleus slides where counterstained with DAPI (labeling DNA).

2.8 Fluorescence Microscopy for Fluorescent Ursodeoxycholic Acid.

Fluorescent-labeled ursodeoxycholic acid (ursodeoxycholyl(UDC)-[Nε-4-nitrobenzo-2-oxa-1,3diazol (NBD)]-lysine, MW 684; provided by Prof. Dr. Alan Hofmann, University of California, San Diego, La Jolla, CA). For this experiment, 3d CBDL mice and SOP controls were injected 100 µmol UDC-Nε-NBD-lysine continuously over 10 minutes into their portal veins [100]. Then, the kidneys of those mice were immediately frozen in liquid nitrogen and cryosections of 3µm thick unfixed kidney tissue immediately screened under a fluorescence microscope.

2.9 Quantification of kidney fibrosis.

Kidney fibrosis was indirectly quantified and compared between the different experimental settings by measurement of renal hydroxyproline, an amino acid present in collagen. Hydroxyproline levels were measured by a calorimetric method from homogenized frozen kidney tissue as described in detail in Fickert P, Krones E et al, Hepatology. 2013;58(6):2056-69 [100].

2.10 Preparation of kidney protein and Western blotting (WB) for vascular cell adhesion molecule-1 (Vcam-1).

Kidney protein was isolated by sonicating kidney tissue in a homogenization buffer (0.25 mol/L sucrose, 10 mmol/L HEPES, pH 7.5, and 1 mmol/L EDTA, pH 8.0) containing protease inhibitors (Thermo Fisher, Halt™ Protease Inhibitor Cocktail, EDTA-free, 10X).

Equal amounts of protein (measured by Pierce™ BCA Protein Assay Kit, Thermo Fisher Scientific, Rockford, USA) were separated on sodium dodecyl sulphate polyacrylamide gel (SDS page), transferred to a nitrocellulose membrane (Biorad Nitrocellulose Membrane), and blotted with specific antibodies against Vcam-1 and beta-actin (mouse Vcam-1/CD106 antibody; dilution, 1:1500, R&D Systems, AF643; Monoclonal Anti-Actin; dilution 1:10000, Sigma-Aldrich, A4700). Antibody binding was detected using peroxidase-conjugated respective immunoglobulins (Dako) and peroxidase activity was visualized using the enhanced chemiluminescence method (ECL) Western blotting detection system.

2.11 Determination of urinary neutrophil-gelatinase associated lipocalin (uNGAL).

NGAL is an iron-transporting protein with increased renal excretion in nephrotoxic or ischemic kidney injury [179]. To detect tubular epithelial injury and to monitor the therapeutic effects of *nor*UDCA, urinary NGAL was measured in urine samples collected at time of harvesting using a commercially available ELISA kit (Lipocalin-2/NGAL DuoSet Mouse, R&D Systems, DY1857) or Western blot using a commercially available antibody. For ELISA, samples were incubated with a detection antibody, labelled with streptavidin-HRP and subsequently measured at 450 nm wavelengths. For Western blot the amount of urine used was normalized to urinary excreted creatinine. Urine samples were centrifuged at 13 000 rpm and 4°C for 5 minutes and pellet proteins were separated on SDS page.

2.12 Bile acid profiling by ultra-performance liquid chromatography-tandem mass spectrometry (UPLC-MS/MS).

The experiments on bile acids profiling were performed in close collaboration with Prof. Hanns Ulrich Marschall (Wallenberg Laboratory, Department of Molecular and Clinical Medicine and Sahlgrenska Center for Cardiovascular and Metabolic Research, University of Gothenburg, 413 45 Gothenburg, Sweden). Profiles of liver, kidney, serum and urine bile acids on an Applied Biosystems AB SCIEX QTRAP 5500 platform as published [180]. Unconjugated and taurine (T) or glucuronic acid (GlcA) conjugated di-, tri-, tetra-

and pentahydroxylated *nor*UDCA metabolites (C23 bile acids) were identified from their molecular anions and quantified in relation to D4-labelled C24-bile acids.

2.13 Determination of renal messenger RNA using quantitative real-time reverse-transcription polymerase chain reaction analysis.

RNA was extracted and reversely transcribed into cDNA. PCR reaction (20 µL) contained 12.5 ng cDNA, 330 nM of each primer and 10.5 µl of SYBR Green Master mix (Applied Biosystems, Carlsbad, USA). The expression levels of all transcripts were normalized to the housekeeping gene 36b4. All primers used are summarized in Table 6.

Gene	Forward Primer	Reverse Primer	Access No.
36b4	gcttcattgtgggagcagaca	catggtgttcttgcccatcag	NM_007475
Colα1(I)	caatgcaatgaagaactggactgt	tcctacatcttctgagtttggtga	NM_007742
F4/80	ttggccaagattctcttcct	tcactgcctccactagcatc	NM_010130
Tgf-β1	tgacgtcactggagttgtacgg	ggttcatgtcatggatggtgc	NM_011577
Vcam-1	taattgctatgaggatggaagactc	ggagatgtcaacaataaatggtttc	NM_011693
Mcp-1	ggctggagagctacaagagg	atgtctggacccattccttc	NM_011333
Lcn2	ccagttcgccatggtatttttc	cacactcaccacccattcagtt	NM_008491
Kim-1	tgtcgagtggagattcctggatggt	ggtcttcctgtagctgtgggcc	NM_001166632

Table 6. Primers used for analysis of mRNA expression.

2.14 Statistical analysis for animal experiments.

Data are reported as arithmetic means ± standard deviation of 4 to 10 animals in each group. Statistical analysis using IBM SPSS statistics 23 included either Student's *t*-test (in case of normal distribution of data) or analysis of variance with Bonferroni post testing when three or more groups were compared. A p value ≤0.05 was considered as significant.

2.15 Retrospective analysis of human cases of cholemic nephropathy.

To substantiate the herein presented concept from animal experiments with human evidence, the archives of the Diagnostic and Research Institute of Pathology of the Medical University of Graz were screened for patients with cholestatic liver disease and cholemic

nephropathy in whom both tissues were available for examination. This was performed in collaboration with Univ.-Doz. Univ. FA Dr. med. Cord Langner from the Diagnostic and Research Institute of Pathology of the Medical University of Graz.

2.16 *In vitro* experiments.

Madin-Darby canine kidney (MDCK) cells, originating from the collecting duct [181], were cultured in Eagle's Minimum Essential Medium, supplied with 10% fetal bovine serum (FBS) and 1% penicillin/streptomycin at 37°C and incubated with taurocholic acid (TCA), cholic acid (CA), chenodeoxycholic acid (CDCA), glycochenodeoxycholic acid (GCDA), (Sigma-Aldrich, Co., St.Louis, USA), and *nor*UDCA (Falk Foundation, Freiburg, Germany) at increasing concentrations (10/50/100 µM for CDCA and GCDCA and 100/500/1000 µM for TCA, CA and *nor*UDCA) for at least 1 hour. After 30 minutes cell morphology was compared. Viability was determined using the water soluble tetrazolium salt (WST-1) assay (CHEMICON International, Inc.).

3 RESULTS

3.1 Modeling cholemic nephropathy in a mouse model of cholestasis – results from animal experiments, tissue, serum and urine analyses

3.1.1 Long-term CBDL as a model for cholemic nephropathy in mice

Obstructive cholestasis and biliary fibrosis was modeled by CBDL for up to 8 weeks (8w). This intervention led to significant cholestasis with elevated AP and bile acids and hepatocellular injury with elevated ALT levels (Table 7) [100]. Upon liver histology, the livers of CBDL mice showed extensive biliary fibrosis. At time of harvesting, the common bile duct of 8w CBDL mice was massively dilated (Fig. 1A). Also, loss of abdominal and epididymal fat was observed but there were no signs of biliary leakage or peritonitis (Fig. 1A) [100]. The kidneys appeared shrunken with an irregular greenish colored surface (Fig. 1B) closely resembling the characteristically described human cholemic nephropathy phenotype [113]. Compared to SOP controls, CBDL mice showed a significantly reduced kidney size and weight (Fig. 1C) although kidney to body weight ratio was almost similar in both groups [100]. The macroscopic findings in 8w CBDL mice were accompanied by increased levels of urea (Fig. 1C, Table 7) and an increased urine volume (5.2 ± 2.0 v.s. 1.3 ± 0.7ml/24h in controls, P .009) [100]. Upon H&E-stained kidney sections of 8w CBDL mice impressively dilated tubules, signs of tubulointerstitial nephritis and kidney fibrosis was found (Fig. 1E, Table 7) [100]. Urine cytology of CBDL mice showed tubular cell cylinders and urinary casts suggestive of tubular epithelial injury (Fig. 1F). The urine of 8w SOP controls was unremarkable (free of cells and cell debris) [100].

	Control	3d CBDL	7d CBDL	3w CBDL	6w CBDL	8w CBDL
ALT (U/L)	69 ± 11	440 ± 246 *	399 ± 85 *	521 ± 30 *	377 ± 497	322 ± 88 *
AP (U/L)	75 ± 12	1274 ± 284 *	1360 ± 761 *	2511 ± 490 *	1096 ± 674	1424 ± 575 *
Bile acids (µmol/l)	10 ± 5	948 ± 493 *	202 ± 132 *	862 ± 9 *	281 ± 182	1499 ± 827 *
Urea (mg/dL)	55 ± 4	NA	NA	NA	NA	98 ± 37
Tubular epithelial lesions	-	+	++	+++	+++	+++
Renal fibrosis	-	-	-	+	++	+++

Table 7. Serum biochemistry and renal phenotypes at different time points following CBDL.

Values shown in the table are expressed as mean ± standard deviation. * $P < 0.05$ compared to 8w SOP (Control) as a representative control group for SOP. ALT, alanine aminotransferase; AP, alkaline phosphatase; NA, not available. Table adapted from Fickert P, Krones E et al, Hepatology. 2013;58(6):2056-69 [100] with permission of Wiley. Table drafted by Elisabeth Tatscher.

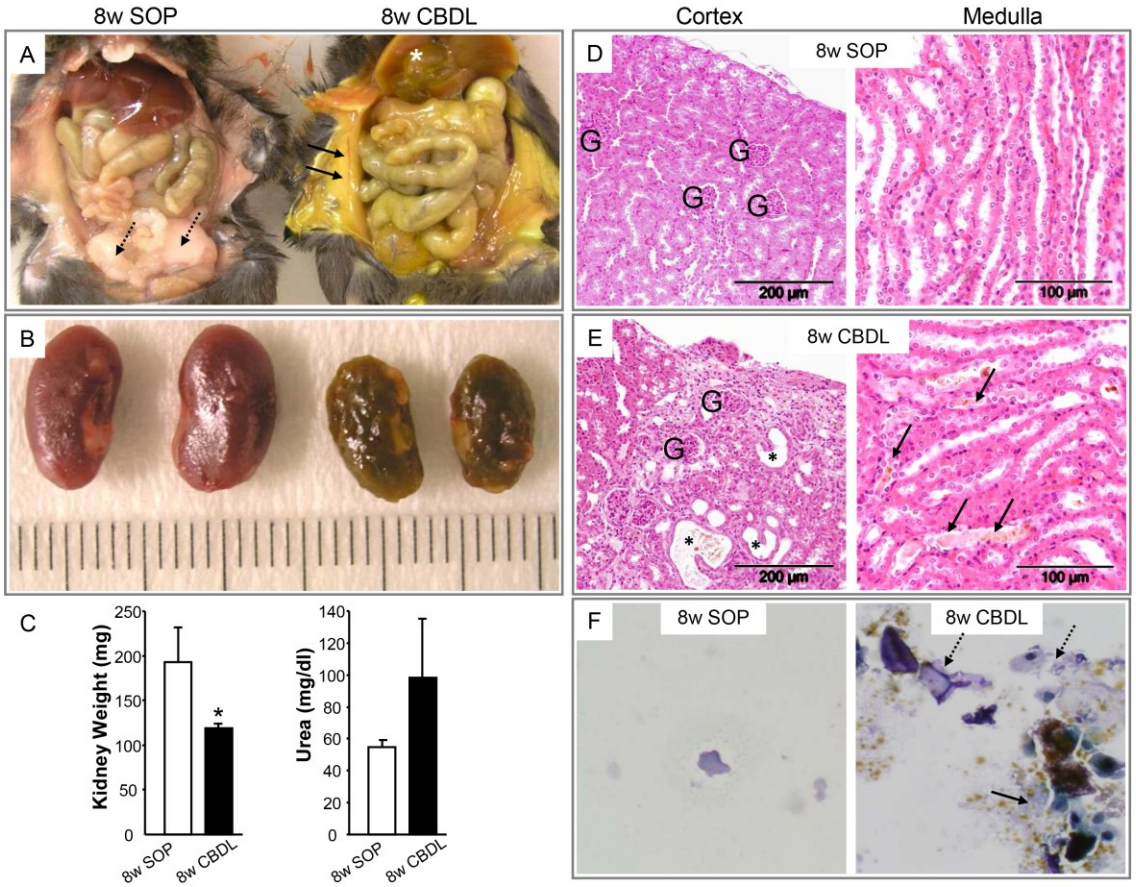

Figure 1: Long-term CBDL mice develop cholemic nephropathy.
(A) Comparison of a SOP control mouse (8w SOP, left) and a 8w CBDL mouse (8w CBDL, right. The 8w CBDL mouse shows a dilated common bile duct (*white asterisk*) and loss of epididymal fat (compared to normal fat indicated by *dashed black arrows* in the SOP control mouse). No signs of peritonitis (*black arrows*). (B) Comparison of kidney macroscopy of a SOP control mouse (*left pair of kidneys*) and an 8w CBDL mouse (*right pair of kidneys*). (C) Significantly reduced kidney weight and increased serum urea levels in 8w CBDL mice (*black bars*) compared to SOP controls (*open bars*) (n=8 in each group; ± SD). * $P < 0.05$ vs. control. (D,E) Dilated tubules (*indicated by black asterisks*) and intraluminal casts (*indicated by black arrows*) as well as signs of tubulointerstitial nephritis and kidney fibrosis upon H&E-stained kidney sections of 8w CBDL mice. G, glomeruli. (F) Tubular cell cylinders (*black arrows*) and cells of the urothelium (*dashed arrows*) upon Papanicolaou staining of urine cytology of a 8w CBDL mouse versus normal urine sediment in a 8w SOP mouse. Figure reproduced from Fickert P, Krones E et al, Hepatology. 2013;58(6):2056-69 [100] with permission of Wiley. Figure drafted by Elisabeth Tatscher.

Unlike the CBDL mouse model, neither macroscopic nor histologic renal alterations were observed in DDC-fed and Mdr2$^{-/-}$ mice (data not shown). Thus, exclusively (long-term) CBDL (with the highest serum bile acid levels) led to pronounced tubulointerstitial renal fibrosis with substantially impaired renal function [100].

3.1.2 Progression of tubular epithelial injury from short-term to long-term CBDL.

Long-term CBDL was the only mouse model leading to the typical cholemic nephropathy phenotype including renal failure and significant renal fibrosis. Thus, further experiments focused on detailed time course studies in this model. The earliest time point CBDL mice were screened for the presence of a renal phenotype was 3d after CBDL. Already at that early time point, tubular epithelial injury with small foci of coagulation necrosis and intratubular cast formation could be observed at the border region between the outer and the inner strip of the medulla (Fig. 2B). These early changes were, however, only detectable on PAS-stained but not on H&E stained kidney sections (Fig. 2B) [100]. As a next step time course studies were performed: After 7 days of CBDL, a higher number of dilated tubules and intraluminal casts (consisting of protein and cell debris) were predominantly observed in distal nephron segments (distal tubules and collecting ducts) (Fig. 2C) [100]. After longer durations of CBDL (3 and 6 weeks, 3w and 6w) the kidneys showed progressive tubular epithelial injury with partial occlusion and subsequent dilatation of distal nephron segments with the full-blown macroscopic phenotype observed after 8 weeks (Fig. 1D-E) [100]. Interestingly also atrophic glomeruli with a dilated Bowman`s space were found at that late time points [100].

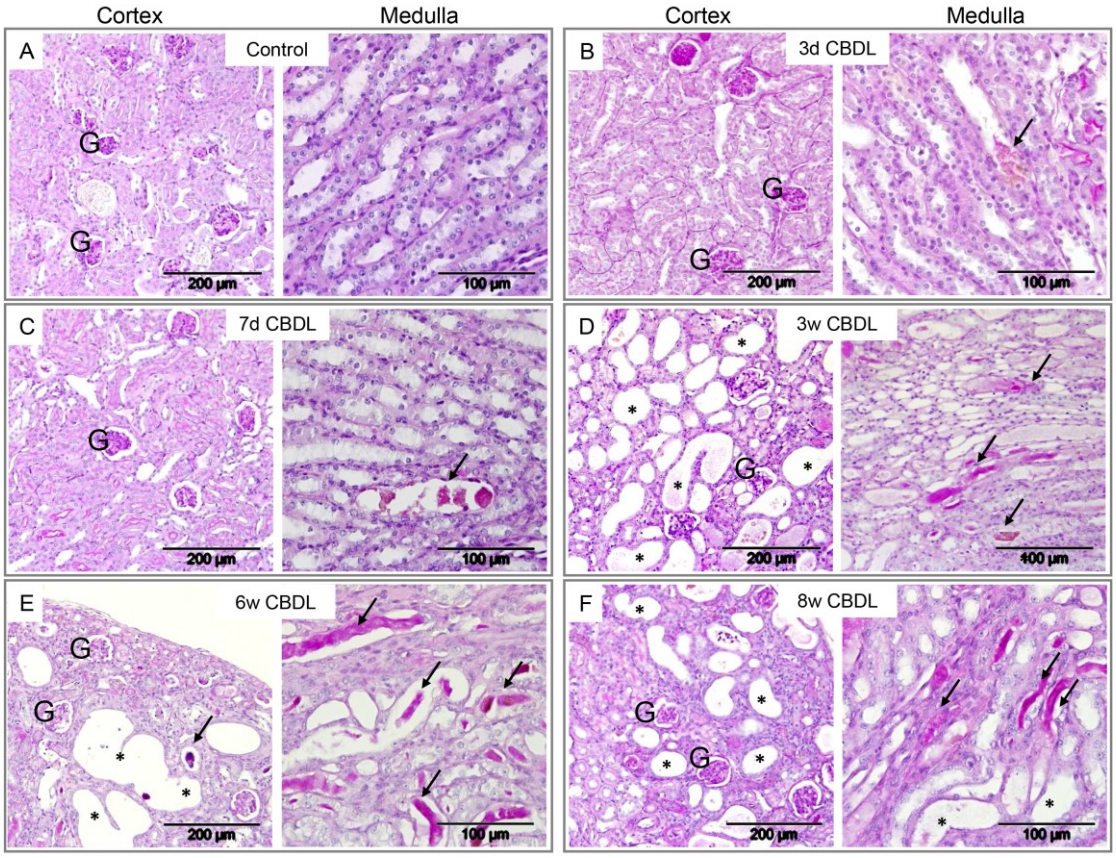

Figure 2. Progressive tubular epithelial kidney injury in CBDL mice.
(A-F) PAS stained kidney sections of CBDL mice show PAS-positive casts (*black arrows)* at the levels of distal nephron segments (distal tubules and collecting ducts) and progressive tubular dilatation (*black asterisks*) after 3w, 6w and 8w of CBDL. G, glomeruli. Figure reproduced from Fickert P, Krones E et al, Hepatology. 2013;58(6):2056-69 [100] with permission of Wiley. Figure drafted by Elisabeth Tatscher.

The fact, that the most initially detected structural alterations after 3d CBDL seemed to be directed towards distal nephron segments (especially collecting ducts) was supported by immunohistochemial and immunofluorescence staining for AQP2, a transporter which is specifically expressed in the apical plasma membrane of collecting duct epithelial cells [182, 183]. Immunohistochemistry and immunofluorescence showed partial lack of AQP2 positivity with parallel loss of nuclear staining indicative of necrotic collecting duct cells (Fig. 3 A,C,D) [100]. Serial sections of PAS stained kidney sections showed tubular epithelial barrier discontinuity corresponding to the collecting duct epithelium upon immunohistochemistry for AQP2 (Fig. 3 D-F). The epithelium of the thick ascending limb of Henle, which were identified by immunohistochemistry for NKCC2, appeared normal without evidence of cell injury (Fig 4) [100].

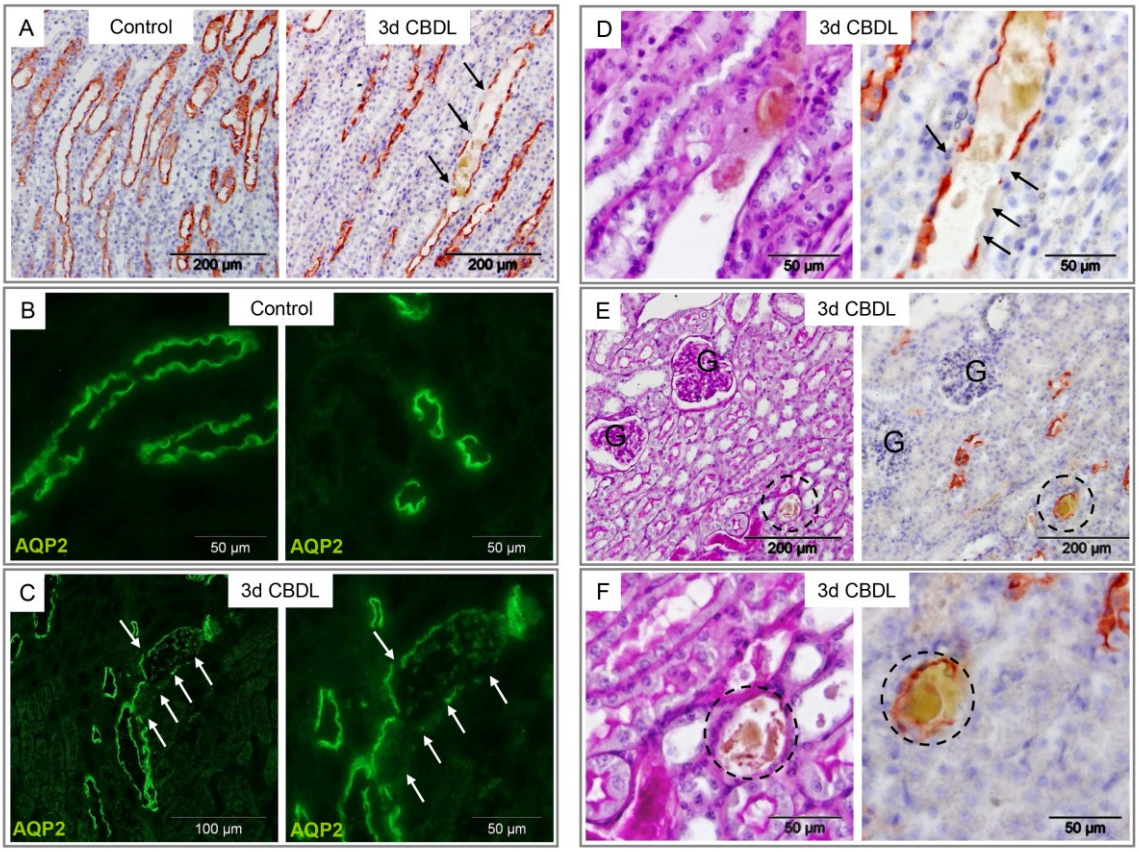

Figure 3. Epithelial barrier discontinuity in collecting ducts of CBDL mice.
(A) AQP2 immunohistochemistry in SOP controls (Control) demonstrates normal, continuous AQP2 expression along the collecting duct epithelium. In contrast, a representative collecting duct of a 3d CBDL mouse (3d CBDL) shows loss of epithelial cell continuity (*indicated by black arrows*) and intraluminal greenish casts. (B) Immunofluorescence for AQP2 shows regular AQP2 staining in a SOP control mouse (Control). In contrast, representative collecting ducts of a 3d CBDL mouse (3d CBDL) again show epithelial cell discontinuity (*indicated by white arrows*). (D-F) Serial sections of PAS stainings and immunohistochemistry for AQP2 demonstrate co-localization of tubular epithelial cell injury (*indicated by black arrows*), cast formation (*dashed circles*) and AQP2 positivity (representing collecting duct epithelial cells). G, glomeruli. Figure reproduced from Fickert P, Krones E et al, Hepatology. 2013;58(6):2056-69 [100] with permission of Wiley. Figure drafted by Elisabeth Tatscher.

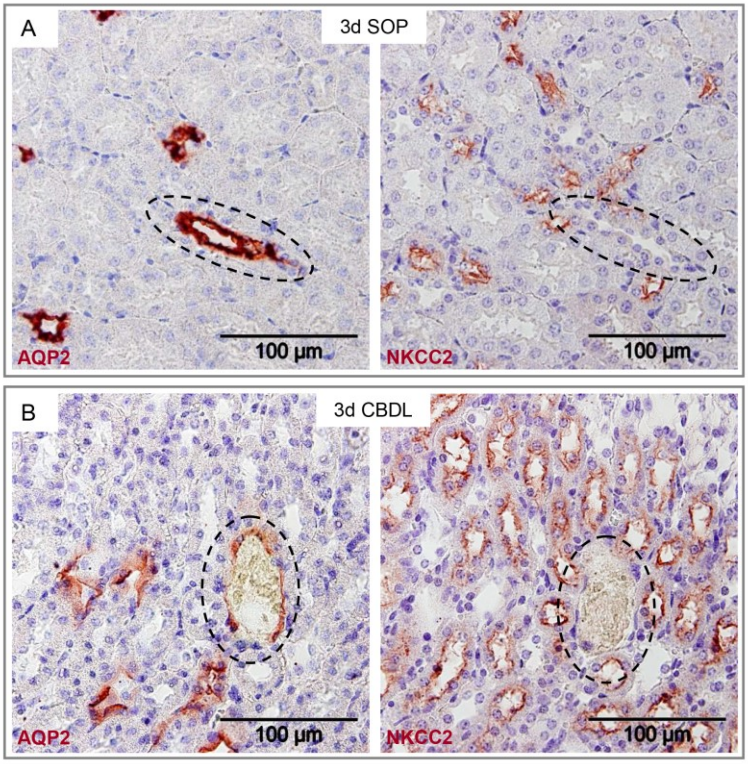

Figure 4. Altered AQP2 expression on collecting ducts but regular NKCC2 expression of the thick ascending limb of Henle in CBDL.
(A,B) Serial sections with immunohistochemistry for AQP2, a collecting duct marker (left image), and NKCC2, staining cells of the thick ascending limb of the Henle's loop (right image), shows (A) normal expression of AQP 2 on collecting duct epithelial cells and normal expression of NKCC2 in cells of the thick ascending limb of the Henle's loop in a 3d SOP control mouse. The *dashed ellipses* indicate the identical collecting duct in both sections. (B) In contrast, AQP2 expression was altered (*dashed ellipse*) in a 3d CBDL mouse (3d CBDL), whereas the surrounding parts of the NKCC2-positive thick ascending limbs of the Henle's loop appear normal. Figure reproduced from Fickert P, Krones E et al, Hepatology. 2013;58(6):2056-69 [100] with permission of Wiley. Figure drafted by Elisabeth Tatscher.

The findings presented in Fig. 3 and 4 indicate loss of collecting duct epithelial barrier continuity in 3d CBDL mice [100]. The next step was thus to search for defective basement membrane by immunofluorescent double labelling with anti-laminin (being a defining component of basement membranes) and anti-AQP2 antibodies (staining collecting ducts) [100]. Compared to SOP controls, showing continuous basement membranes (Fig. 5A), 3d CBDL mice showed basement membrane discontinuity and exfoliated epithelial cells coalescing to intraluminal cell casts (Fig. 5B) [100].

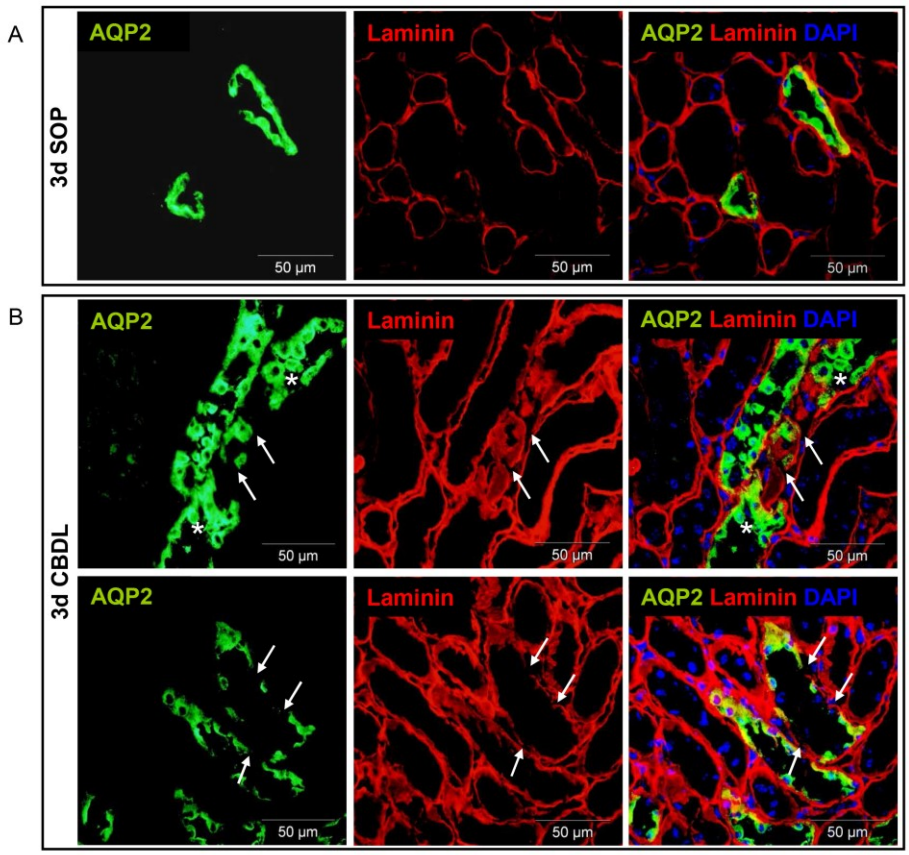

Figure 5. Loss of collecting duct basement membrane continuity in CBDL mice. Immunofluorescence labelling for AQP2 (*green*), laminin (*red*) and DAPI (*staining DNA*) in kidneys of a SOP control (A) and a 3d CBDL mouse (B). Normal continuous basement membranes of the collecting duct epithelium in a representative SOP control mouse (A), versus collecting ducts in a 3d CBDL mouse showing alterations of epithelial cell integrity and basement membrane discontinuity (*white arrows*). Intraluminal casts consist of exfoliated epithelial cells (*white asterisk*). Figure reproduced from Fickert P, Krones E et al, Hepatology. 2013;58(6):2056-69 [100] with permission of Wiley. Figure drafted by Elisabeth Tatscher.

The next step was to demonstrate the functional relevance of these findings. This was achieved by portal vein injection of renally excreted UDC-(Nε-NBD)-lysine in CBDL mice. In contrast, SOP control kidneys, that stained almost negative after portal vein injection of UDC-(Nε-NBD)-lysine (not shown), CBDL mice showed leakage of this fluorescent marker from collecting duct lumina (Fig. 6) [100]. In line with that and reflecting the principle of bile acid leakage in a well-established experimental condition, hepatic bile infarcts (as a well-known result of obstructive cholestasis) of the same CBDL mouse also stained positive for fluorescent UDC-NBD-lysine (Fig. 7) [100].

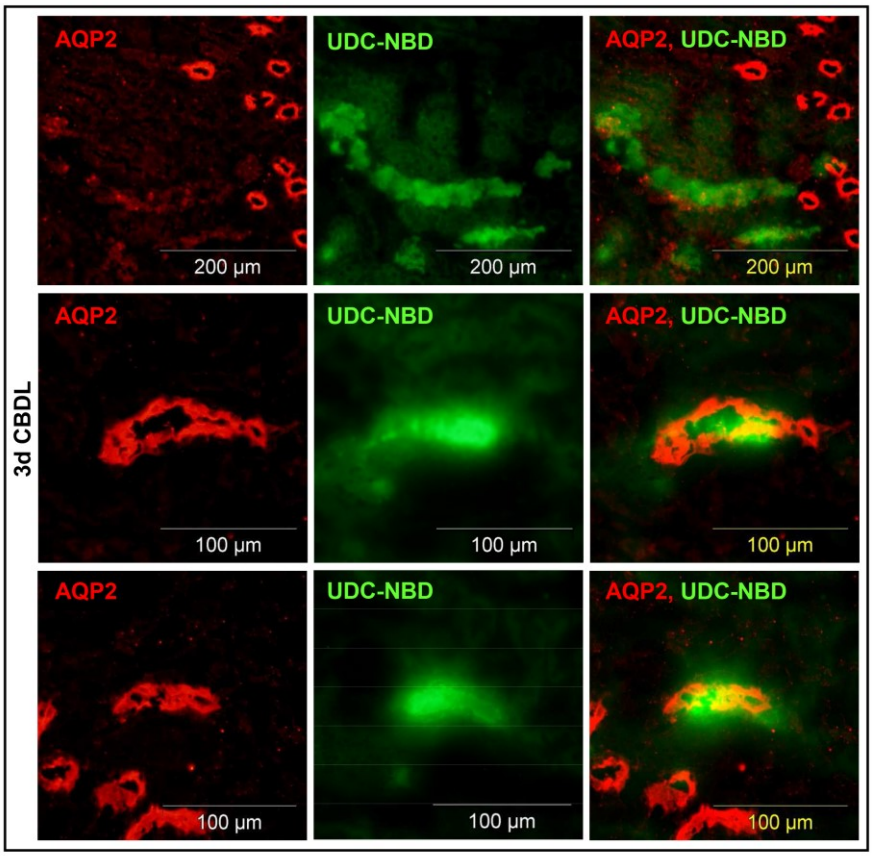

Figure 6. Leaky collecting ducts demonstrated by portal vein injection of UDC-(Nε-NBD)-lysine in CBDL mice.
Serial sections of a 3d CBDL mouse kidney showing collecting ducts staining positive for AQP2 (*red*) and fluorescent UDC-(Nε-NBD)-lysine (*green*) (UDC-NBD). Upper panel of images: Longitudinal section of a collecting duct with diminished AQP2 positivity (suggestive of collecting duct epithelial cell injury) and leakage of UDC-(Nε-NBD)-lysine. The lower panel of images shows higher magnifications of the same section with leakage of intraluminal enriched UDC-(Nε-NBD)-lysine from AQP2 positive collecting ducts. Figure reproduced from Fickert P, Krones E et al, Hepatology. 2013;58(6):2056-69 [100] with permission of Wiley. Figure drafted by Elisabeth Tatscher.

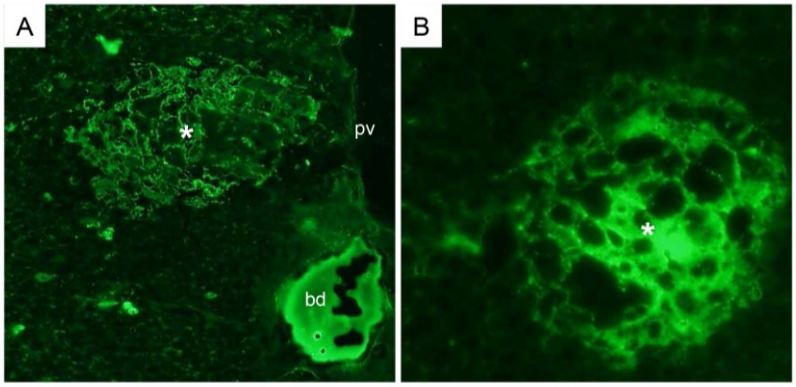

Figure 7. Bile ducts and bile infarcts in livers of CBDL mice stain positive for portal vein injected UDC-(Nε-NBD)-lysine.
(A,B) Injection of UDC-(Nε-NBD)-lysine (green) into the portal vein (pv) of a 3d CBDL mouse results in intense luminal staining of an intrahepatic bile duct (bd) and UDC-(Nε-NBD)-lysine leakage into bile infarcts (*white asterisks*); (B) shows a higher magnification of a bile infarct staining positive for UDC-(Nε-NBD)-lysine. Figure reproduced from Fickert P, Krones E et al, Hepatology. 2013;58(6):2056-69 [100] with permission of Wiley. Figure drafted by Elisabeth Tatscher.

The findings observed upon immunofluorescence studies and the UDC-(Nε-NBD)-lysine experiments demonstrate that the collecting duct epithelium obviously represents the most initial location of injury further leading to the characteristic morphological phenotype of cholemic nephropathy.

3.1.3 CBDL results in interstitial nephritis and kidney fibrosis.

Inflammation, almost always preceding renal fibrosis, involves lymphocytes, dendritic cells, macrophages and monocytes (among others) [184]. Thus, renal Vcam-1 and macrophage/dendritic cell marker F4/80 expression was studied using immunohistochemistry, Western blotting and measurement of mRNA levels. In contrast to SOP controls, that did not show significant alterations, CBDL mice showed pronounced renal Vcam-1 and F4/80 protein expression following different time points after CBDL [100]. In CBDL, induced Vcam-1 expression with an increase over time was primarily observed in tubular epithelial cells (Fig. 8A) [100]. In parallel, a significant increase of Vcam-1 mRNA and protein expression levels was observed (Fig. 8A B,C) [100]. Immunohistochemical expression of the macrophage/dendritic cell marker F4/80 was

primarily found in cells of the renal interstitium in CBDL mice (Fig. 9A) [100]. In parallel, renal overexpression of F4/80 and Mcp-1 mRNA was observed (Figs. 9B,C) [100].

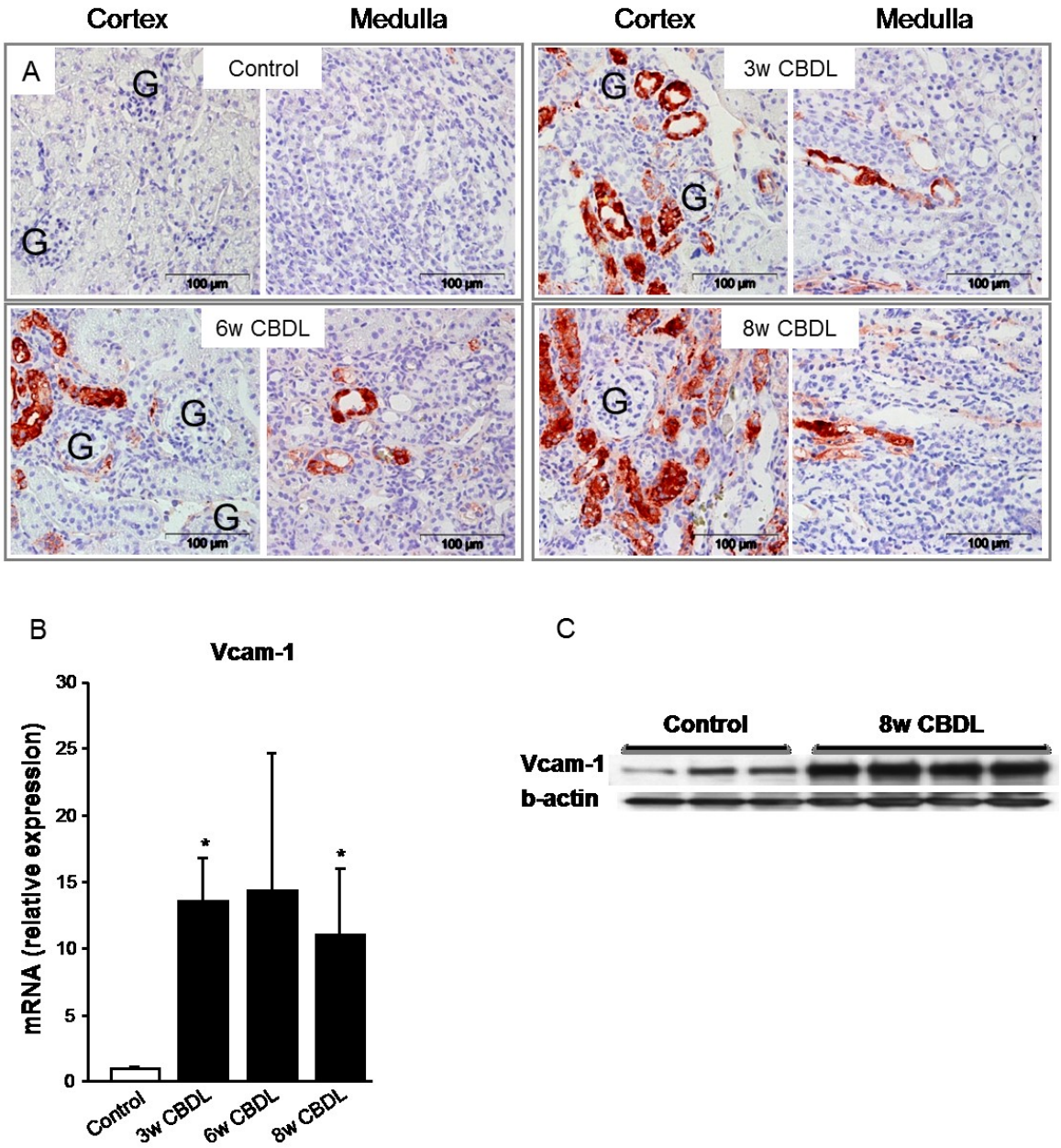

Figure 8. Overexpression of Vcam-1 in kidneys of CBDL mice.
(A) Longitudinal increase of renal Vcam-1 expression in 3w, 6w, and 8w CBDL mice. G, glomeruli. (B) Renal Vcam-1 m-RNA expression levels compared between SOP controls (8w SOP) and 3w, 6w, and 8w CBDL mice; * $P < 0.05$ vs. control. (C) Western blotting shows induced protein expression of Vcam-1 in 8w CBDL mouse kidneys. Figure reproduced from Fickert P, Krones E et al, Hepatology. 2013;58(6):2056-69 [100] with permission of Wiley. Figure drafted by Elisabeth Tatscher.

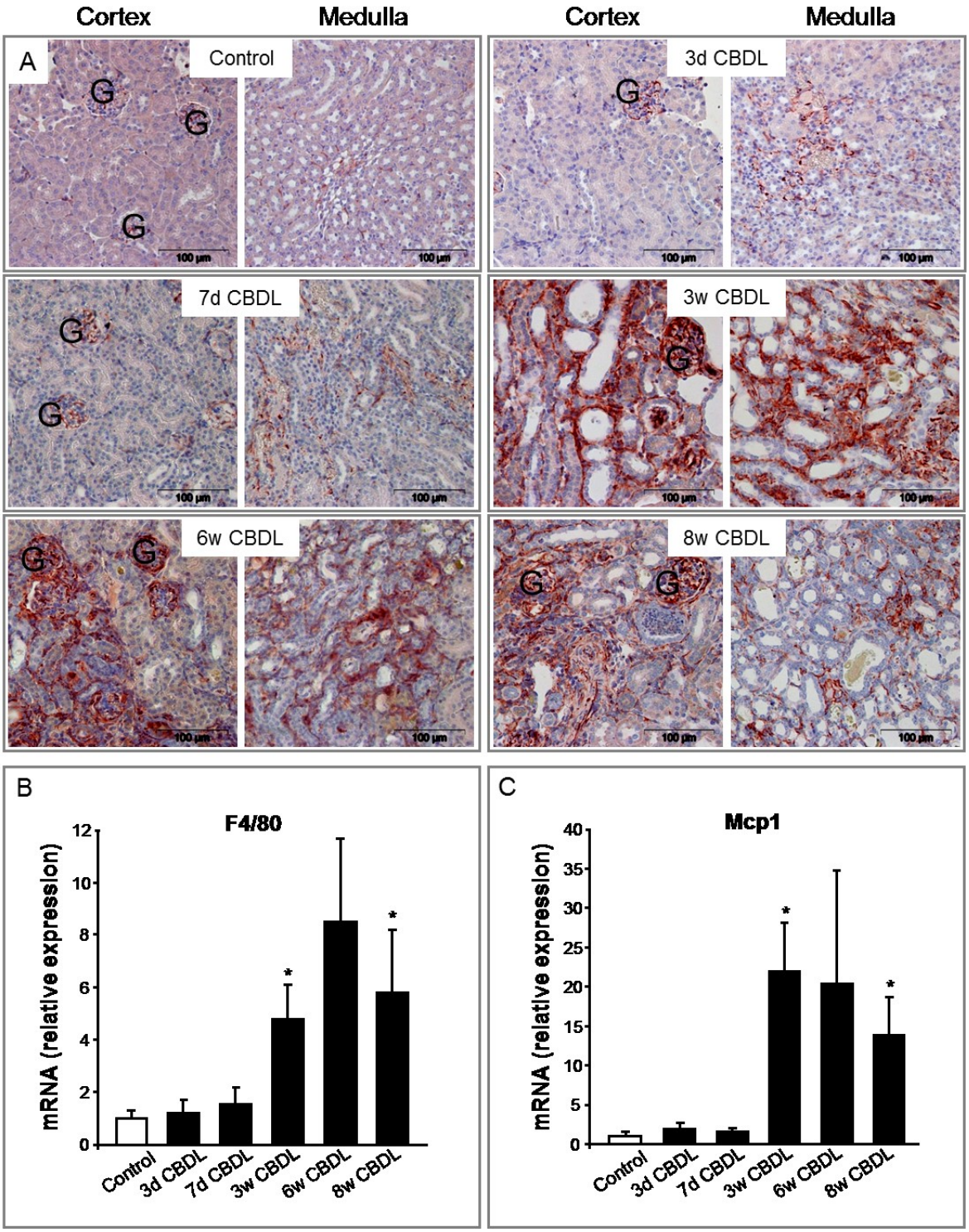

Figure 9. Overexpression of F4/80 and Mcp-1 in kidneys of CBDL mice.
(A) Pronounced expression of F4/80 in kidneys of 3w, 6w and 8w CBDL mice. G, glomeruli. (B,C) Pronounced F4/80 (B) and Mcp-1 (C) mRNA expression in 3w, 6w and 8w CBDL mice. * $P < 0.05$ vs. control. Figure reproduced from Fickert P, Krones E et al, Hepatology. 2013;58(6):2056-69 [100] with permission of Wiley. Figure drafted by Elisabeth Tatscher.

3.1.4 Long-term CBDL results in tubulointerstitial kidney fibrosis.

Sirius red-stained kidney sections at several time points following CBDL were compared to Sirius red-stained kidney sections of SOP control mice in order to study the development of kidney fibrosis in CBDL. Renal fibrosis was additionally quantified by measurement of renal Colα1(I) and Tgf-β1 mRNA expression levels and measurement of renal hydroxyproline levels. Already 3 weeks after CBDL (3w CBDL) significant renal fibrosis was observed, which was even more impressive after 6w and 8w CBDL were the full-blown cholemic nephropathy phenotype was developed (Fig. 10A) [100]. Besides histological evidence for renal fibrosis, mRNA levels of key genes of fibrosis, namely Colα1(I) and Tgf- β1, were induced in CBDL mice (Fig. 10B). Also, renal hydroxyproline levels were significantly elevated in CBDL mouse kidneys (Fig. 10C) [100].

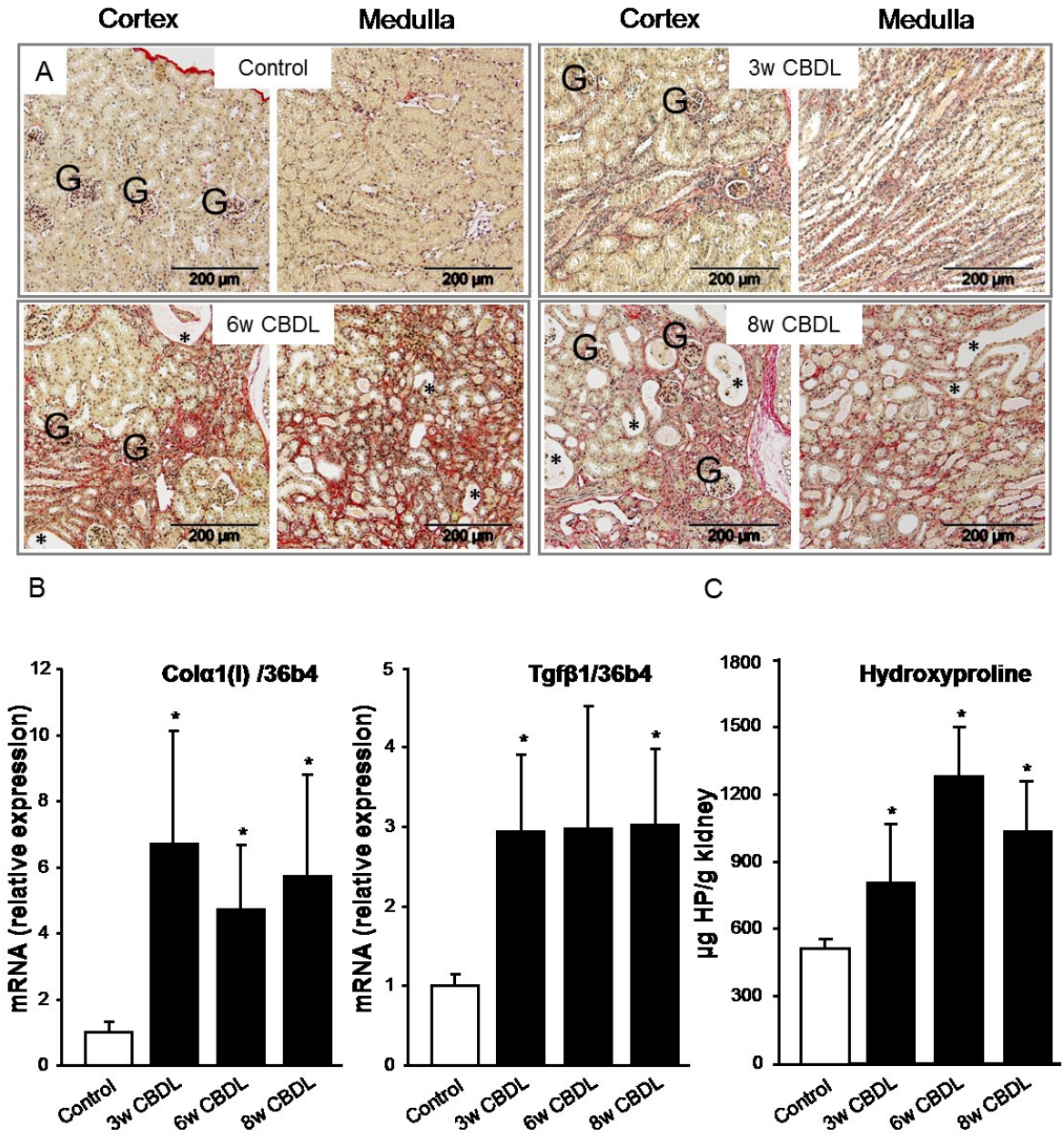

Figure 10. Tubulointerstitial kidney fibrosis in long-term CBDL.
(A) Enhanced Sirius red staining indicative of renal fibrosis can be observed from 3w following CBDL. Kidney fibrosis increases over time and is mostly pronounced after 8w of CBDL. At that time point dilated tubules (*indicated by asterisks*) are surrounded by fibrous septa. G, glomeruli. (B) Regarding mRNA expression levels, significant overexpression of Colα1(I) and Tgfβ1 mRNA levels can be found in kidneys of CBDL mice (*black bars*) compared to controls (8w SOP, *open bars*). * $P < 0.05$ vs. control. (C) Measurement of renal hydroxyproline content shows significantly increased renal hydroxyproline levels in 3w, 6w and 8w CBDL mice (*black bars*) compared to SOP controls (8w SOP, *open bars*). * $P < 0.05$ vs. control. Figure reproduced from Fickert P, Krones E et al, Hepatology. 2013;58(6):2056-69 [100] with permission of Wiley. Figure drafted by Elisabeth Tatscher.

3.2 Amelioration of the renal phenotype in cholemic nephropathy by modulation of the bile acid pool.

Since the initial renal changes were observed already 3d after CBDL (where serum bile acid levels are very high) at the level of collecting ducts, it's tempting to speculate that this might be due to potentially cytotoxic agents with a presumably very high local concentration (such as bile acids that are alternatively excreted via the kidney in cholestasis) resulting in cellular damage at the level of distal nephron segments [100]. The following experiments aimed to study the renal phenotype in conditions with a modified bile acid pool towards more hydrophilicity and thus less toxicity. This was granted by using (I) a genetically modified mouse model exhibiting a more hydrophilic bile acid pool (i.e. the $FXR^{-/-}$ mouse model) or (II) a mouse model with dietary modulation of the bile acid pool towards more hydrophilicity by feeding *nor*UDCA, the side chain modified derivative of UDCA which was shown to ameliorate the liver phenotype in a mouse model of PSC (i.e. the $Mdr2^{-/-}$ mouse) and to undergo renal elimination [175, 178] making it an attractive therapeutic compound for cholemic nephropathy.

3.2.1 CBDL FXR knockout mice ($FXR^{-/-}$) are protected from developing renal fibrosis.

CBDL $FXR^{-/-}$ mice have been shown to excrete high levels of polyhydroxylated hydrophilic and therefore less toxic bile acids than those eliminated in WT controls [185]. Assuming that potentially toxic bile acids could lead to tubular epithelial injury in the CBDL mouse model, it was tempting to speculate that $FXR^{-/-}$ CBDL mice could be protected from developing cholemic nephropathy. PAS stained kidney sections of 3d CBDL mice, however, showed the characteristic tubular epithelial injury in both genotypes, $FXR^{-/-}$ CBDL mice and $FXR^{+/+}$ CBDL mice (Fig. 11A) [100]. Interestingly, Sirius red stained kidney sections of long-term (8w) CBDL $FXR^{-/-}$ mice showed impressively less kidney fibrosis and this could also be quantified by a significantly lower renal hydroxyproline content in these mice (Fig. 11B) [100]. In line with previously published results [185], $FXR^{-/-}$ mice at later time points following CBDL (8w) showed lower bile acid levels (110 ± 21µmol/l) compared to 20-fold higher serum bile acid levels

in WT mice (2851 ± 1097µmol/l) (Table 8) which could be an explanation for the amelioration of the renal phenotype in this model. To rule out a general resistance of $FXR^{-/-}$ mice towards renal fibrosis development, the degree of renal fibrosis in response to UUL (as a non-cholestatic condition) was compared and no difference in the fibrotic response after UUL in $FXR^{-/-}$ mice compared to WT mice (Fig. 11C) was observed [100]. The findings of 3d CBDL $FXR^{-/-}$ mice showing equal levels of tubular epithelial injury compared to WT ($FXR^{+/+}$) CBDL mice on the one hand and long-term CBDL $FXR^{-/-}$ mice being protected from developing cholemic kidney fibrosis on the other hand might be explained by gradually declining and more hydrophilic bile acids in $FXR^{-/-}$ mice (but not WT mice) [100].

Genotype	Procedure	ALT (U/L)	AP (U/L)	Bile acids (µmol/L)	Tubular epithelial lesions	Renal fibrosis
WT	3d CBDL	440 ± 246	1274 ± 284	948 ± 493	-	-
$FXR^{-/-}$	3d CBDL	1437 ± 1024 *	602 ± 284 *	1879 ± 689 *	+	-
WT	8w SOP	58 ± 9	72 ± 8	48 ± 78	-	-
$FXR^{-/-}$	8w SOP	333 ± 187	77 ± 6	24 ± 17	-	-
WT	8w CBDL	197 ± 15	2072 ± 405	2851 ± 1098	+++	+++
$FXR^{-/-}$	8w CBDL	534 ± 215 *	591 ± 128 *	110 ± 21 *	-	-
WT	2w UUL	60 ± 5	80 ± 11	14 ± 2	+++	+++
$FXR^{-/-}$	2w UUL	134 ± 61	59 ± 10 *	37 ± 8 *	+++	+++

Table 8. Serum biochemistry and blinded scorings of the kidney phenotype under various experimental conditions.
Table reproduced from Fickert P, Krones E et al, Hepatology. 2013;58(6):2056-69 [100] with permission of Wiley. Table drafted by Elisabeth Tatscher. Values are expressed as mean ± standard deviation. * P <.05 compared to respective WT controls (WT). ALT, alanine aminotransferase; AP, alkaline phosphatase; NA, not available; UUL, unilateral ureter ligation; WT, wildtype.

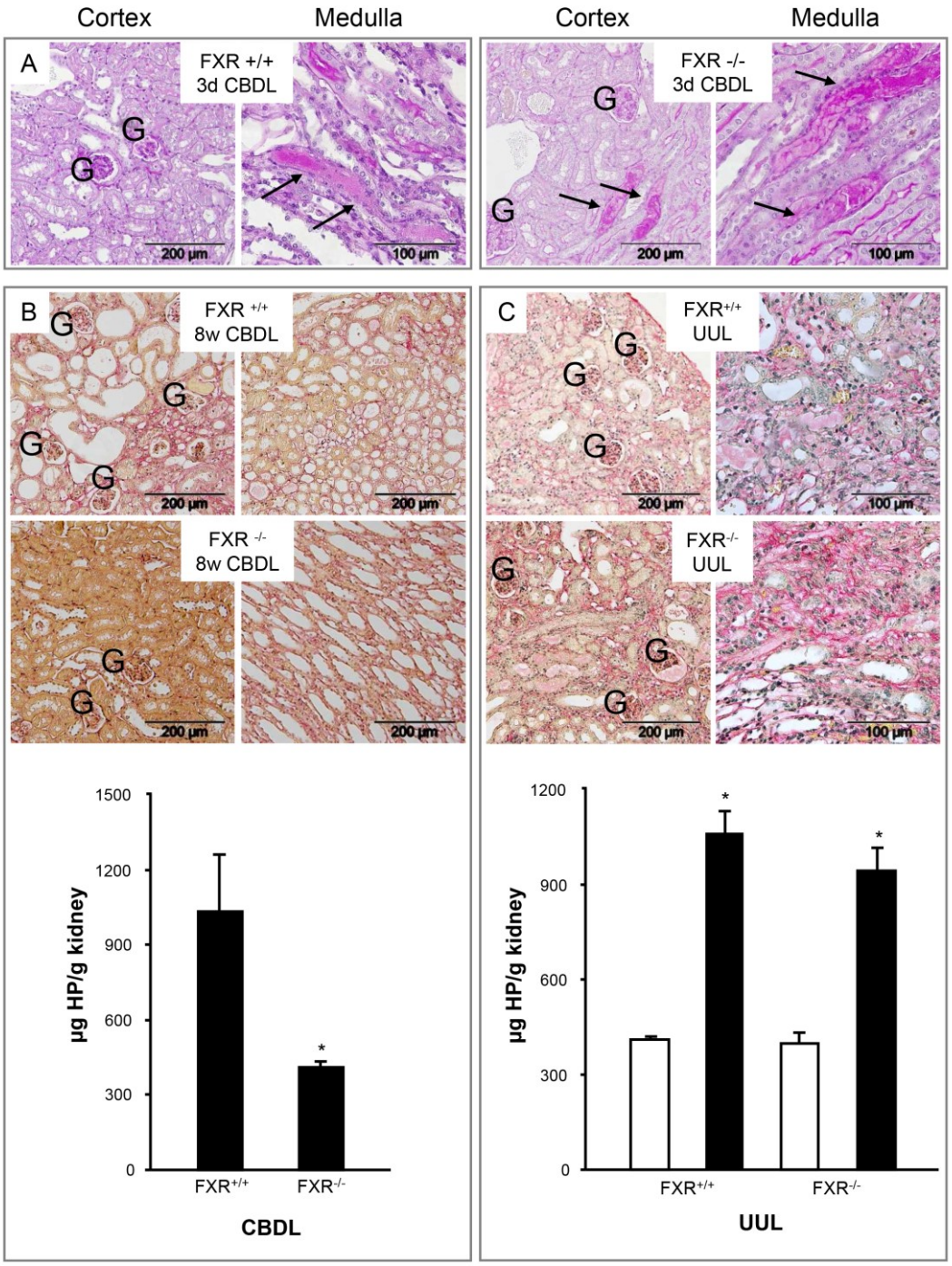

Figure 11. FXR$^{-/-}$ mice are protected from kidney fibrosis development in response to common bile duct ligation (CBDL) but show a similar degree of renal fibrosis in obstructive uropathy (i.e. unilateral ureter ligation, UUL).
(A) Equal degrees of tubular epithelial injury and intratubular cast formation in 3d FXR$^{-/-}$ (FXR$^{-/-}$ CBDL) CBDL and WT CBDL mice (FXR$^{+/+}$ CBDL) (*black arrows*). (B) Impressive amelioration of kidney fibrosis in 8w CBDL FXR$^{-/-}$ mice compared to WT controls (FXR$^{+/+}$ 8w CBDL). G, Glomeruli. Significantly reduced renal hydroxyproline content in 8w FXR $^{-/-}$ CBDL mice compared to WT controls (*left bar graph*). * $P < 0.05$ vs. control. (C) In contrast, no difference between the two genotypes could be observed in response to UUL (*right bar graph, black bars*). * $P < 0.05$ vs. control. Both genotypes also showed a comparable degree of renal fibrosis upon Sirius red stained kidney sections.

Figure reproduced from in Fickert P, Krones E et al, Hepatology. 2013;58(6):2056-69 [100] with permission of Wiley. Figure drafted by Elisabeth Tatscher.

3.2.2 *nor*UDCA ameliorates cholemic nephropathy in CBDL mice.

Since genetic modification of the bile acid pool toward more hydrophilicity in $FXR^{-/-}$ mice protected from full blown cholemic nephropathy, the next step was to test the effect of dietary modification of the bile acid pool. Thus, CBDL mice were prefed *nor*UDCA, a hydrophilic bile acid, that was shown to undergo substantial renal elimination [175], 7 days prior to CBDL in order to test whether this could prevent the development of cholemic nephropathy. Indeed, 3d CBDL mice showed to evidence of tubular epithelial injury or intraluminal casts upon PAS- and AQP2-stained kidney sections (Fig 12) [100].

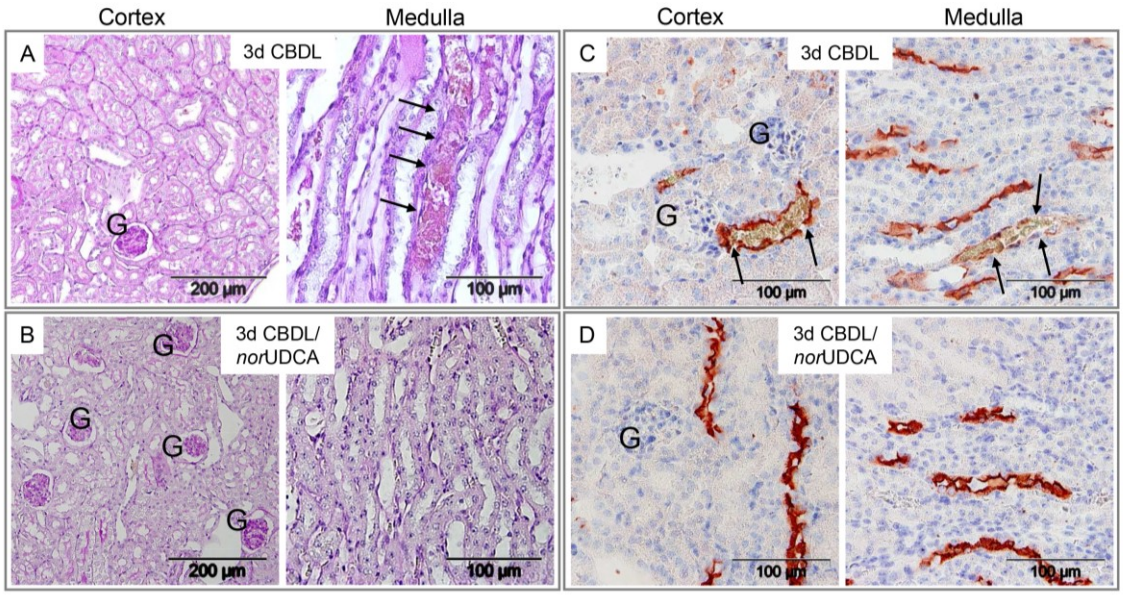

Figure 12. *Nor*UDCA prevents tubular epithelial injury in 3d CBDL mice.
(A,B) In contrast to chow-fed CBDL mice (3d CBDL) (A) PAS stained kidney sections of 3d CBDL mice that were fed a *nor*UDCA-enriched diet prior to CBDL (3d CBDL/*nor*UDCA) (B) show no evidence for collecting duct tubular epithelial injury or intraluminal cast formation (*black arrows*) (C,D) Immunohistochemistry for AQP2 shows discontinuous AQP2 staining (*black arrows*) and intraluminal casts in chow-fed CBDL mice (C) whereas the kidney histology/AQP2 immunohistochemistry of *nor*UDCA-fed 3d CBDL mice appeared normal (D). Figure reproduced from Fickert P, Krones E et al, Hepatology. 2013;58(6):2056-69 [100] with permission of Wiley. Figure drafted by Elisabeth Tatscher.

3.2.3 *Nor*UDCA protects long-term CBDL mice from cholemic nephropathy.

As described in methods section, the effects of dietary hydrophilization of the bile acid pool by feeding *nor*UDCA was not only studied in short-term (3d), but also in long term CBDL using two experimental setups (*norUDCA for Prevention* and *norUDCA for Rescue, see Methods section,* Fig 13A) [186]. In contrast to chow-fed CBDL mice, which developed substantial impairment of renal function with significantly elevated serum urea levels along with the characteristic morphological kidney alternations suggestive of cholemic nephropathy (Figures 1, 2 and 10), both experimental conditions, that were studied in order to unravel the therapeutic effects of *nor*UDCA in cholemic nephropathy (*norUDCA for Prevention* and *norUDCA for Rescue,* Fig.13A*),* led to a significantly ameliorated renal phenotype [186]. In detail and as shown before, long-term CBDL in chow-fed CBDL mice led to the characteristic macroscopic cholemic nephropathy phenotype consisting of shrunken greenish kidneys (Fig. 13B, left pair of kidneys, see also Fig. 1). In contrast, kidneys of *nor*UDCA-fed CBDL mice (*norUDCA for Prevention*, Fig. 13B, right pair of kidneys) showed an almost normal macroscopic appearance [186]. In line with that, urine cytology appeared almost normal (Fig. 13B, lower right panel) in *nor*UDCA-fed CBDL mice (*norUDCA for Prevention*). In contrast, microscopic urinalysis of chow-fed CBDL mice was suggestive of acute tubular injury showing renal tubular epithelial cells and cell cylinders (Fig. 13B, lower left panel, see also Fig. 1) [186].

NGAL is an iron-transporting protein with increased renal excretion in nephrotoxic or ischemic kidney injury. Compared to chow-fed CBDL mice, *nor*UDCA-fed CBDL mice had significantly lower uNGAL levels suggesting a lesser degree of tubular epithelial injury (Fig. 13B) [186]. Urinary NGAL measurement was therefore suggested to represent a suitable test for monitoring the degree of injury and reflecting therapeutic effects in the cholemic nephropathy mouse model.

Also upon histology, *nor*UDCA-fed CBDL kidneys showed significantly less evidence for tubular epithelial injury and kidney fibrosis compared to chow-fed CBDL mice. Compared to chow-fed controls, PAS-stainings of *nor*UDCA-fed CBDL mouse kidneys showed impressively less dilatation of tubules, less intraluminal cast formation and significantly less fibrosis (*norUDCA for Prevention*: Fig. 13C, Table 9; for *norUDCA for Rescue* see Fig. 14, Table 9) [186]. Being suggestive of a lesser degree of kidney injury, also serum urea levels were lower in *nor*UDCA-fed CBDL mice compared to chow-fed

CBDL mice (Fig. 13C) [186]. Also mRNA expression levels lipocalin 2 (Lcn2) and kidney injury molecule-1 (Kim-1) were found to be significantly downregulated in *nor*UDCA-fed CBDL mice (*norUDCA for Prevention* and *norUDCA for Rescue*) (Fig. 13D) [186].

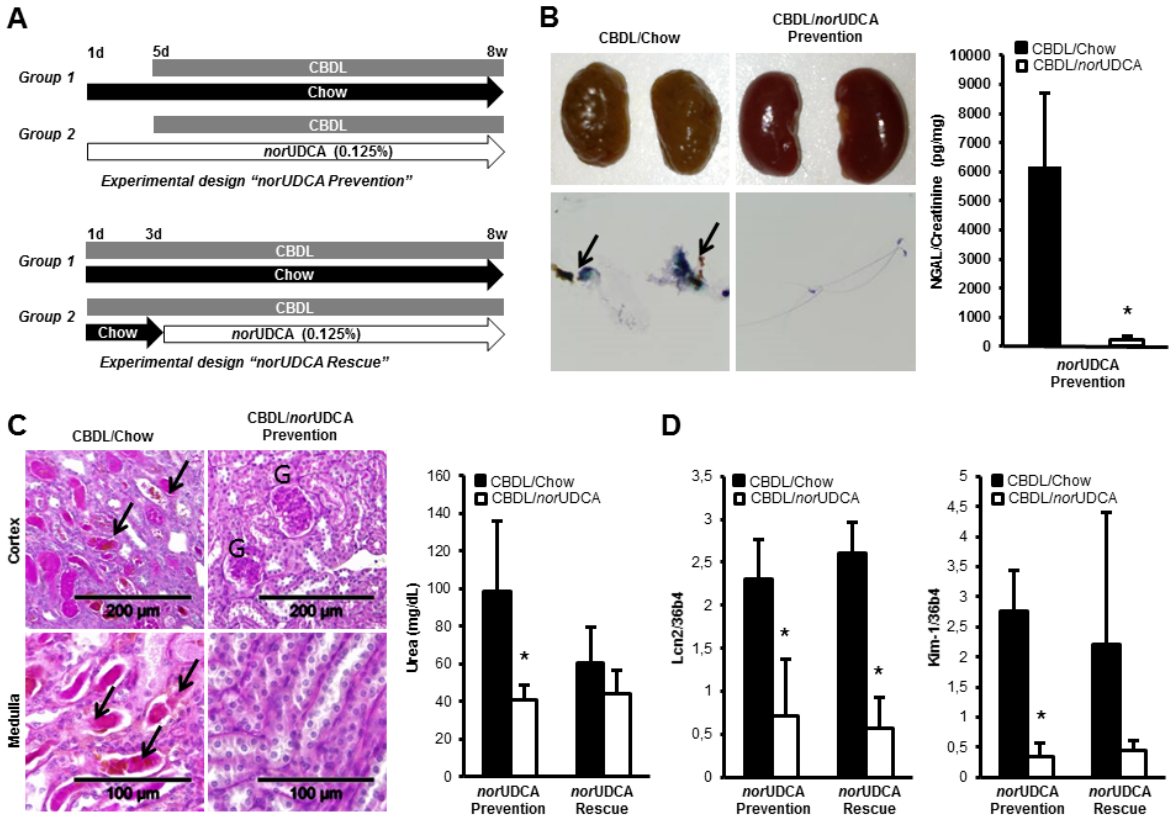

Figure 13. Therapeutic efficacy of *nor*UDCA in long-term common bile duct-ligated (CBDL) mice.

(A) The potential therapeutic effects of *nor*UDCA in cholemic nephropathy was studied in two experimental setups: For *norUDCA Prevention*, *nor*UDCA 0.125% was given 5 days prior to CBDL and continued for 8 weeks until harvesting. For *norUDCA Rescue*, *nor*UDCA 0.125% was started 3 days after CBDL was performed and continued for 8 weeks until harvesting. (B) Results of *norUDCA Prevention:* Kidney macroscopy of *nor*UDCA-fed CBDL mice (CBDL/*nor*UDCA Prevention, *right pair of kidneys*) was almost normal when compared to chow-fed CBDL mouse kidneys (CBDL/chow, *left pair of kidneys*). Also, n*or*UDCA-fed CBDL mice (CBDL/*nor*UDCA Prevention) had an almost normal urine cytology when compared to chow-fed CBDL mice (CBDL/chow) showing signs of acute tubular injury including high amounts of urinary excreted tubular epithelial cells (*arrows*). Urinary NGAL levels (normalized to urinary creatinine) were significantly lower in *nor*UDCA-fed CBDL mice (*open bars*) (6195 ± 2508 pg/mg in chow-fed CBDL mice vs. 230 ± 133 pg/mg in *nor*UDCA-fed CBDL mice (CBDL/*nor*UDCA Prevention),* p = 0.05). (C) *norUDCA Prevention:* Kidney histology of *nor*UDCA-fed CBDL mice (CBDL/*nor*UDCA Prevention) appears almost unremarkable while PAS stainings of chow-fed CBDL mouse kidneys reveals the typical phenotype of cholemic nephropathy [i.e. intraluminal cast formation (*arrows*), dilated tubules]. G, glomeruli. Also serum urea levels were significantly lower in *nor*UDCA-fed CBDL mice

(*open bar*, *norUCDA Prevention*) (*norUDCA Prevention:* 98 ± 37 mg/dL in chow-fed CBDL mice vs. 40 ± 9 mg/dL in *nor*UDCA-fed CBDL mice, * p = 0.024; *norUDCA Rescue:* 61 ± 19 mg/dL in chow-fed CBDL mice vs. 44 ± 12 mg/dL in *nor*UDCA-fed CBDL mice, n.s.). (D) *norUDCA Prevention and norUDCA Rescue: nor*UDCA-fed CBDL mice (*open bars*) show significantly downregulated mRNA expression levels of lipocalin 2 (Lcn2) and kidney injury molecule-1 (Kim-1). Expression levels of transcripts were normalized to the housekeeping gene 36b4. * p< 0.05 vs. control. Figure reproduced from Krones E et al, J Hepatol. 2017;67(1):110-119 [186] with permission of Elsevier. Figure drafted by Elisabeth Tatscher.

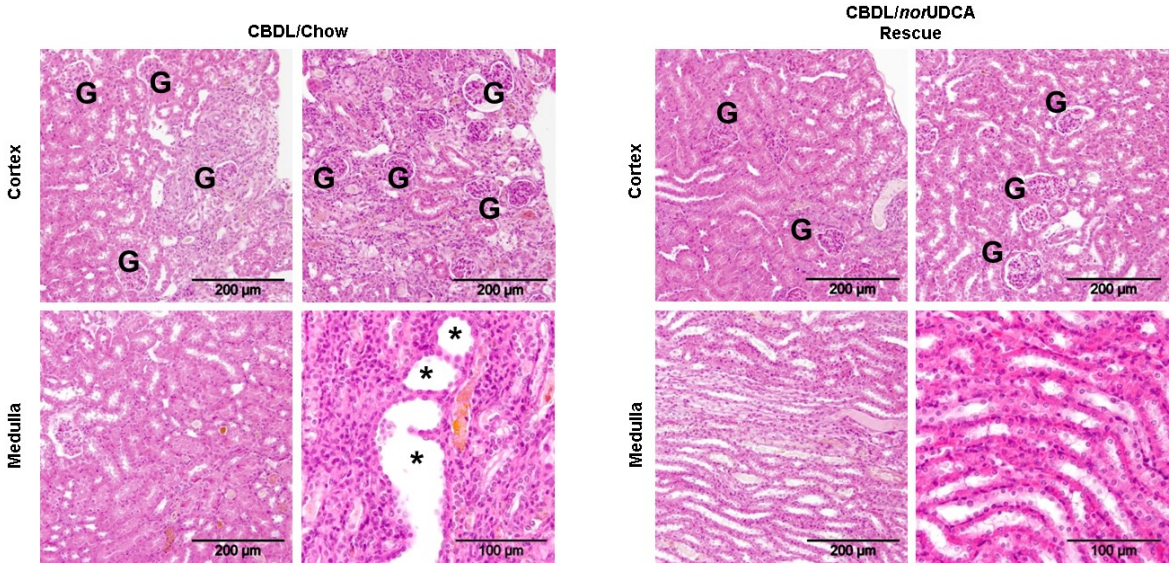

Figure 14. *Nor*UDCA leads to amelioration of cholemic nephropathy in long-term common bile duct-ligated (CBDL) mice.
norUDCA Rescue: The *left panel of images* shows intraluminal cast formation (*arrows*) and dilated tubules upon of chow-fed CBDL mice. On the contrary, PAS stainings of *nor*UDCA-fed CBDL mice (*norUDCA Rescue)* do not show evidence of acute kidney injury (*right panel of images)*. G, glomeruli. (Original magnification x20, x40 for the right lower pictures of each panel) Figure reproduced from Krones E et al, J Hepatol. 2017;67(1):110-119 [186] with permission of Elsevier. Figure drafted by Elisabeth Tatscher.

		norUDCA Prevention		*norUDCA Rescue*	
Intervention	Diet	Tubular dilatation	Fibrosis	Tubular dilatation	Fibrosis
SOP	Chow	-	-		
SOP	Chow	-	-		
CBDL	Chow	+++	+++	++	+++
CBDL	Chow	++(+)	++(+)	++(+)	+++
CBDL	Chow	++(+)	+++	++	++
CBDL	Chow	++(+)	++(+)	+++	+++
CBDL	Chow	+++	+++	++	+++
CBDL	*nor*UDCA	+	+	+	+
CBDL	*nor*UDCA	(+)	-	(+)	(+)
CBDL	*nor*UDCA	(+)	(+)	-	(+)
CBDL	*nor*UDCA	+	(+)	+	+
CBDL	*nor*UDCA	+	+	-	-

Table 9. *Nor*UDCA-associated amelioration of cholemic nephropathy in long-term common bile duct ligated mice.
Blinded scoring of PAS- and Sirius Red-stained kidney sections of SOP mice (n=2) and chow- and *nor*UDCA-fed CBDL mice from the *norUDCA Prevention (5 vs. 5 mice)* and the *norUDCA Rescue(5 vs.5 mice)* arm.–indicates "no dilated tubules" and "no fibrosis"; + indicates "single dilated tubules" and "single fibrotic septa"; ++ indicates "<50% dilated tubules per HPF" and "<50% fibrosis per HPF; +++ indicates ">50% dilated tubules per HPF" and ">50% fibrosis per HPF". SOP; Sham Operation; CBDL, Common bile duct ligation; *nor*UDCA, *nor*Ursodeoxycholic acid. Table reproduced from Krones E et al, J Hepatol. 2017;67(1):110-119 [186] with permission of Elsevier. Figure drafted by Elisabeth Tatscher.

3.2.4 *Nor*UDCA feeding prevents interstitial nephritis in CBDL.

As shown earlier in this thesis, induced expression of renal adhesion molecule Vcam-1 and macrophage/dendritic cell marker F4/80 was found in chow-fed CBDL mouse kidneys (Fig. 9). In the *norUDCA for Prevention* arm, renal expression of F4/80 (Fig. 15A, left panel), and Vcam-1 was significantly reduced (Fig. 15A, right panel, 15B) [186]. In line with that, mRNA expression levels of F4/80, Vcam-1, and Mcp-1were significantly downregulated (Fig. 15D) [186]. Also in the second experimental setup (*norUDCA for Rescue*) a reduced renal protein expression of F4/80 (Fig. 15C, left panel) and Vcam-1 (Fig. 15C, right panel) was observed, however, gene expression levels of F4/80, Vcam-1,

and Mcp-1 mRNA were not significantly reduced in this experimental setup (Fig. 15D) [186].

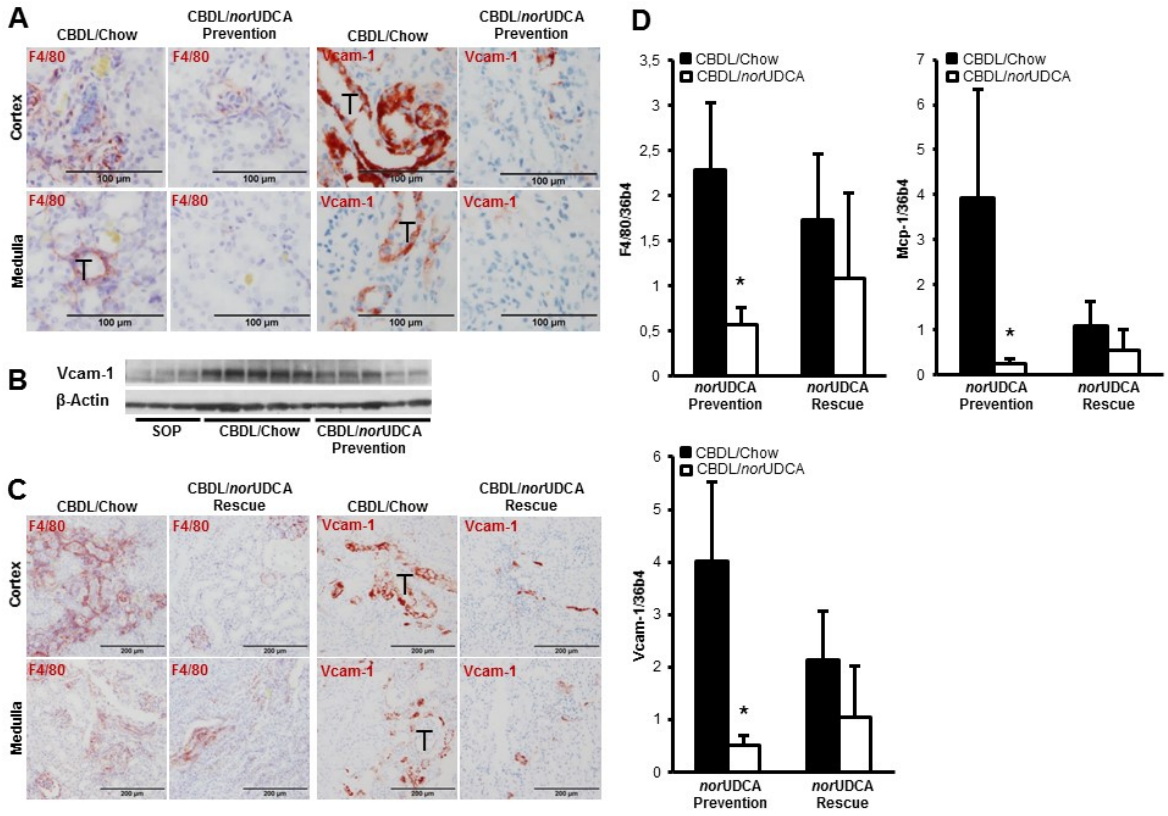

Figure 15. Ameliorated inflammation in kidneys of *nor*UDCA-fed long-term common bile duct-ligated (CBDL) mice.
(A) *norUDCA Prevention*: Less pronounced F4/80 and Vcam-1 expression in kidneys of *nor*UDCA-fed CBDL mice (CBDL/*nor*UDCA Prevention) upon immunohistochemistry. T, tubule. (Original magnification x40) (B) *norUDCA Prevention*: Renal Vcam-1 protein expression is induced to a lesser degree in *nor*UDCA-fed CBDL mice (CBDL/*nor*UDCA) compared to chow-fed CBDL mice (CBDL/chow). (C) Also in the *norUDCA Rescue* arm, less pronounced F4/80 and Vcam-1 expression in kidneys of *nor*UDCA-fed CBDL mice (CBDL/*nor*UDCA Rescue) can be observed upon immunohistochemistry. T, tubule. (Original magnification x20). (D) In the *norUDCA Prevention* arm, key genes of inflammation including F4/80, Vcam-1 and Mcp-1 are significantly downregulated in *nor*UDCA-fed CBDL mice (*open bars*) compared to chow-fed CBDL mice (*black bars*). In the *norUDCA Rescue* arm, the reduction did not reach statistical significance. Expression levels of transcripts were normalized to the housekeeping gene 36b4. * $p < 0.05$ vs. control. Figure reproduced from Krones E et al, J Hepatol. 2017;67(1):110-119 [186] with permission of Elsevier. Figure drafted by Elisabeth Tatscher.

3.2.5 *Nor*UDCA impressively ameliorates fibrosis in long-term CBDL mice.

Sirius red stained kidney sections, renal hydroxyproline content, and gene expression levels of Colα1(I) and Tgf-β1 were compared between *nor*UDCA- and chow-fed CBDL mice in order to investigate whether *nor*UDCA feeding ameliorates fibrosis in CBDL kidneys [186]. As described earlier in this thesis (Fig. 10), enhanced Sirius red staining suggestive of tubulointerstitial kidney fibrosis could be observed in chow-fed CBDL mice (Fig. 16A, left panel). In contrast, kidneys of *nor*UDCA-fed CBDL mice (*norUDCA for Prevention and for Rescue*) showed significantly less fibrosis upon Sirius red stainings (Fig. 16A, right panel; Fig. 16C, Table 9) [186]. In line with that, quantification of fibrosis by measurement of renal hydroxyproline levels revealed a significantly reduced renal hydroxyproline content in *nor*UDCA-fed CBDL mice (Fig. 16D) [186]. Also key genes of fibrosis (i.e. Colα1(I) and Tgf-β1) were significantly repressed in the *norUDCA for Prevention* arm; however, similar to key genes of inflammation, expression levels of Colα1(I) and Tgf-β1 were not significantly different in chow- and *nor*UDCA-fed CBDL mice in the *norUDCA for Rescue* setup (Fig. 16E) [186].

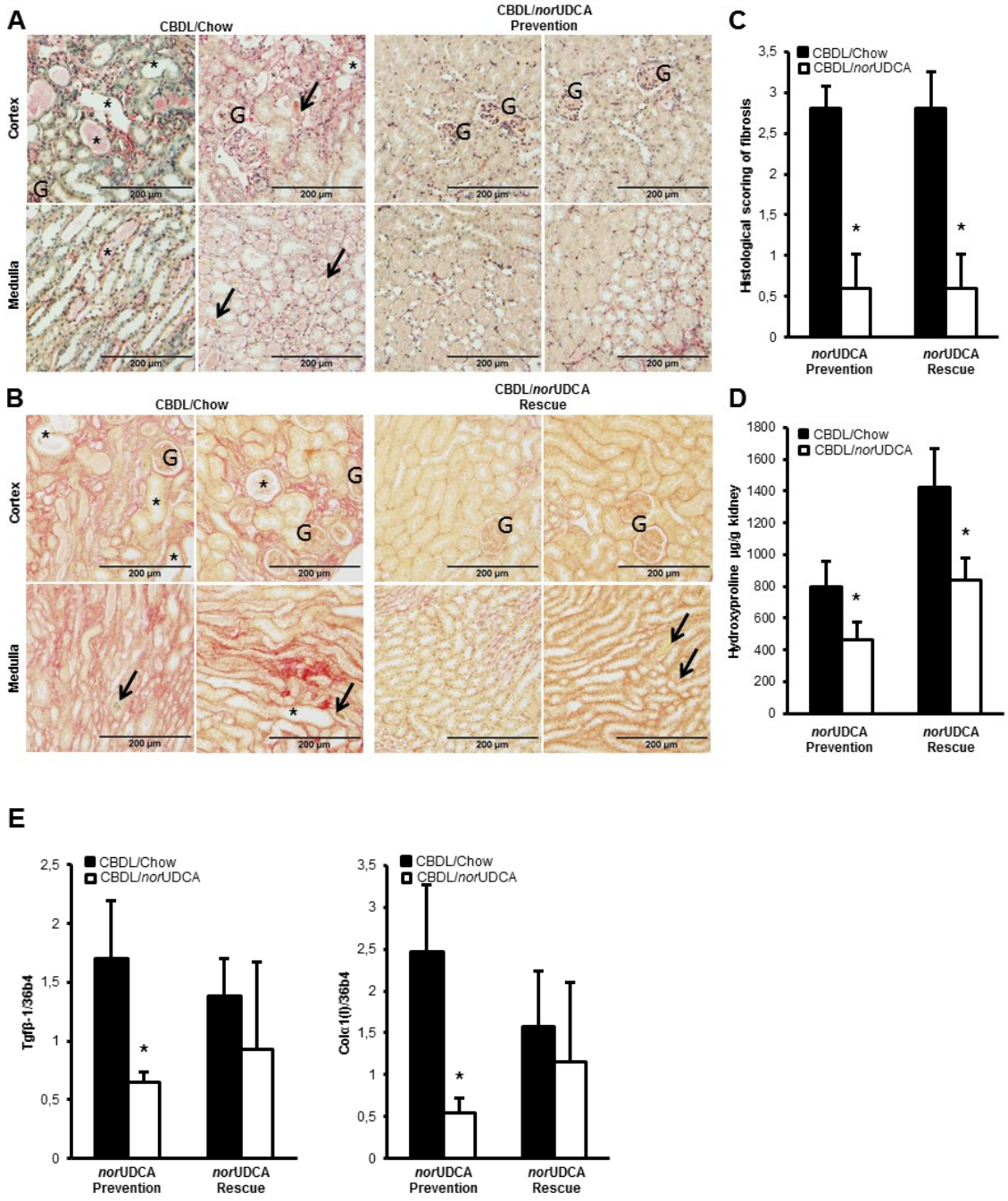

Figure 16. *Nor*UDCA impressively ameliorates fibrosis in long-term common bile duct-ligated (CBDL) mouse kidneys.

(A) *norUDCA Prevention:* Dilated tubules *(asterisks)* and enhanced Sirius red staining upon kidney sections of chow-fed CBDL mice (CBDL/chow). In contrast, Sirius red stained kidney sections of *nor*UDCA-fed CBDL mice (CBDL/*nor*UDCA Prevention) show an impressively lesser degree of fibrosis despite evidence of some intraluminal bile casts *(arrows)* (Original magnification x20). (B) Also in the *norUDCA Rescue* arm less fibrosis is observed in kidneys of *nor*UDCA-fed CBDL mice (CBDL/*nor*UDCA Rescue) when compared to kidneys of chow-fed CBDL mice (CBDL/chow). (Original magnification x20). (C) Blinded scoring of Sirius Red-stained kidney sections of chow- and *nor*UDCA-fed CBDL mice (see also Suppl. Table 3) from the *norUDCA Prevention (5 vs. 5 mice)* and the *norUDCA Rescue (5 vs.5 mice)* arm. * $p < 0.05$ vs. control. (D) Renal hydroxyproline

levels were significantly lower in *nor*UDCA-fed CBDL mice (*open bars*) (*norUDCA Prevention:* 797 ± 160 µg/g kidney in chow-fed CBDL mice vs. 466 ± 106 µg/g kidney in *nor*UDCA-fed CBDL mice, * p 0.004; *norUDCA Rescue:* 1422 ± 242 µg/g kidney in chow-fed CBDL mice vs. 838 ± 143 µg/g kidney in *nor*UDCA-fed CBDL mice, * p 0.002). (E) Key genes of fibrosis including Colα1(I) and Tgfβ-1 were significantly (in the *norUDCA Prevention* arm) downregulated in *nor*UDCA-fed CBDL mice (*open bars*). Expression levels were normalized to the housekeeping gene 36b4. * $p < 0.05$ vs. control. Figure reproduced from Krones E et al, J Hepatol. 2017;67(1):110-119 [186] with permission of Elsevier. Figure drafted by Elisabeth Tatscher.

3.2.6 *Nor*UDCA´s effects on cholestatic liver injury in long-term CBDL mice.

One might speculate, that the kidney-protective effect of *nor*UDCA were secondary to amelioration of liver disease. Liver injury was thus compared between chow- and *nor*UDCA-fed CBDL mice. Similar to chow-fed CBDL mice, liver histology revealed enlarged and broadened portal tracts with ductular proliferation and fibrosis of the biliary type in both experimental conditions using *nor*UDCA (*norUDCA for Prevention and for Rescue;* Fig. 17A, B*)* [186]. Bile infarcts were, however, more frequently present in chow-fed CBDL mice (Fig. 17A left upper panel, B left upper panel; Table 10) which is in line with previously published data [187]. Serum levels of cholestatic liver injury (i.e. ALT and AP) (Fig. 17C) as well as liver hydroxyproline levels (Fig. 17D) did also not significantly differ between chow- and *nor*UDCA-fed CBDL mice (both experimental designs) [186]. Taken together, this observations suggest that the beneficial effects of *nor*UDCA observed in the kidneys of long-term CBDL mice were not attributable to (significant) amelioration of liver disease [186].

		norUDCA Prevention			*norUDCA Rescue*		
Intervention	Diet	Ductular Proliferation	Bile Infarcts	Fibrosis	Ductular Proliferation	Bile Infarcts	Fibrosis
SOP	Chow	-	-	-			
SOP	Chow	-	-	-			
CBDL	Chow	+++	+++	+++	++(+)	++	++
CBDL	Chow	++(+)	+	++	++(+)	-	++(+)
CBDL	Chow	++(+)	++	+++	++	-	++
CBDL	Chow	++	+	++(+)	+++	+	++
CBDL	Chow	+++	+	+++	+++	+	++
CBDL	*nor*UDCA	++	-	+(+)	++	-	++
CBDL	*nor*UDCA	+++	+++	+(+)	++	-	++
CBDL	*nor*UDCA	+(+)	-	+(+)	++	-	++
CBDL	*nor*UDCA	++(+)	+	++(+)	++(+)	-	++(+)
CBDL	*nor*UDCA	+++	+	++(+)	++(+)	+	++(+)

Table 10. *Nor*UDCA does not significantly ameliorate liver disease in long-term common bile duct ligated mice.

Blinded scoring of liver sections (H&E and SR) of SOP (n=2) and chow- and *nor*UDCA-fed CBDL mice from the *norUDCA for Prevention* (5 vs. 5 mice) and the *norUDCA for Rescue* (5 vs.5 mice) arms. Apart from bile infarcts, which are found to a lesser degree in *nor*UDCA-fed CBDL mice, liver histology does not show significant differences between chow- and *nor*UDCA-fed CBDL mice, neither in the *norUDCA for Prevention (5 vs. 5 mice)* nor in the *norUDCA for Rescue (5 vs.5 mice)* arms. – indicates "no ductular proliferation", "no bile infarcts" and "no fibrosis"; + indicates "mild ductular proliferation", "single bile infarcts" and "mild fibrosis expansion of some portal areas"; ++ indicates "moderate ductular proliferation", "< 2 bile infarcts per HPF" and "fibrosis expansion of most portal areas"; +++ indicates "marked ductular proliferation", "> 2 bile infarcts per HPF" and "fibrosis expansion of most portal areas with marked portal to portal bridging". SOP; Sham Operation; CBDL, Common bile duct ligation; *nor*UDCA, *nor*Ursodeoxycholic acid. Table reproduced from Krones E et al, J Hepatol. 2017;67(1):110-119 [186] with permission of Elsevier. Table drafted by Elisabeth Tatscher.

.

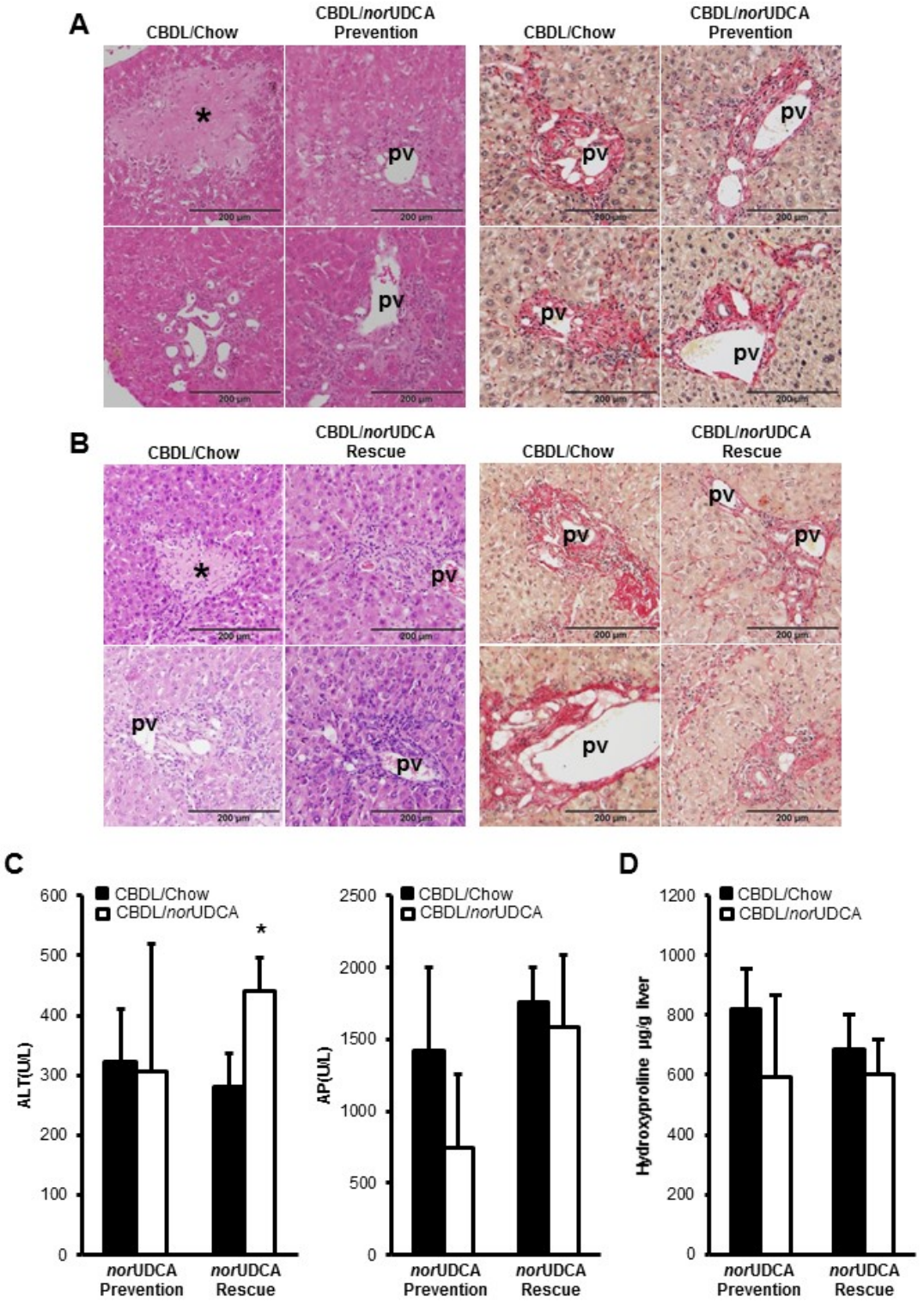

Figure 17. *Nor*UDCA does not significantly affect the cholestatic phenotype of liver injury in long-term common bile duct ligated (CBDL) mice.
(A, B) (A) H&E and (B) Sirius Red stained liver sections of chow- and *nor*UDCA-fed CBDL mice (*norUDCA Prevention;* A, *norUDCA Rescue,* B) show enlarged and broadened portal tracts with ductular proliferation and biliary type of fibrosis in all groups. Only bile infarcts *(asterisk)* are more frequently found in chow-fed CBDL mice. pv, portal vein. (C) *norUDCA Prevention and norUDCA Rescue:* Serum ALT and AP levels did not significantly differ between chow(*black bars*)- and *nor*UDCA-fed (*open bars*) CBDL mice

(*norUDCA Prevention:* ALT: 322 ± 88 U/L vs. 306 ± 214 U/L in chow- and *nor*UDCA-fed CBDL mice, respectively, p = 0.877; AP: 1424 ± 575 U/L vs. 742 ± 514 U/L in chow- and *nor*UDCA-fed CBDL mice, respectively, p = 0.067; *norUDCA Rescue:* ALT: 281 ± 56 U/L vs. 442 ± 54 U/L in chow- and *nor*UDCA-fed CBDL mice, respectively, * p = 0.002; AP: 1759 ± 240 U/L vs. 1584 ± 507 U/L in chow- and *nor*UDCA-fed CBDL mice, respectively, p = 0.505). (D) *norUDCA Prevention and norUDCA Rescue:* Liver tissue hydroxyproline levels did not significantly differ between chow (*black bars*)- and *nor*UDCA-fed (*open bars*) CBDL mice (*norUDCA Prevention:* 818 ± 136 µg/g vs. 593 ± 272 µg/g in chow- and *nor*UDCA-fed CBDL mice, respectively, p = 0.129; *norUDCA Rescue:* 684 ± 118 µg/g vs. 601 ± 115 µg/g in chow- and *nor*UDCA-fed CBDL mice, respectively, p = 0.390). Figure reproduced from Krones E et al, J Hepatol. 2017;67(1):110-119 [186] with permission of Elsevier. Figure drafted by Elisabeth Tatscher.

3.2.7 Effects of *nor*UDCA on liver, kidney, serum and urine bile acid composition in CBDL mice.

UPLC-MSMS was used to analyze and compare liver, kidney, serum and urine bile acid profiles. Three experimental groups were compared: SOP and chow- or *nor*UDCA-fed CBDL mice. Individual endogenous (C24) bile acids and *nor*UDCA (C23) metabolites in liver, kidney, serum and urine of SOP and chow- or *nor*UDCA-fed CBDL mice were separated [186]. In total, 27 different metabolites of *nor*UDCA were quantified: unconjugated and taurine- (T) conjugated nor-diols (n= 3), -triols (n=6), -tetrols (n=8), and -pentols (n=4), and otherwise unconjugated *nor*diol- and *nor*triol glucuronides (n=6) [186]. Of total *nor* bile acids in liver, kidney and serum, 18.5%, 25.3%, and 1.3% consisted of native *nor*UDCA [186]. However, native *nor*UDCA was absent in urine [186]. In livers of chow-fed CBDL mice, a shift from TCA towards Tβ-MCA and formation of tetra- and pentahydroxylated bile acids (i.e. cholestasis-typical changes in bile acid profiles) was observed (Fig. 18A) [186]. No significant difference was observed compared to *nor*UDCA-fed CBDL mice where bile acid profiles rather in addition consisted of about 10% *nor*UDCA metabolites [186]. In kidneys of *nor*UDCA-fed animals, three times higher total amounts of bile acids were measured as compared to kidneys of chow-fed CBDL mice [186]. This was entirely attributable to *nor*UDCA-metabolites that consisted 74.9% of all kidney bile acids (Fig. 18A) [186]. Chow-fed and *nor*UDCA-fed mice showed a comparable urinary output (2.4 ± 0.8 mL/12 hours in controls vs. 3.9 ± 1.5 mL/12 hours in *nor*UDCA-fed mice, n.s) (Fig. 18B, C) and fluid intake was similar in both groups (92.5 ± 3.5 mL/12 hours in control vs. 90 ± 0 mL/12 hours in *nor*UDCA-fed group) [186]. In

serum of *nor*UDCA-fed CBDL mice, total bile acids were about one third lower when compared to chow-fed CBDL mice (1.33 mmol/L vs. 1.05 mmol/L, respectively; 6% *nor*UDCA-metabolites in *nor*UDCA-fed animals) [186]. Although this difference was not statistically significant (p=0.06), it was reflected by an increase of total urinary excretion of bile acids, from 885.2 ± 397.6 nmol/12h to 2757.2 ± 2296.1 nmol/12h (45% *nor*UDCA metabolites) [186]. Taken together, these findings show that hydrophilic *nor*UDCA is extensively metabolized towards even more hydrophilic metabolites that are significantly enriched in kidney tissue and excreted via urine [186].

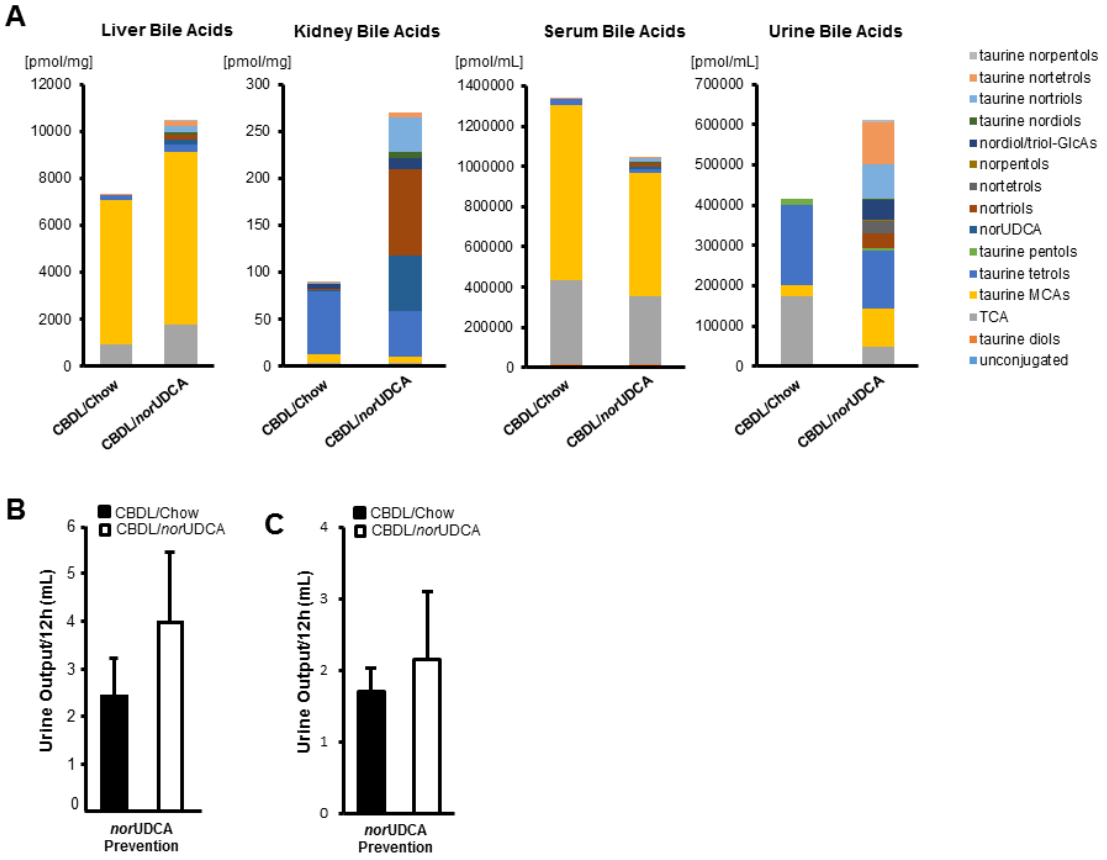

Figure 18. Liver, kidney, serum and urine bile acid profiles and urine output in chow- and *nor*UDCA-fed CBDL mice.
(A) The liver bile acid composition of chow- and *nor*UDCA-fed CBDL mice shows a shift from TCA towards βMCA and the formation of tetra- and pentahydroxylated bile acids (i.e. cholestasis-typical changes) with additional *nor*UDCA metabolites in *nor*UDCA-fed CBDL mice. Kidneys of *nor*UDCA-fed animals show three-times higher total amounts of bile acids when compared to kidneys of chow-fed CBDL mice, however, *nor*UDCA-metabolites represent the most abundant bile acid compound. Urine bile acid profiles in *nor*UDCA-fed animals were comparable to what was found in kidney tissue. (B) *norUDCA Prevention:* A slightly but not significantly higher 12h urine output was observed in 5 days *nor*UDCA-fed mice compared to chow-fed animals (pooled urine samples of 4 vs. 4 mice), 2.4 ± 0.8 ml/12h in chow-fed mice vs. 3.9 ± 1.5 ml/12h in

*nor*UDCA-fed mice, n.s.). (C) *norUDCA Prevention:* A slightly but not significantly higher 12h urine output was observed in 3 days *nor*UDCA-fed mice (pooled urine samples of 4 vs. 4 mice), 1.7 ± 0.3 ml/12h in chow-fed mice vs. 2.1 ± 0.9 ml/12h in *nor*UDCA-fed mice, statistically n.s.). Figure reproduced from Krones E et al, J Hepatol. 2017;67(1):110-119 [186] with permission of Elsevier. Figure drafted by Elisabeth Tatscher.

3.2.8 *Nor*UDCA exerts no protective effects in ischemia/reperfusion (I/R)-induced kidney injury, unilateral ureter ligation (UUL)-induced kidney fibrosis, and LPS-induced kidney injury.

To determine whether the therapeutic effect of *nor*UDCA is specific for in cholemic nephropathy or could also be observed in other kidney injury models, the effects of *nor*UDCA were studied in the I/R-induced kidney injury model, in unilateral ureter ligation (UUL)-induced kidney fibrosis, and in LPS-induced kidney injury [186]. A comparable degree of tubular epithelial injury was found for chow- and *nor*UDCA-fed mice in the I/R-induced kidney injury model (Fig. 19A) [186]. As such, no significant differences between chow- and *nor*UDCA-fed mice were observed regarding active caspase-3 expression (18 hrs after I/R), the proliferation marker Ki-67 (48 hrs after I/R) (Fig. 19B, C) and uNGAL excretion 18 hrs and 48 hrs after I/R (Fig. 19D) [186]. Also in the UUL-induced kidney fibrosis model, morphological analysis of SFOG stained kidney sections and renal hydroxyproline levels (Fig. 19E, F) did not show apparent differences between chow- and *nor*UDCA-fed mice [186].

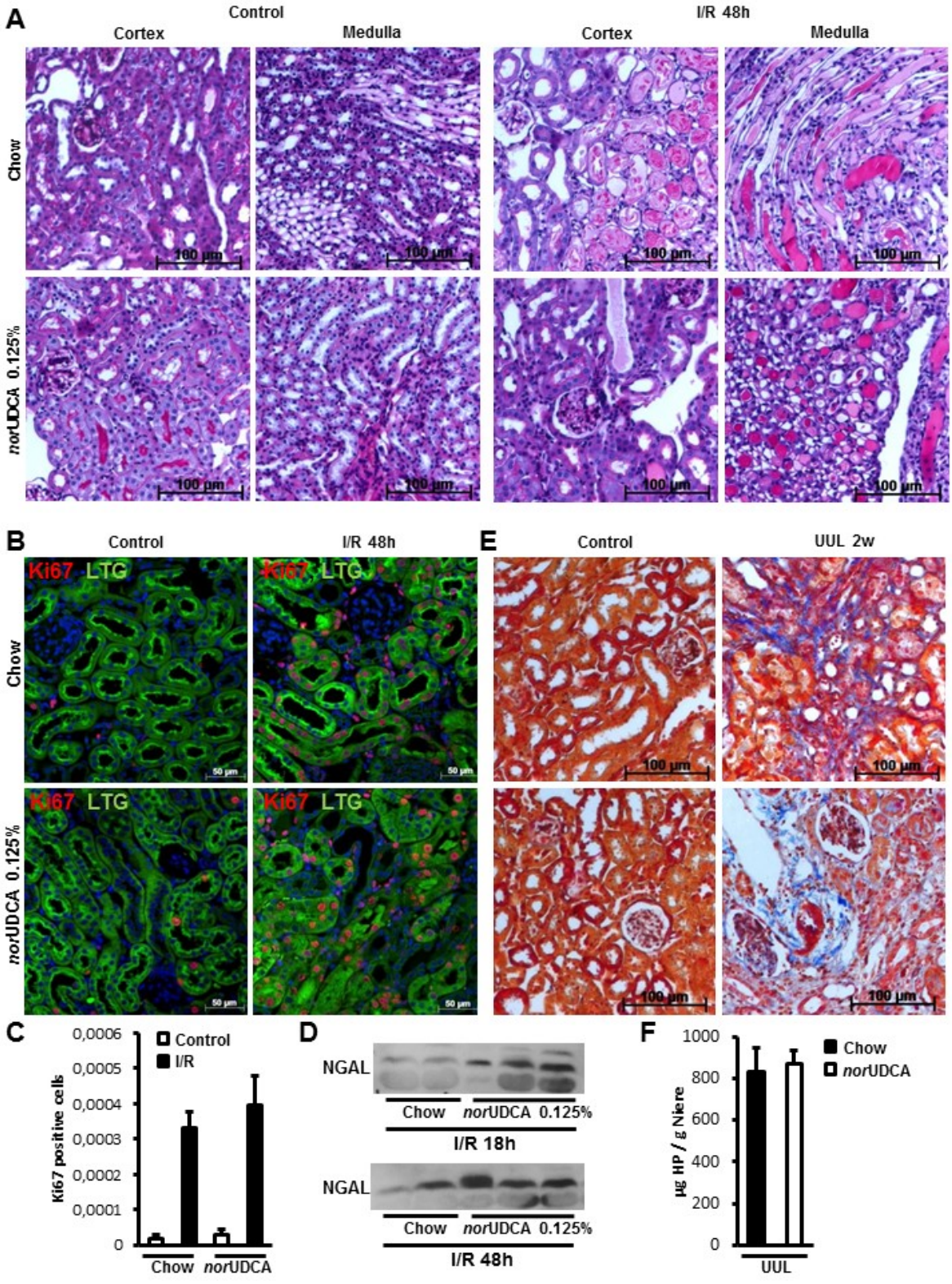

Figure 19. *Nor*UDCA does not lead to amelioration of the renal phenotype in ischemia/reperfusion injury (I/R) and unilateral ureter ligation (UUL).
(A) I/R resulted in acute tubular injury in chow- and *nor*UDCA-fed mice (harvested 18 hrs and 48 hrs after I/R). (B,C) No difference between the two groups upon immunofluorescence for the proliferation marker Ki-67 (48 hrs after I/R). (D) No difference in urinary NGAL excretion 18 hrs and 48 hrs after I/R between chow- and *nor*UDCA-fed CBDL mice. (E,F) Equal amount of kidney fibrosis determined by

morphological analysis of SFOG stained kidney sections and measurement of the renal hydroxyproline content (830 ± 116 µg/g in chow-fed UUL mice vs. 870 ± 67 µg/g in *nor*UDCA-fed UUL mice, statistically n.s.) in a mouse model of unilateral ureter ligation (UUL) fed either *nor*UDCA or standard diet. Data (C, F) are presented as mean ± SD, unpaired Student's t test was used to compare each group. Figure reproduced from Krones E et al, J Hepatol. 2017;67(1):110-119 [186] with permission of Elsevier. Figure drafted by Elisabeth Tatscher.

Compared to vehicle injected controls, intraperitoneal (i.p.) injection of LPS for 12 hrs led to acute kidney injury with a significant increase in serum urea levels and NGAL/Creatinine levels (Fig. 20) [186]. Prefeeding of *nor*UDCA (0.5%) enriched diets did, however, not result in significant amelioration of this phenotype (Fig. 20B) [186]. As such, mRNA expression levels of Lcn2, Kim-1, F4/80, Mcp-1 and Vcam-1 did not show a significant difference between chow- (Ctrl) and *nor*UDCA-fed, LPS-treated mice (Fig. 20C) [186].

To sum up, *nor*UDCA did not affect kidney injury and/or renal function in I/R-associated AKI, obstructive uropathy and in LPS-associated AKI. The fact that no therapeutic effect of *nor*UDCA was observed for this three different models argues for a specific effect of this hydrophilic compound in cholemic nephropathy and again underlines the role of bile acids in its pathogenesis [186].

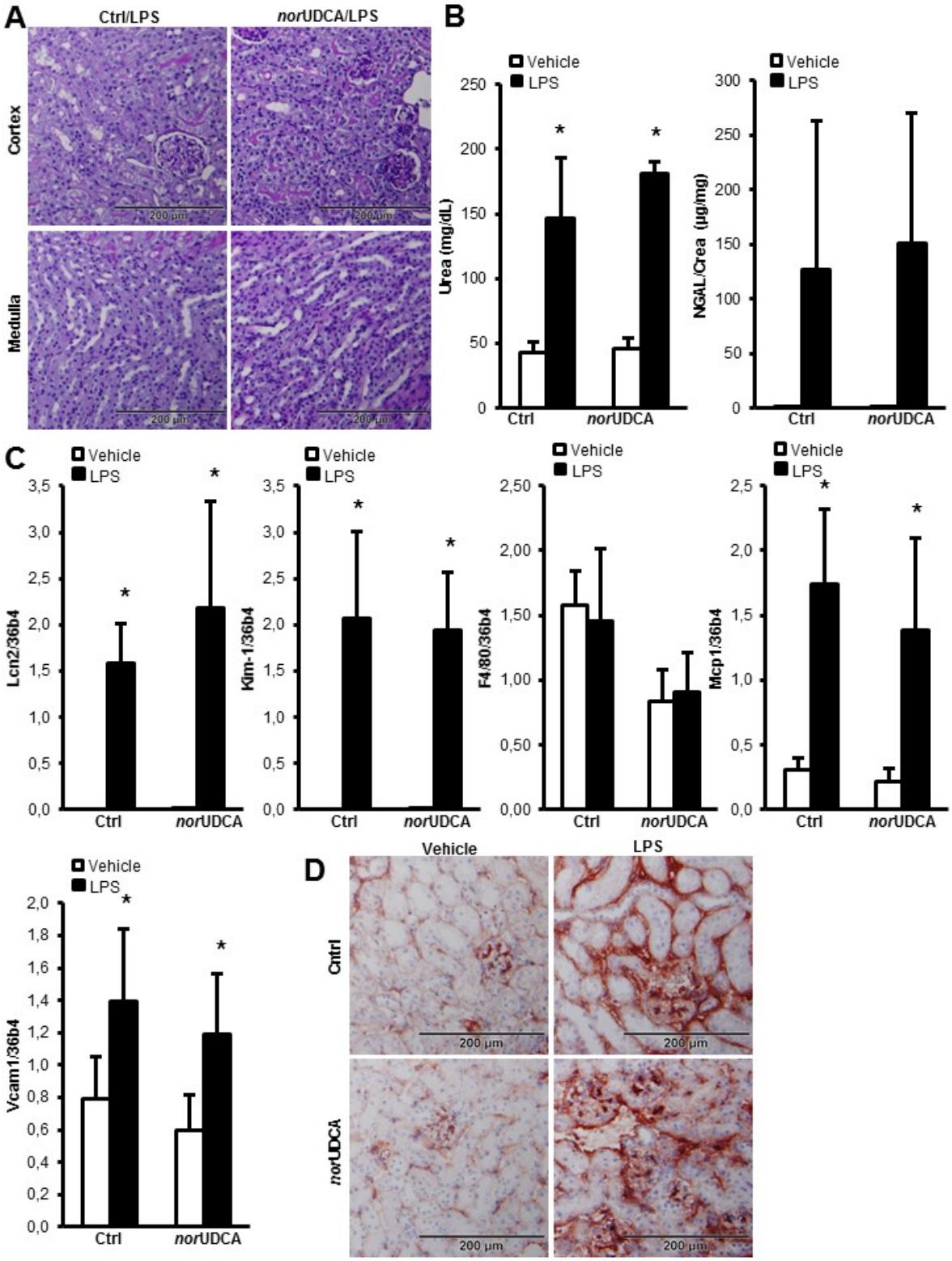

Figure 20. *Nor*UDCA does not ameliorate the renal phenotype in lipopolysaccharide (LPS)-challenged kidneys.

(A) PAS stained kidney sections revealed no difference in histomorphology between *nor*UDCA (0.5%) and chow-fed (Ctrl) LPS-injected mice (original magnification x40). (B) Compared to vehicle injected controls, intraperitoneal (i.p.) injection of LPS for 12 hrs led to acute kidney injury with a significant increase in serum urea levels (Ctrl/Vehicle 43 ± 8 mg/dL vs. Ctrl/LPS 146 ± 47 mg/dL, p=0.000; *nor*UDCA/Vehicle: 46 ± 8 mg/dL vs.

*nor*UDCA/LPS: 181 ± 9mg/dL, p=0.000) and elevation of NGAL/Creatinine levels (Ctrl/Vehicle 0.4 ± 0.2 µg/mg vs. Ctrl/LPS 127 ± 136 µg/mg, p=0.229; *nor*UDCA/Vehicle: 0.2 ± 0.1 µg/mg vs. *nor*UDCA/LPS: 151 ± 119 µg/mg, p=0.133). However, no statistical significant difference was observed between chow- (Ctrl) and *nor*UDCA (0.5%)-fed mice. Both were equally susceptible towards LPS challenge. (Urea: Ctrl/LPS 146 ± 47 mg/dL vs. *nor*UDCA/LPS: 181 ± 9mg/dL, p=0.307; NGAL/Creatinine: Ctrl/LPS 127 ± 136 µg/mg vs. *nor*UDCA/LPS: 151 ± 119 µg/mg, p=1.000). (C) Significant differences for mRNA expression levels of Lcn2, Kim-1, Mcp-1 and Vcam-1 were observed when vehicle- and LPS-injected mice were compared (* indicates $p<0.05$). However, no difference between chow- (Ctrl) and *nor*UDCA-fed LPS-challenged mice was observed. Data (B, C) are presented as mean ± SD, analysis of variance with Bonferroni post testing was used for comparison between the groups. (D) Compared to kidneys of vehicle-injected mice (Vehicle), kidneys of LPS-injected mice (LPS) show less pronounced Vcam-1 expression upon immunohistochemistry. However, no difference was observed between chow- (Ctrl) and *nor*UDCA-fed (*nor*UDCA) LPS-challenged mice (original magnification x40). Figure reproduced from Krones E et al, J Hepatol. 2017;67(1):110-119 [186] with permission of Elsevier. Figure drafted by Elisabeth Tatscher.

3.3 Human Evidence

As described earlier in this thesis, patients with cholemic nephropathy show tubular epithelial injury and intraluminal casts at the level of distal nephron segments (Table 4). In order to substantiate the findings from the above described animal with human evidence the archives of the Diagnostic and Research Institute of Pathology of the Medical University of Graz were screened for patients with cholestatic liver disease and cholemic nephropathy in whom both tissues were available for examination. This was performed in collaboration with Univ.-Doz. Univ. FA Dr. med. Cord Langner from the Diagnostic and Research Institute of Pathology of the Medical University of Graz [100]. Only 4 patients with cholestatic (end-stage) liver disease and cholemic nephropathy described in their autopsy reports were identified. In line with what was found in cholemic mouse kidneys, kidney histology of these patients showed collecting duct epithelial injury, tubular cast formation, signs of interstitial nephritis, and tubulointerstitial fibrosis (Fig. 21) [100]. As it's the case for other autopsy reports on cholemic nephropathy, these findings are limited by numerous potential confounding factors such as critical illness leading to death (e.g. use of vasoconstrictors, shock, potentially nephrotoxic medication) as well as ischemia time and autolysis [100].

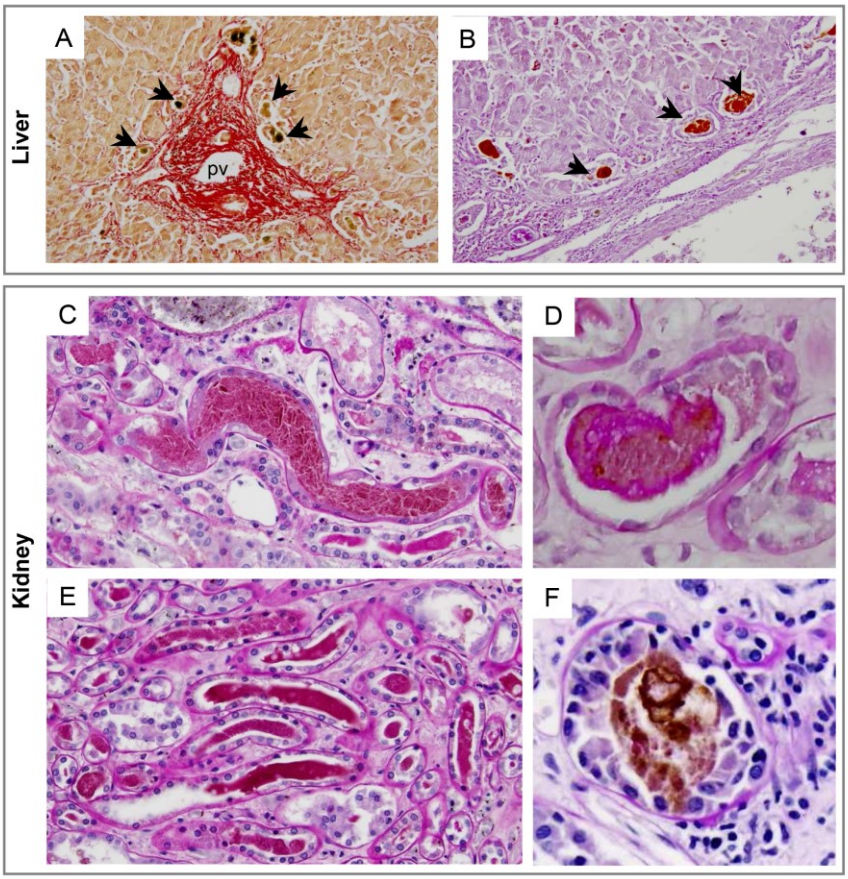

Figure 21. Human evidence for cholemic nephropathy with intraluminal casts and tubulointerstitial nephritis in cholestatic liver disease.
(A-B) Representative liver histology of cholestatic liver disease. Sirius red (A) and PAS stainings (B) show enlarged and broadened portal tracts with ductular proliferation and biliary type of liver fibrosis (*ductular cholestasis indicated by black arrowheads*). pv, portal vein. (C-F) Intraluminal cast formation at the level of distal tubules and collecting ducts upon PAS stained kidney sections of two different cholestatic patients with end-stage liver disease. (F) Peritubular inflammatory infiltrate around an intraluminal cast. Original magnification x20 for A and B, x40 for C and E, x60 for D and F. Figure reproduced from Fickert P, Krones E et al, Hepatology. 2013;58(6):2056-69 [100] with permission of Wiley. Figure drafted by Elisabeth Tatscher.

3.4 *In vitro* experiments

3.4.1 Bile acids induce dose-dependent collecting duct epithelial cell death.

Combined morphological analysis and WST-1 assay revealed a dose-dependent cytotoxic effect of CDCA on MDCK cells already at concentrations of 100 µM after 30 minutes. In contrast, CA and *nor*UDCA (tested even at millimolar concentrations) did not induce MDCK cell death (Fig 22).

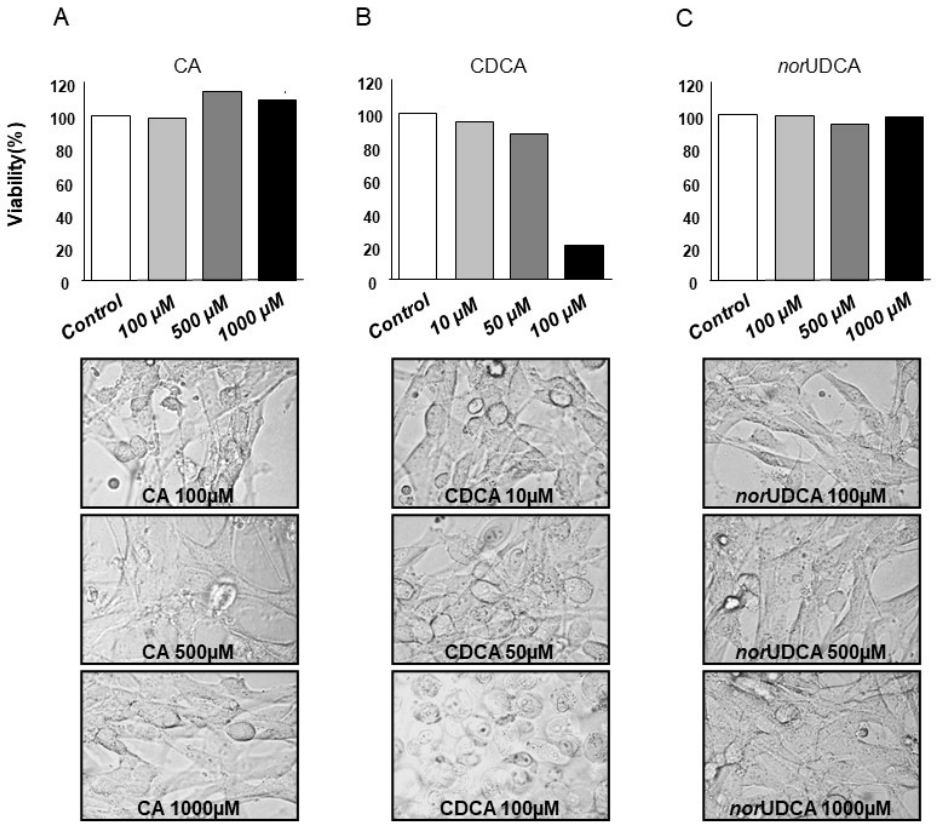

Figure 22. Chenodeoxycholic acid (CDCA) induces dose-dependent collecting duct epithelial cell death in vitro.
A-C. CDCA induced MDCK cell death already at 100 µM. Morphological analysis of cells reveals MCDK cell death after 30 minutes of treatment (B). In contrast, neither CA (A) nor *nor*UDCA (C) induced MDCK cell death, even at millimolar concentrations.

4 DISCUSSION

AKI in patients with ACLD has been known for decades as a diagnostically and therapeutically challenging complication with a high risk of mortality [90]. Besides all different forms of AKI (prerenal, intrinsic and postrenal), the most well described and prevailing mechanism of AKI in ACLD/cirrhosis is altered hemodynamics, suggesting AKI to be functional in its origin (i.e. HRS-AKI), however, only a minority of patients with HRS-AKI seem to suffer from "pure" functional HRS [188]. Superimposed on the hemodynamic abnormalities due to portal hypertension, other factors, including inflammation, bacterial translocation and potential nephrotoxins (such as bilirubin or bile acids) may contribute to a rather "mixed bag" of AKI in ACLD in most patients. This hypothesis is further supported by the fact that a large proportion of patients do not adequately respond to vasoactive therapy. As such, HRS-AKI reversal was only reported in 32% of patients under terlipressin treatment in a recent multicenter placebo-controlled randomized trial investigating the effect of terlipressin versus placebo on HRS reversal and mortality in HRS-AKI patients [68]. Response rates to terlipressin in ACLF are even worse with only 18% in a large prospectively studied cohort with ACLF and AKI 3 [139], notably, in that cohort, a large proportion of those patients were reported to have structural renal changes upon post-mortem renal histopathology. Also other autopsy studies revealed patients who were initially classified as HRS-AKI to have substantial parenchymal kidney injury, which would preclude the diagnosis of HRS-AKI [113, 163]. From a clinical point of view, this underlines the well-known difficulty to accurately establish a (non-invasive) diagnosis of HRS-AKI, which in turn guides the further therapeutic steps [69].

Besides several well-known entities that might lead to AKI in ACLD/cirrhosis including prerenal azotemia, HRS-AKI, intrinsic renal disease (e.g. IgA nephropathy, glomerulonephritis, glomerulosclerosis) and –although very rare- postrenal causes [69], cholemic nephropathy represents an underestimated and still poorly understood cause of AKI in ACLD and cirrhosis. A human study from 2019 revealed that cholemic nephropathy is even more frequently found in the condition of AKI (17.8%) than CKD and that elevated serum bilirubin, AP, and urinary bilirubin and urobilinogen are predictors for the diagnosis of cholemic nephropathy [134]. According to a substantial number of cases

published since 2000, cholemic nephropathy as a potential cause of AKI has to especially kept in mind in (deeply) jaundiced patients with (obstructive) cholestasis decompensated liver, ASH or ACLF [69].

The aim of this thesis was to show, that (obstructive) cholestasis in mice with systemic accumulation and exaggerated urinary elimination of potentially toxic cholephiles (such as bilirubin and bile acids) leads to AKI and distinct histological renal changes, closely resembling those described in human cholemic nephropathy. To address this aim, an in vivo model for progressive cholestatic liver disease/biliary cirrhosis associated with tubulointerstitial nephritis, renal fibrosis and impaired renal function, the features of cholemic nephropathy, was established. This CBDL mouse model offered new perspectives to study the complex pathophysiology of this condition.

Longitudinal studies in CBDL mice revealed that the first phenotypical changes of cholemic nephropathy could already be observed after 3d CBDL with renal tubular epithelial injury and basement membrane defects predominantly at the level of AQP2-positive collecting ducts. This initial changes were followed by by formation of obstructive intraluminal casts, dilation of tubules, interstitial nephritis and renal fibrosis in 3-, 6-, and 8-week CBDL mice [100].

Loss of AQP2 expression in collecting ducts, meanwhile also observed in human histopathology samples with cholemic nephropathy [134], may be secondary to bile acid toxicity with resulting tubular cell injury and death or due to a direct tubular effect of bile acids downregulating the number of AQP2 channels [69].

While the cholemic nephropathy kidney phenotype was not observed in other models of sclerosing cholangitis and biliary type of liver fibrosis (i.e. 8w DDC-fed and 8w $Mdr2^{-/-}$ mice), the characteristic kidney alterations were repeatedly found at different time points of CBDL. In contrast to DDC-fed and $Mdr2^{-/-}$ mice, CBDL mice significantly higher serum bile acid levels; it is therefore highly likely that bile acids represent the key pathogenic factor for the renal pathology specifically observed in CBDL mice [51-53].

This is further supported by the fact that 3d CBDL $FXR^{-/-}$ mice, which were previously shown to have high urinary bile acid levels 3 days following surgery but later on excrete

mainly polyhydroxylated/nontoxic bile acids [43], showed tubular injury after 3d CBDL but were protected from renal fibrosis in the long-term course [100].

Not only genetic modification of the bile acid pool but also dietary modulation via (pre)treatment of CBDL mice with hydrophilic *nor*UDCA), which is has been shown to be excreted via urine [44], led to effective amelioration of cholemic nephropathy in long-term CBDL mice [186]. Since *nor*UDCA feeding had no positive effect on cholestatic liver injury in this model of long-term obstructive cholestasis, the kidney protective effects of *nor*UDCA cannot be explained by improvement of liver disease [186]. The results presented in Figures 12-16 and table 9 nicely show that *nor*UDCA effectively and significantly ameliorates the renal phenotype in long-term CBDL mice [186]. This seems to be due to a kidney-specific effect of *nor*UDCA which therefore could represent a new medical treatment for this extrahepatic manifestation of (obstructive) cholestasis [186]. Commencing *nor*UDCA treatment prior to CBDL (*norUDCA for Prevention*) almost completely prevented the development of kidney injury (Figure 13). Starting *nor*UDCA 3 days after CBDL was performed (*norUDCA for Rescue*) also resulted in less inflammation and significantly less fibrosis after 8 weeks [186]. This therapeutic effect was specific for cholemic nephropathy, since no beneficial effect was observed in 3 additionally studied non-cholestatic models of kidney injury (i.e. ischemia/reperfusion and LPS-induced AKI) and kidney fibrosis (i.e. the UUL model) (Figures 19 and 20) [186], which again argues for a key pathogenetic role of bile acids in cholemic nephropathy.

According to kidney, urine, serum, and liver bile acid profiles (Figure 18), the beneficial effect of *nor*UDCA in cholemic nephropathy might primarily be attributable to replacement of potentially cytotoxic endogenous bile acids by hydrophilic non-toxic *nor*UDCA metabolites [186]. As such, a trend towards decreased endogenous serum and increased endogenous urinary bile acids in *nor*UDCA- compared to chow-fed CBDL mice was observed [186]. In addition, the analyses of bile acid composition provided two major findings: First, enrichment of *nor*UDCA and its metabolites in kidney tissue despite a tendency for lower total serum bile acid levels and second, a substantial difference of *nor*UDCA metabolite profiles between kidney and urine [186]. These argues for a biologically relevant enrichment of *nor*UDCA and its metabolites in kidney tissue of *nor*UDCA-fed CBDL mice. It may be thus attractive to conclude that the substantial anti-inflammatory and antifibrotic effects that were observed in the *nor*UDCA-fed experimental

arms (*norUDCA for Prevention*; *norUDCA for Rescue,* Figures 15 and 16) were triggered by highly hydrophilic *nor*UDCA [186].

The data summarized within this thesis strongly argue for a role of bile acids in the pathogenesis of cholemic nephropathy [100, 186]. Under physiological conditions, the synthesis and transport of bile acids, sterol-derived compounds that are essential for the metabolism of lipids, proteins and glucose, is tightly regulated by specific receptors (including FXR and the G-protein–coupled bile acid receptor). These regulatory mechanisms involve the liver, small intestine and kidney. After synthesis and conjugation in the liver, bile acids are secreted into the small intestine and 95% are reabsorbed and enter the enterohepatic circulation. The small amount that spills into systemic circulation is glomerularly filtrated and almost completely reuptaken at the level of proximal tubules via the apical sodium-dependent transporter (ASBT) and organic solute transporter α/β (OST α/β) [73]. Besides this very low amount of urinary excreted bile acids under physiological conditions, the kidney compensates systemic accumulation of bile acids in experimental and clinical cholestasis via markedly induced renal elimination and urinary excretion.

The herein presented experiments revealed a bile acid peak around day 3 after CBDL [100, 140, 189] which conincides with the beginning of structural and functional renal alterations, namely detection of basement membrane defects, sloughing of tubular epithelial cells, discrete cast formations upon PAS-stained kidney sections and elevaed urinary NGAL levels [100, 186].

Also, increasing the hydrophilicity of the bile acid pool either genetically, by the use of $Fxr^{-/-}$ mice that exhibit a much more hydrophilic bile acid pool and were protected from development of cholemic nephropathy although beeing equally susceptible to kidney injury in response to UUL [100], or dietary by feeding hydrophilic *nor*UDCA significantly ameliorates the cholemic nephropathy typical renal changes in CBDL mice [186].

Throughout experimental studies between 1940 and 1950 mainly dogs were used and structural renal alterations including interstitial nephritis and renal fibrosis in cholestasis were described [100, 190]. In the subsequent years most laboratories changed to rats and the renal alterations in response to CBDL reported in this rodents are notoriously mild [100, 140, 191, 192]. Based on the impressive findings in CBDL mice it is tempting to

speculate that species-specific differences in bile acid metabolism might be an explanation for this phenotypical differences [100, 192].

This might also be a matter of bile acid concentration since no renal phenotype was observed in 8w DDC-fed and 8w Mdr2$^{-/-}$ mice which have lower serum bile acid levels compared to the CBDL mouse model [100, 166, 171]. Although the degree of liver injury, ductular reaction, and biliary type of fibrosis is more or less comparable in CBDL, DDC-fed, and Mdr2$^{-/-}$ mice, serum bile acid levels have been shown to be 5-fold (vs. 8w DDC) to 94-fold (vs. Mdr2$^{-/-}$) higher in CBDL mice [100, 166].

Also dynamics of serum bile acid increase may come into play since CBDL mice show a rather sudden bile acid increase (i.e. a 40-fold increase within 24 hours), while serum bile acid levels in DDC-fed mice rather rise continuously and slowly and can even normalize after 4 weeks [100, 171]. This might also hold true from a clinical perspective since common clinical features of cholemic nephropathy reported in a significant number of case reports/case series since 2000 include markedly elevated bilirubin levels with mean values of 30 mg/dl or even higher (Table 4) [107, 112, 113, 117, 120, 127, 130, 139]. As such, patients with severe alcoholic steatohepatitis, usually being deeply jaundiced, have a notoriously high risk for AKI [100, 193] (which could be at least in part caused by cholemic nephropathy).

The exact mechanism how bile acids lead to tubular epithelial injury and finally cholemic nephropathy remains enigmatic. It is unknown whether bile acids are acting via perturbations to renal and systemic hemodynamics, directly toxic upon tubular cells, or indirectly via other involved mechanisms [69, 194]. There is some evidence for a hemodynamic-driven mechanism [69]. As such, bile acids were shown negatively impact on cardiac function (i.e. decreased cardiac output caused by negative effects on contractility, induction of cardiomyocyte apoptosis and electrical conductance defects) and systemic hemodynamics (i.e. splanchnic vasodilatation and reduced systemic vascular resistance) which in turn compromises renal perfusion [69, 195, 196]. Reduced enteral bile acid concentrations in cholestasis facilitate bacterial translocation and systemic endotoxemia. Thus, alternative pathogenetic factors such as activation of toll-like receptor pathways through increased bacterial translocation [64] need to be considered as important cofactors and need to be studied in detail in future studies.

Besides bile acids, conjugated bilirubin is alternatively eliminated via the kidney in cholestasis. Unlike conjugated bilirubin, unconjugated bilirubin has been shown to be of nephrotoxic potential through mitochondrial damage [144, 145, 194, 197, 198]. Kidneys from CBDL mice do not show intratubular bilirubin accumulation or tubular casts containing abundant amounts of bilirubin [69]. Bilirubin might even have renoprotective effects. As such, it was shown to increase expression of heme oxygenase-1 (HO-1) in CBDL kidneys [199-204], which inherits a protective role in AKI. Whether accumulation of bilirubin in cholemic nephropathy, as described in human cases as "greenish" autopsy kidneys (attributable to the conversion of bilirubin to biliverdin due to formalin fixation and thus being an artifact), causes or at least contributes to tubular epithelial injury or only accumulates as a consequence of tubular epithelial injury and cast formation is so far unknown.

To date, cholemic nephropathy was referred to with different synonyms such as bile cast nephropathy [113], bile acid induced nephropathy [112] and icteric nephrosis among many others. The term bile cast nephropathy refers to the typical histological appearance, however, it remains controversial whether the formation ob intraluminal tubular casts represent the cause or consequence of cholemic nephropathy. Since histology remains the gold standard of diagnosis, cholemic nephropathy is mainly diagnosed upon autopsy and intraluminal casts might also be caused by autolysis. Bile acid nephropathy suggests the so far not entirely clarified pathogenetic mechanism; nevertheless the data shown within this thesis strongly suggest a pathogenetic role for bile acids. Using the "umbrella term" cholemic nephropathy might be advantageous since it neither restricts to a specific phenotype nor to a distinct pathogenesis.

In the absence of reliable non-invasive diagnostic tests, histological analysis of kidney biopsies or autopsy kidneys remains the only established diagnostic test and current gold standard to diagnose cholemic nephropathy. Performing a kidney biopsy, however, might often not be feasible and carries a substantial risk of bleeding in patients with ACLF, ACLD or cirrhosis considering the presence of coagulopathy. Also, the diagnostic lesions at the level of distal nephron segments (i.e. collecting ducts located on the boarder at the inner and outer strip and especially in the inner medulla) are likely to be missed by a conventional percutaneous kidney biopsy [100]. And last, performing a kidney biopsy

requires that the course of the suspected disease could be positively influenced by an available treatment option which is currently not the case in cholemic nephropathy. Regarding the risks of the procedure, Bräsen and Mederacke *et al.* reported on serious, potentially life-threatening (bleeding) complications when obtaining kidney biopsies for diagnosis of cholemic nephropathy (4/79, 5%) [134]. In this series, 2 bleeding events required coiling or even surgery [134, 165]. A considerably better safety profile can be obtained by using a transjugular route, however, this approach harbors the disadvantage of probably missing the relevant (distal) nephron segment and can only be performed in experienced centers.

Although all reported clinical cases and animal studies describe characteristic histological alterations consisting of tubular epithelial injury (predominantly in distal nephron segments) accompanied by intraluminal formation of bile casts, the histological criteria for diagnosing cholemic nephropathy are poorly defined [53, 165]. This so-called "characteristic histological alterations" may be easily missed on histology or could only present the tip of the iceberg in very severe forms of cholemic nephropathy. Also, histologic evaluation of the kidneys for bile casts which are typically described as red-brown, granular casts may be challenging since they might be easily missed on routine staining (such as H&E) and Hall's bilirubin stain is a more specialized and difficult stain to perform [163]. For milder lesions, as observed in earlier CBDL stages (3 or 7d CBDL) in murine models, kidney sections had to be accurately screened. Such milder, earlier observations could be loss of aquaporin 2 (AQP2) expression, which was observed in our CBDL mouse model but also in human cases of cholemic nephropathy [134]. Interestingly, this phenomenon was not only observed in full-blown cholemic nephropathy, but also in patients with AKI and hyperbilirubinaemia without clear histological evidence for cholemic nephropathy [134].

Urinary biomarkers may be used to differentiate between HRS-AKI and renal AKI such as cholemic nephropathy. In this context, the best validated biomarker is the urine neutrophil gelatinase-associated lipocalin (uNGAL) [205]. A uNGAL value of ≥220-244 µg/g creatinine identified the presence of ATN-AKI with a high sensitivity and specificity [42]. Also in the cholemic nephropathy mouse model, urinary expression for NGAL and increased mRNA expression for Lcn2 and Kim-1, another biomarker for tubular injury, could be found. A very simple parameter, namely the fractional excretion of sodium

(FENa) with a very low cut-off of <0.2% was reported to be suggestive of renal vasoconstriction with (levels <0.1% being highly predictive) may be considered in differential diagnosis [20, 206]. However, further studies are needed to confirm this results.

From a clinical point of view and due to limited availability, it seems unlikely that these- rather unspecific - markers are helpful for differentiating between functional HRS-AKI and cholemic nephropathy or cholemic nephropathy and other forms of tubular epithelial injury in daily routine [165].

In contrast, microscopic urinalysis could be promising. Bile casts and renal tubular epithelial cells have been found in animal models of cholemic nephropathy and bile-stained casts, leucocytes and renal epithelial cells containing granular or crystalline bilirubin have been described in case reports on cholemic nephropathy [112, 120, 128].

Defining clear diagnostic criteria would be of utmost importance. The clinical suspicion of cholemic nephropathy should be raised in the setting of AKI in deeply jaundiced patients (bilirubin levels > 20mg/dL) or distinct etiologies such as ASH or ACLF, especially when there is no response to vasoconstrictor treatment. Cholemic nephropathy with bile acid toxicity directed toward the kidneys could be an important factor for poor or even nonresponse to vasopressor therapy in (HRS-)AKI. As such, terlipressin was effective in only 13% of patients with HRS-AKI with serum bilirubin > 10 mg/dl, compared with 67% of patients with serum bilirubin < 10 mg/dl in a study by Nazar *et al* [207, 208]. Assuming that these patients had elevated serum bile acid levels because of their elevated bilirubin measures, this indicates that the degree of cholestasis is an important prognostic factor in HRS-AKI [69]. A study published by van Slambrouck *et al.* in 2013 reported the presence of bile casts 85% of the patients classified as HRS-AKI (13 out of 44 patients were classified as HRS-AKI, in 11 (85%) bile casts were found) [113], however, it has to be kept in mind that this could be confounded by the fact that mainly autopsy kidneys were screened. Another autopsy study found Hall-stain positive bile casts in 55% of 114 autopsy cases (patients with cirrhosis) [163]. The most common etiology of cirrhosis in this study was hepatitis C and hepatitis C combined with alcoholic liver disease. In the group with Hall-stain positive bile casts, eGFR was significantly reduced [163]. In this series, 4 out of 5 cases with a premortem diagnosis of HRS; were found to have bile casts, which is comparable to the 11 of 13 HRS cases with bile casts reported by van Slambrouck *et al*

[113, 163]. Interestingly and in contrast to many other caser reports an case series, bile casts in this study were found at much lower serum bilirubin levels (10,4 ± 12 mg/dL) – again – it has to kept in mind that this were autopsy kidneys, thus, the results may be compromised by *post mortem* preparation artifacts [163, 209].

Cholemic nephropathy has been described in a variety of acute or chronic liver alterations leading to jaundice. Interestingly, reversibility has been reported in cholemic nephropathy due to obstructive jaundice while most patients with cholemic nephropathy due to ACLF had a poor outcome (Table 4) [134, 135, 139]. This raises the question whether there are even subgroups of cholemic nephropathy such as a pure cholestatic subtype and an inflammatory subtype which could be the case in ACLF where inflammation plays a major role. This is, however, highly speculative so far and should be clarified in further studies.

4.1 Conclusion

Despite an increasing number of clinical cases and the awareness that etiopathogenesis of AKI in ACLD rather represents a “mixed bag” than a pure “functional” origin caused by altered hemodynamics, cholemic nephropathy remains an underdiagnosed entity. This could stem from the difficulty in assessing renal function in patients with ACLD/cirrhosis, a general lack of awareness of this condition as a diagnostic entity and difficulties in establishing its diagnosis since renal histology remains the gold standard and renal biopsies are uncommonly performed in patients with ACLD/cirrhosis. To better understand the pathophysiology and to be able to develop targeted therapeutic strategies, further clinical research in this area should aim on the development of (non-invasive) diagnostic biomarkers and study of their clinical impact. The experiments presented in that thesis suggest that bile acids are the key players in the pathogenesis of cholemic nephropathy and may also serve as a druggable target to treat cholemic nephropathy, measurement of serum and/or urinary bile acids and bile acid composition might thus be a useful source of biomarkers for diagnosing cholemic nephropathy.

4.2 Project-related presentations at national and international scientific conferences

Krones E, Pollheimer M, Durchschein F, Trauner M, Fickert P. *nor*UDCA protects CBDL mice from bile acid-induced collecting duct tubular injury. Submitted to XXII International Bile Acid Meeting - Hepatic and Extrahepatic Targets of Bile Acid Signalling 2012; Vienna, Austria. (Poster)

Krones E, Pollheimer M, Durchschein F, Trauner M, Fickert P. The effects of bile acids on renal collecting duct epithelial cell death – are bile acids the culprits in cholemic nephropathy? The 63rd Annual Meeting of the American Association for the Study of Liver Diseases: The Liver Meeting 2012, Boston, USA (Poster)

Krones E, Pollheimer MJ, Durchschein F, Kinslechner K, Deutschmann A, Trauner M, Fickert P. *nor*UDCA protects common bile duct ligated mice from collecting duct tubular epithelial lesions. Doctoral Day 2012, Graz, Austria (Oral presentation)

Krones E, Pollheimer MJ, Durchschein F, Kinslechner K, Deutschmann A, Eller K, Rosenkranz A, Trauner M, Fickert P. *nor*UDCA ameliorates cholemic nephropathy in long-term common bile duct ligated mice. EASL International Liver Congress 2013, Amsterdam, The Netherlands (Oral presentation)

Krones E, Pollheimer MJ, Durchschein F, Kinslechner K, Deutschmann A, Eller K, Kirsch A, Rosenkranz A, Marschall HU, Trauner M, Fickert P. *nor*UDCA – A novel therapeutic option for cholemic nephropathy? ISC – International Student Congress 2013, Graz, Austria (Oral presentation)

Krones E, Eller K, Rosenkranz A, Deutschmann A, Kinslechner K, Durchschein F, Pollheimer MJ, Trauner M, Fickert P. *nor*UDCA als Therapie der cholämischen Nephropathie. Jahrestagung der österreichischen Gesellschaften für Hypertensiologie und Nephrologie 2013, Linz, Austria (Oral presentation)

Krones E et al. Harn NGAL Spiegel reflektieren die therapeutischen Effekte von *nor*UDCA im Mausmodell der cholämischen Nephropathie. Jahrestagung der österreichischen Gesellschaft für Innere Medizin 2014, Salzburg, Austria (Poster)

Krones E. Cholämische Nephropathie – eine glomeruläre Erkrankung? Kongress für Nephrologie. 6. Jahrestagung Deutschen Gesellschaft für Nephrologie, Berlin, Germany (Oral presentation, invited lecture)

Krones E et al. Urinary NGAL Levels Reflect the Therapeutic Effects of *nor*UDCA in Mice with Cholemic Nephropathy. AASLD, The Liver Meeting® 2014, Boston, USA (Poster)

Krones E. Cholemic Nephropathy. Mini-Symposium "The immune system in kidney and liver disease" 21st April 2015. Medical University of Graz, Austria [Oral presentation]

4.3 Project-related peer-reviewed publications

Fickert P*, Krones E*, Pollheimer MJ, Thueringer A, Moustafa T, Silbert D, Halilbasic E, Yang M, Jaeschke H, Stokman G, Wells RG, Eller K, Rosenkranz AR, Eggertsen G, Langner C, Denk H, Wagner CA, Trauner M. (*P.F. and E.K. contributed equally to this paper) Bile Acids Trigger Cholemic Nephropathy in Common Bile-Duct-ligated Mice. Hepatology. 2013 Dec;58(6):2056-69.

Krones E, Eller K, Pollheimer MJ, Racedo S, Kirsch AH, Frauscher B, Wahlström A, Ståhlman M, Trauner M, Grahammer F, Huber TB, Wagner K, Rosenkranz AR, Marschall HU, Fickert P. NorUrsodeoxycholic Acid Ameliorates Cholemic Nephropathy in Bile Duct Ligated Mice. J Hepatol. 2017 Jul;67(1):110-119.

Krones, E; Wagner, M; Eller, K; Rosenkranz, AR; Trauner, M; Fickert, P. Bile acid-induced Cholemic Nephropathy. (Review) Dig Dis. 2015;33(3):367-75. doi: 10.1159/000371689.

Krones E, Pollheimer MJ, Rosenkranz AR, Fickert P. Cholemic Nephropathy – A Clinical Consequence of Altered Bile Acid Metabolism? Biochim Biophys Acta. 2018 Apr;1864(4 Pt B):1356-1366. doi: 10.1016/j.bbadis.2017.08.028. Epub 2017 Aug 26.

5 REFERENCES

1. Wiesner, R., et al., Model for end-stage liver disease (MELD) and allocation of donor livers. Gastroenterology, 2003. **124**(1): p. 91-6.
2. Jalan, R., et al., Development and validation of a prognostic score to predict mortality in patients with acute-on-chronic liver failure. J Hepatol, 2014. **61**(5): p. 1038-47.
3. Jalan, R., et al., The CLIF Consortium Acute Decompensation score (CLIF-C ADs) for prognosis of hospitalised cirrhotic patients without acute-on-chronic liver failure. J Hepatol, 2015. **62**(4): p. 831-40.
4. Louvet, A., et al., The Lille model: a new tool for therapeutic strategy in patients with severe alcoholic hepatitis treated with steroids. Hepatology, 2007. **45**(6): p. 1348-54.
5. Wong, F., et al., New consensus definition of acute kidney injury accurately predicts 30-day mortality in patients with cirrhosis and infection. Gastroenterology, 2013. **145**(6): p. 1280-8 e1.
6. Tsien, C.D., R. Rabie, and F. Wong, Acute kidney injury in decompensated cirrhosis. Gut, 2013. **62**(1): p. 131-7.
7. de Carvalho, J.R., et al., Acute kidney injury network criteria as a predictor of hospital mortality in cirrhotic patients with ascites. J Clin Gastroenterol, 2012. **46**(3): p. e21-6.
8. Bera, C. and F. Wong, Management of hepatorenal syndrome in liver cirrhosis: a recent update. Therap Adv Gastroenterol, 2022. **15**: p. 17562848221102679.
9. Moreau, R. and D. Lebrec, Acute renal failure in patients with cirrhosis: perspectives in the age of MELD. Hepatology, 2003. **37**(2): p. 233-43.
10. Nair, S., S. Verma, and P.J. Thuluvath, Pretransplant renal function predicts survival in patients undergoing orthotopic liver transplantation. Hepatology, 2002. **35**(5): p. 1179-85.
11. Kamath, P.S., et al., A model to predict survival in patients with end-stage liver disease. Hepatology, 2001. **33**(2): p. 464-70.
12. Durand, F. and D. Valla, Assessment of the prognosis of cirrhosis: Child-Pugh versus MELD. J Hepatol, 2005. **42 Suppl**(1): p. S100-7.
13. Moreau, R., et al., Acute-on-chronic liver failure is a distinct syndrome that develops in patients with acute decompensation of cirrhosis. Gastroenterology, 2013. **144**(7): p. 1426-37, 1437 e1-9.
14. Garcia-Tsao, G., C.R. Parikh, and A. Viola, Acute kidney injury in cirrhosis. Hepatology, 2008. **48**(6): p. 2064-77.
15. Angeli, P., et al., Diagnosis and management of acute kidney injury in patients with cirrhosis: revised consensus recommendations of the International Club of Ascites. J Hepatol, 2015. **62**(4): p. 968-74.
16. Nadim, M.K., et al., Hepatorenal syndrome: the 8th International Consensus Conference of the Acute Dialysis Quality Initiative (ADQI) Group. Crit Care, 2012. **16**(1): p. R23.
17. Gerbes, A.L., Liver Cirrhosis and Kidney. Dig Dis, 2016. **34**(4): p. 387-90.
18. Angeli, P., et al., Diagnosis and management of acute kidney injury in patients with cirrhosis: revised consensus recommendations of the International Club of Ascites. Gut, 2015. **64**(4): p. 531-7.

19. Wong, F., The evolving concept of acute kidney injury in patients with cirrhosis. Nat Rev Gastroenterol Hepatol, 2015. **12**(12): p. 711-9.
20. Angeli, P., et al., News in pathophysiology, definition and classification of hepatorenal syndrome: A step beyond the International Club of Ascites (ICA) consensus document. J Hepatol, 2019. **71**(4): p. 811-822.
21. Fede, G., et al., Renal failure and cirrhosis: a systematic review of mortality and prognosis. J Hepatol, 2012. **56**(4): p. 810-8.
22. Mindikoglu, A.L., et al., Performance of chronic kidney disease epidemiology collaboration creatinine-cystatin C equation for estimating kidney function in cirrhosis. Hepatology, 2014. **59**(4): p. 1532-42.
23. Francoz, C., et al., The evaluation of renal function and disease in patients with cirrhosis. J Hepatol, 2010. **52**(4): p. 605-13.
24. Francoz, C., et al., Inaccuracies of creatinine and creatinine-based equations in candidates for liver transplantation with low creatinine: impact on the model for end-stage liver disease score. Liver Transpl, 2010. **16**(10): p. 1169-77.
25. Cholongitas, E., et al., Review article: renal function assessment in cirrhosis - difficulties and alternative measurements. Aliment Pharmacol Ther, 2007. **26**(7): p. 969-78.
26. Sherman, D.S., D.N. Fish, and I. Teitelbaum, Assessing renal function in cirrhotic patients: problems and pitfalls. Am J Kidney Dis, 2003. **41**(2): p. 269-78.
27. Randers, E. and E.J. Erlandsen, Serum cystatin C as an endogenous marker of the renal function--a review. Clin Chem Lab Med, 1999. **37**(4): p. 389-95.
28. De Souza, V., et al., Creatinine- versus cystatine C-based equations in assessing the renal function of candidates for liver transplantation with cirrhosis. Hepatology, 2014. **59**(4): p. 1522-31.
29. Orlando, R., et al., Diagnostic value of plasma cystatin C as a glomerular filtration marker in decompensated liver cirrhosis. Clin Chem, 2002. **48**(6 Pt 1): p. 850-8.
30. Seo, Y.S., et al., Serum cystatin C level is a good prognostic marker in patients with cirrhotic ascites and normal serum creatinine levels. Liver Int, 2009. **29**(10): p. 1521-7.
31. Ustundag, Y., et al., Analysis of glomerular filtration rate, serum cystatin C levels, and renal resistive index values in cirrhosis patients. Clin Chem Lab Med, 2007. **45**(7): p. 890-4.
32. Xirouchakis, E., et al., Comparison of cystatin C and creatinine-based glomerular filtration rate formulas with 51Cr-EDTA clearance in patients with cirrhosis. Clin J Am Soc Nephrol, 2011. **6**(1): p. 84-92.
33. Gerbes, A.L., et al., Evaluation of serum cystatin C concentration as a marker of renal function in patients with cirrhosis of the liver. Gut, 2002. **50**(1): p. 106-10.
34. Stevens, L.A., et al., Factors other than glomerular filtration rate affect serum cystatin C levels. Kidney Int, 2009. **75**(6): p. 652-60.
35. Francoz, C., M.K. Nadim, and F. Durand, Kidney Biomarkers in Cirrhosis. J Hepatol, 2016.
36. Wu, H., et al., IL-18 contributes to renal damage after ischemia-reperfusion. J Am Soc Nephrol, 2008. **19**(12): p. 2331-41.
37. Ichimura, T., et al., Kidney injury molecule-1 (KIM-1), a putative epithelial cell adhesion molecule containing a novel immunoglobulin domain, is up-regulated in renal cells after injury. J Biol Chem, 1998. **273**(7): p. 4135-42.
38. Furuhashi, M. and G.S. Hotamisligil, Fatty acid-binding proteins: role in metabolic diseases and potential as drug targets. Nat Rev Drug Discov, 2008. **7**(6): p. 489-503.

39. Kamijo-Ikemori, A., et al., Roles of human liver type fatty acid binding protein in kidney disease clarified using hL-FABP chromosomal transgenic mice. Nephrology (Carlton), 2011. **16**(6): p. 539-44.
40. Fagundes, C., et al., Urinary neutrophil gelatinase-associated lipocalin as biomarker in the differential diagnosis of impairment of kidney function in cirrhosis. J Hepatol, 2012. **57**(2): p. 267-73.
41. Belcher, J.M., et al., Kidney biomarkers and differential diagnosis of patients with cirrhosis and acute kidney injury. Hepatology, 2014. **60**(2): p. 622-32.
42. Huelin, P., et al., Neutrophil Gelatinase-Associated Lipocalin for Assessment of Acute Kidney Injury in Cirrhosis: A Prospective Study. Hepatology, 2019. **70**(1): p. 319-333.
43. Ariza, X., et al., Analysis of a urinary biomarker panel for clinical outcomes assessment in cirrhosis. PLoS One, 2015. **10**(6): p. e0128145.
44. Slack, A.J., et al., Predicting the development of acute kidney injury in liver cirrhosis--an analysis of glomerular filtration rate, proteinuria and kidney injury biomarkers. Aliment Pharmacol Ther, 2013. **37**(10): p. 989-97.
45. Makris, K., et al., Urinary neutrophil gelatinase-associated lipocalin (NGAL) as an early marker of acute kidney injury in critically ill multiple trauma patients. Clin Chem Lab Med, 2009. **47**(1): p. 79-82.
46. Mishra, J., et al., Identification of neutrophil gelatinase-associated lipocalin as a novel early urinary biomarker for ischemic renal injury. J Am Soc Nephrol, 2003. **14**(10): p. 2534-43.
47. Mishra, J., et al., Amelioration of ischemic acute renal injury by neutrophil gelatinase-associated lipocalin. J Am Soc Nephrol, 2004. **15**(12): p. 3073-82.
48. Wheeler, D.S., et al., Serum neutrophil gelatinase-associated lipocalin (NGAL) as a marker of acute kidney injury in critically ill children with septic shock. Crit Care Med, 2008. **36**(4): p. 1297-303.
49. Otto, G.P., et al., Impact of sepsis-associated cytokine storm on plasma NGAL during acute kidney injury in a model of polymicrobial sepsis. Crit Care, 2013. **17**(2): p. 419.
50. Macdonald, S.P., et al., Sustained elevation of resistin, NGAL and IL-8 are associated with severe sepsis/septic shock in the emergency department. PLoS One, 2014. **9**(10): p. e110678.
51. Bianchi, C., et al., Reappraisal of serum beta2-microglobulin as marker of GFR. Ren Fail, 2001. **23**(3-4): p. 419-29.
52. Shinkai, S., et al., Beta2-microglobulin for risk stratification of total mortality in the elderly population: comparison with cystatin C and C-reactive protein. Arch Intern Med, 2008. **168**(2): p. 200-6.
53. Krones, E., et al., Cholemic nephropathy - Historical notes and novel perspectives. Biochim Biophys Acta Mol Basis Dis, 2018. **1864**(4 Pt B): p. 1356-1366.
54. Siew, E.D., L.B. Ware, and T.A. Ikizler, Biological markers of acute kidney injury. J Am Soc Nephrol, 2011. **22**(5): p. 810-20.
55. EASL clinical practice guidelines on the management of ascites, spontaneous bacterial peritonitis, and hepatorenal syndrome in cirrhosis. J Hepatol, 2010. **53**(3): p. 397-417.
56. Arroyo, V., et al., Definition and diagnostic criteria of refractory ascites and hepatorenal syndrome in cirrhosis. International Ascites Club. Hepatology, 1996. **23**(1): p. 164-76.
57. Arroyo, V., J. Fernandez, and P. Gines, Pathogenesis and treatment of hepatorenal syndrome. Semin Liver Dis, 2008. **28**(1): p. 81-95.

58. Gines, P. and R.W. Schrier, Renal failure in cirrhosis. N Engl J Med, 2009. **361**(13): p. 1279-90.
59. Arroyo, V., M. Guevara, and P. Gines, Hepatorenal syndrome in cirrhosis: pathogenesis and treatment. Gastroenterology, 2002. **122**(6): p. 1658-76.
60. Arroyo, V., C. Terra, and P. Gines, Advances in the pathogenesis and treatment of type-1 and type-2 hepatorenal syndrome. J Hepatol, 2007. **46**(5): p. 935-46.
61. Bernardi, M., et al., Mechanisms of decompensation and organ failure in cirrhosis: From peripheral arterial vasodilation to systemic inflammation hypothesis. J Hepatol, 2015. **63**(5): p. 1272-84.
62. Prowle, J.R. and R. Bellomo, Sepsis-associated acute kidney injury: macrohemodynamic and microhemodynamic alterations in the renal circulation. Semin Nephrol, 2015. **35**(1): p. 64-74.
63. Shah, N., et al., Increased renal expression and urinary excretion of TLR4 in acute kidney injury associated with cirrhosis. Liver Int, 2013. **33**(3): p. 398-409.
64. Shah, N., et al., Prevention of acute kidney injury in a rodent model of cirrhosis following selective gut decontamination is associated with reduced renal TLR4 expression. J Hepatol, 2012. **56**(5): p. 1047-53.
65. Jouet, P., et al., Transjugular renal biopsy in the treatment of patients with cirrhosis and renal abnormalities. Hepatology, 1996. **24**(5): p. 1143-7.
66. Trawale, J.M., et al., The spectrum of renal lesions in patients with cirrhosis: a clinicopathological study. Liver Int, 2010. **30**(5): p. 725-32.
67. Mandal, A.K., M. Lansing, and A. Fahmy, Acute tubular necrosis in hepatorenal syndrome: an electron microscopy study. Am J Kidney Dis, 1982. **2**(3): p. 363-74.
68. Wong, F., et al., Terlipressin plus Albumin for the Treatment of Type 1 Hepatorenal Syndrome. N Engl J Med, 2021. **384**(9): p. 818-828.
69. Fickert, P. and A.R. Rosenkranz, Bile Acids Are Important Contributors to AKI Associated with Liver Disease: PRO. Kidney360, 2022. **3**(1): p. 17-20.
70. Wagner, M. and M. Trauner, Recent advances in understanding and managing cholestasis. F1000Res, 2016. **5**.
71. Wagner, M., G. Zollner, and M. Trauner, New molecular insights into the mechanisms of cholestasis. J Hepatol, 2009. **51**(3): p. 565-80.
72. Dawson, P.A., T. Lan, and A. Rao, Bile acid transporters. J Lipid Res, 2009. **50**(12): p. 2340-57.
73. Stiehl, A., Bile salt sulphates in cholestasis. Eur J Clin Invest, 1974. **4**(1): p. 59-63.
74. Weiner, I.M., J.E. Glasser, and L. Lack, Renal Excretion of Bile Acids: Taurocholic, Glycocholic, and Colic Acids. Am J Physiol, 1964. **207**: p. 964-70.
75. Wilson, F.A., et al., Sodium-coupled taurocholate transport in the proximal convolution of the rat kidney in vivo and in vitro. J Clin Invest, 1981. **67**(4): p. 1141-50.
76. Christie, D.M., et al., Comparative analysis of the ontogeny of a sodium-dependent bile acid transporter in rat kidney and ileum. Am J Physiol, 1996. **271**(2 Pt 1): p. G377-85.
77. Craddock, A.L., et al., Expression and transport properties of the human ileal and renal sodium-dependent bile acid transporter. Am J Physiol, 1998. **274**(1 Pt 1): p. G157-69.
78. Ballatori, N., et al., OSTalpha-OSTbeta: a major basolateral bile acid and steroid transporter in human intestinal, renal, and biliary epithelia. Hepatology, 2005. **42**(6): p. 1270-9.
79. Popper, H. and F. Schaffner, Pathophysiology of cholestasis. Hum Pathol, 1970. **1**(1): p. 1-24.

80. Zollner, G. and M. Trauner, Mechanisms of cholestasis. Clin Liver Dis, 2008. **12**(1): p. 1-26, vii.
81. Wagner, M., et al., Role of farnesoid X receptor in determining hepatic ABC transporter expression and liver injury in bile duct-ligated mice. Gastroenterology, 2003. **125**(3): p. 825-38.
82. Zollner, G., et al., Role of nuclear bile acid receptor, FXR, in adaptive ABC transporter regulation by cholic and ursodeoxycholic acid in mouse liver, kidney and intestine. J Hepatol, 2003. **39**(4): p. 480-8.
83. Denk, G.U., et al., Multidrug resistance-associated protein 4 is up-regulated in liver but down-regulated in kidney in obstructive cholestasis in the rat. J Hepatol, 2004. **40**(4): p. 585-91.
84. Boyer, J.L., et al., Upregulation of a basolateral FXR-dependent bile acid efflux transporter OSTalpha-OSTbeta in cholestasis in humans and rodents. Am J Physiol Gastrointest Liver Physiol, 2006. **290**(6): p. G1124-30.
85. Mennone, A., et al., Mrp4-/- mice have an impaired cytoprotective response in obstructive cholestasis. Hepatology, 2006. **43**(5): p. 1013-21.
86. Zollner, G., et al., Coordinated induction of bile acid detoxification and alternative elimination in mice: role of FXR-regulated organic solute transporter-alpha/beta in the adaptive response to bile acids. Am J Physiol Gastrointest Liver Physiol, 2006. **290**(5): p. G923-32.
87. Zollner, G., et al., Expression of bile acid synthesis and detoxification enzymes and the alternative bile acid efflux pump MRP4 in patients with primary biliary cirrhosis. Liver Int, 2007. **27**(7): p. 920-9.
88. Krones, E., et al., Bile acid-induced cholemic nephropathy. Dig Dis, 2015. **33**(3): p. 367-75.
89. Walker, J.G., Renal failure in jaundice. Proc R Soc Med, 1962. **55**: p. 570.
90. Dawson, J.L., Acute post-operative renal failure in obstructive jaundice. Ann R Coll Surg Engl, 1968. **42**(3): p. 163-81.
91. Zollinger, R.M. and R.D. Williams, Surgical aspects of jaundice. Surgery, 1956. **39**(6): p. 1016-30.
92. Williams, R.D., D.W. Elliott, and R.M. Zollinger, The effect of hypotension in obstructive jaundice. Arch Surg, 1960. **81**: p. 334-40.
93. Dawson, J.L., The Incidence of Postoperative Renal Failure in Obstructive Jaundice. Br J Surg, 1965. **52**: p. 663-5.
94. Armstrong, C.P., et al., Surgical experience of deeply jaundiced patients with bile duct obstruction. Br J Surg, 1984. **71**(3): p. 234-8.
95. Neuhaus, T.J., et al., Familial progressive tubulo-interstitial nephropathy and cholestatic liver disease -- a newly recognized entity? Eur J Pediatr, 1997. **156**(9): p. 723-6.
96. Harris, H.W., Jr., et al., Progressive tubulointerstitial renal disease in infancy with associated hepatic abnormalities. Am J Med, 1986. **81**(1): p. 169-76.
97. Popovic-Rolovic, M., et al., Progressive tubulointerstitial nephritis and chronic cholestatic liver disease. Pediatr Nephrol, 1993. **7**(4): p. 396-400.
98. Proesmans, W., et al., Fatal tubulo-intestitial nephropathy with chronic cholestatic liver disease. Acta Paediatr Belg, 1976. **29**(4): p. 231-8.
99. Henrot, B., et al., Progressive tubulointerstitial nephropathy with hepatic involvement in an infant. Eur J Pediatr, 1990. **149**(5): p. 365-7.
100. Fickert, P., et al., Bile acids trigger cholemic nephropathy in common bile-duct-ligated mice. Hepatology, 2013. **58**(6): p. 2056-69.

101. Montini, G., et al., Chronic cholestatic liver disease with associated tubulointerstitial nephropathy in early childhood. Pediatrics, 1997. **100**(3): p. E10.
102. Tekin, N., et al., Clinical and pathological aspects of ARC (arthrogryposis, renal dysfunction and cholestasis) syndrome in two siblings. Turk J Pediatr, 2005. **47**(1): p. 67-70.
103. Papadia, F., et al., Biliary malformation with renal tubular insufficiency in two male infants: third family report. Clin Genet, 1996. **49**(5): p. 267-70.
104. Mikati, M.A., et al., Renal tubular insufficiency, cholestatic jaundice, and multiple congenital anomalies--a new multisystem syndrome. Helv Paediatr Acta, 1984. **39**(5-6): p. 463-71.
105. Gentilini, P. and G. La Villa, Liver-kidney pathophysiological interrelationships in liver diseases. Dig Liver Dis, 2008. **40**(12): p. 909-19.
106. Bairaktari, E., et al., Partially reversible renal tubular damage in patients with obstructive jaundice. Hepatology, 2001. **33**(6): p. 1365-9.
107. Betjes, M.G. and I. Bajema, The pathology of jaundice-related renal insufficiency: cholemic nephrosis revisited. J Nephrol, 2006. **19**(2): p. 229-33.
108. Holmes, T.W., Jr., The histologic lesion of cholemic nephrosis. J Urol, 1953. **70**(5): p. 677-85.
109. Lenti, G., et al., [Pathogenetic aspects of cholemic nephropathy]. Minerva Med, 1978. **69**(47): p. 3203-14.
110. Pasero, G. and G. Tamagnini, [Cholemic tubulo-nephrosis; functional symptomatology of the kidney in icteric syndromes]. Omnia Ther Suppl, 1958. **36**(1-2): p. 1-35.
111. Sant, S.M. and N.M. Purandare, Cholemic Nephrosis--an Autopsy and Experimental Study. J Postgrad Med, 1965. **11**: p. 79-89.
112. Luciano, R.L., et al., Bile acid nephropathy in a bodybuilder abusing an anabolic androgenic steroid. Am J Kidney Dis, 2014. **64**(3): p. 473-6.
113. van Slambrouck, C.M., et al., Bile cast nephropathy is a common pathologic finding for kidney injury associated with severe liver dysfunction. Kidney Int, 2013. **84**(1): p. 192-7.
114. Bal, C., et al., Renal function and structure in subacute hepatic failure. J Gastroenterol Hepatol, 2000. **15**(11): p. 1318-24.
115. Kiewe, P., et al., Unusual sites of Hodgkin's lymphoma: CASE 3. Cholemic nephrosis in Hodgkin's lymphoma with liver involvement. J Clin Oncol, 2004. **22**(20): p. 4230-1.
116. Uslu, A., et al., Human kidney histopathology in acute obstructive jaundice: a prospective study. Eur J Gastroenterol Hepatol, 2010. **22**(12): p. 1458-65.
117. Bredewold, O.W., J.W. de Fijter, and T. Rabelink, A case of mononucleosis infectiosa presenting with cholemic nephrosis. NDT Plus, 2011. **4**(3): p. 170-2.
118. Rafat, C., et al., Bilirubin-associated acute tubular necrosis in a kidney transplant recipient. Am J Kidney Dis, 2013. **61**(5): p. 782-5.
119. van der Wijngaart, H., et al., A 73-year-old male with jaundice and acute kidney injury. Bile cast nephropathy. Neth J Med, 2014. **72**(2): p. 95, 99.
120. Jain, K., et al., Bile cast nephropathy. Kidney Int, 2015. **87**(2): p. 484.
121. Sequeira, A. and X. Gu, Bile cast nephropathy: an often forgotten diagnosis. Hemodial Int, 2015. **19**(1): p. 132-5.
122. Tabatabaee, S.M., R. Elahi, and S. Savaj, Bile cast nephropathy due to cholestatic jaundice after using stanozolol in 2 amateur bodybuilders. Iran J Kidney Dis, 2015. **9**(4): p. 331-4.

123. Patel, J., et al., Bile cast nephropathy: A case report and review of the literature. World J Gastroenterol, 2016. **22**(27): p. 6328-34.
124. Sens, F., et al., Efficacy of extracorporeal albumin dialysis for acute kidney injury due to cholestatic jaundice nephrotoxicity. BMJ Case Rep, 2016. **2016**.
125. Werner, C.R., et al., [Acute kidney injury in liver failure]. Dtsch Med Wochenschr, 2016. **141**(21): p. 1559.
126. Alkhunaizi, A.M., et al., Acute bile nephropathy secondary to anabolic steroids. Clin Nephrol, 2016. **85**(2): p. 121-6.
127. Alnasrallah, B., J.F. Collins, and L.J. Zwi, Bile Nephropathy in Flucloxacillin-Induced Cholestatic Liver Dysfunction. Case Rep Nephrol, 2016. **2016**: p. 4162674.
128. Mohapatra, M.K., et al., Urinary bile casts in bile cast nephropathy secondary to severe falciparum malaria. Clin Kidney J, 2016. **9**(4): p. 644-8.
129. Leclerc, M., et al., [Bile salt nephropathy/cholemic nephrosis]. Nephrol Ther, 2016. **12**(6): p. 460-462.
130. Aniort, J., et al., Bile Cast Nephropathy Caused by Obstructive Cholestasis. Am J Kidney Dis, 2017. **69**(1): p. 143-146.
131. Sood, V., et al., Cholemic or Bile Cast Nephropathy in a Child with Liver Failure. J Clin Exp Hepatol, 2017. **7**(4): p. 373-375.
132. Nayak, S., et al., Cholemic Nephrosis from Acute Hepatitis E Virus Infection: A Forgotten Entity? Indian J Nephrol, 2018. **28**(3): p. 250-251.
133. Ravi, R., et al., Bile cast nephropathy causing acute kidney injury in a patient with nonfulminant acute hepatitis A. Saudi J Kidney Dis Transpl, 2018. **29**(6): p. 1498-1501.
134. Brasen, J.H., et al., Cholemic Nephropathy Causes Acute Kidney Injury and Is Accompanied by Loss of Aquaporin 2 in Collecting Ducts. Hepatology, 2019. **69**(5): p. 2107-2119.
135. Mukherjee, T., et al., Cholemic nephrosis (bile cast nephropathy) with severe liver dysfunction. Med J Armed Forces India, 2019. **75**(2): p. 216-218.
136. Chango Azanza, J.J., N. Lopetegui Lia, and P.M. Calle Sarmiento, Bile Cast Nephropathy Secondary to Hemophagocytic Lymphohistiocytosis With Liver Failure. Cureus, 2020. **12**(9): p. e10226.
137. Priyaa, V., et al., Cholemic Nephrosis: An Autopsy Study of a Forgotten Entity. Turk Patoloji Derg, 2021. **37**(3): p. 212-218.
138. Al Awadhi, H., et al., Bile acid nephropathy induced by anabolic steroids: A case report and review of the literature. Clin Nephrol Case Stud, 2021. **9**: p. 123-129.
139. Maiwall, R., et al., Natural history, spectrum and outcome of stage 3 AKI in patients with acute-on-chronic liver failure. Liver Int, 2022.
140. Kaler, B., et al., Are bile acids involved in the renal dysfunction of obstructive jaundice? An experimental study in bile duct ligated rats. Ren Fail, 2004. **26**(5): p. 507-16.
141. Haessler, H., P. Rous, and G.O. Broun, The Renal Elimination of Bilirubin. J Exp Med, 1922. **35**(4): p. 533-52.
142. Levy, M. and H. Finestone, Renal response to four hours of biliary obstruction in the dog. Am J Physiol, 1983. **244**(5): p. F516-25.
143. Topuzlu, C. and W.M. Stahl, Effect of bile infusion on the dog kidney. N Engl J Med, 1966. **274**(14): p. 760-3.
144. Gollan, J.L., B.H. Billing, and S.N. Huang, Ultrastructural changes in the isolated rat kidney induced by conjugated bilirubin and bile acids. Br J Exp Pathol, 1976. **57**(5): p. 571-81.

145. Rivera-Huizar, S., et al., Renal dysfunction as a consequence of acute liver damage by bile duct ligation in cirrhotic rats. Exp Toxicol Pathol, 2006. **58**(2-3): p. 185-95.
146. Bomzon, A., S. Holt, and K. Moore, Bile acids, oxidative stress, and renal function in biliary obstruction. Semin Nephrol, 1997. **17**(6): p. 549-62.
147. Kramer, H.J., Impaired renal function in obstructive jaundice: roles of the thromboxane and endothelin systems. Nephron, 1997. **77**(1): p. 1-12.
148. Kramer, H.J., K. Schwarting, and A. Backer, Impaired renal function in obstructive jaundice: enhanced glomerular thromboxane synthesis and effects of thromboxane receptor blockade in bile duct-ligated rats. Clin Sci (Lond), 1995. **88**(1): p. 39-45.
149. Kramer, H.J., et al., Renal endothelin system in obstructive jaundice: its role in impaired renal function of bile-duct ligated rats. Clin Sci (Lond), 1997. **92**(6): p. 579-85.
150. Panozzo, M.P., et al., Altered lipid peroxidation/glutathione ratio in experimental extrahepatic cholestasis. Clin Exp Pharmacol Physiol, 1995. **22**(4): p. 266-71.
151. Panozzo, M.P., et al., Renal functional alterations in extrahepatic cholestasis: can oxidative stress be involved? Eur Surg Res, 1995. **27**(5): p. 332-9.
152. Parks, R.W. and B.J. Rowlands, Renal dysfunction and endotoxaemia in obstructive jaundice. Natl Med J India, 1995. **8**(6): p. 249-51.
153. Clements, W.D., et al., Role of the gut in the pathophysiology of extrahepatic biliary obstruction. Gut, 1996. **39**(4): p. 587-93.
154. Hampel, H., et al., Risk factors for the development of renal dysfunction in hospitalized patients with cirrhosis. Am J Gastroenterol, 2001. **96**(7): p. 2206-10.
155. Terg, R., et al., Serum creatinine and bilirubin predict renal failure and mortality in patients with spontaneous bacterial peritonitis: a retrospective study. Liver Int, 2009. **29**(3): p. 415-9.
156. Leem, J., et al., Serum Total Bilirubin Levels Provide Additive Risk Information over the Framingham Risk Score for Identifying Asymptomatic Diabetic Patients at Higher Risk for Coronary Artery Stenosis. Diabetes Metab J, 2015. **39**(5): p. 414-23.
157. Riphagen, I.J., et al., Bilirubin and progression of nephropathy in type 2 diabetes: a post hoc analysis of RENAAL with independent replication in IDNT. Diabetes, 2014. **63**(8): p. 2845-53.
158. Boon, A.C., et al., Endogenously elevated bilirubin modulates kidney function and protects from circulating oxidative stress in a rat model of adenine-induced kidney failure. Sci Rep, 2015. **5**: p. 15482.
159. Nath, K.A., Heme oxygenase-1: a provenance for cytoprotective pathways in the kidney and other tissues. Kidney Int, 2006. **70**(3): p. 432-43.
160. Kawaguchi, K. and M. Koike, Glomerular alterations associated with obstructive jaundice. Hum Pathol, 1987. **18**(11): p. 1149-54.
161. Sequeira, A. and X. Gu, Bile cast nephropathy: An often forgotten diagnosis. Hemodial Int, 2014.
162. Song J., C.A., Jaundice-associated acute kidney injury. NDT Plus, 2009. **2**: p. 82-83.
163. Foshat, M., et al., Bile Cast Nephropathy in Cirrhotic Patients: Effects of Chronic Hyperbilirubinemia. Am J Clin Pathol, 2017. **147**(5): p. 525-535.
164. Torrealba, J., et al., Bile Cast Nephropathy: A Pathologic Finding with Manifold Causes Displayed in an Adult with Alcoholic Steatohepatitis and in a Child with Wilson's Disease. Case Rep Nephrol Dial, 2018. **8**(3): p. 207-215.

165. Mandorfer, M. and M. Hecking, The Renaissance of Cholemic Nephropathy: A Likely Underestimated Cause of Renal Dysfunction in Liver Disease. Hepatology, 2019. **69**(5): p. 1858-1860.
166. Pollheimer, M.J., M. Trauner, and P. Fickert, Will we ever model PSC? - "It's hard to be a PSC model!". Clin Res Hepatol Gastroenterol, 2011.
167. Pollheimer, M.J. and P. Fickert, Animal models in primary biliary cirrhosis and primary sclerosing cholangitis. Clin Rev Allergy Immunol, 2015. **48**(2-3): p. 207-17.
168. Fickert, P., et al., Regurgitation of bile acids from leaky bile ducts causes sclerosing cholangitis in Mdr2 (Abcb4) knockout mice. Gastroenterology, 2004. **127**(1): p. 261-74.
169. Popov, Y., et al., Mdr2 (Abcb4)-/- mice spontaneously develop severe biliary fibrosis via massive dysregulation of pro- and antifibrogenic genes. J Hepatol, 2005. **43**(6): p. 1045-54.
170. Ackermann, D., et al., Sodium retention and ascites formation in a cholestatic mice model: role of aldosterone and mineralocorticoid receptor? Hepatology, 2007. **46**(1): p. 173-9.
171. Fickert, P., et al., A new xenobiotic-induced mouse model of sclerosing cholangitis and biliary fibrosis. Am J Pathol, 2007. **171**(2): p. 525-36.
172. Fickert, P., et al., Lithocholic acid feeding induces segmental bile duct obstruction and destructive cholangitis in mice. Am J Pathol, 2006. **168**(2): p. 410-22.
173. Trauner, M., et al., New therapeutic concepts in bile acid transport and signaling for management of cholestasis. Hepatology, 2016.
174. Schaap, F.G., M. Trauner, and P.L. Jansen, Bile acid receptors as targets for drug development. Nat Rev Gastroenterol Hepatol, 2014. **11**(1): p. 55-67.
175. Hofmann, A.F., et al., Novel biotransformation and physiological properties of norursodeoxycholic acid in humans. Hepatology, 2005. **42**(6): p. 1391-8.
176. Fickert, P., et al., norUrsodeoxycholic acid improves cholestasis in primary sclerosing cholangitis. J Hepatol, 2017. **67**(3): p. 549-558.
177. Fickert, P., et al., 24-norUrsodeoxycholic acid is superior to ursodeoxycholic acid in the treatment of sclerosing cholangitis in Mdr2 (Abcb4) knockout mice. Gastroenterology, 2006. **130**(2): p. 465-81.
178. Halilbasic, E., et al., Side chain structure determines unique physiologic and therapeutic properties of norursodeoxycholic acid in Mdr2-/- mice. Hepatology, 2009. **49**(6): p. 1972-81.
179. Bolignano, D., et al., Neutrophil gelatinase-associated lipocalin (NGAL) as a marker of kidney damage. Am J Kidney Dis, 2008. **52**(3): p. 595-605.
180. Tremaroli, V., et al., Roux-en-Y Gastric Bypass and Vertical Banded Gastroplasty Induce Long-Term Changes on the Human Gut Microbiome Contributing to Fat Mass Regulation. Cell Metab, 2015. **22**(2): p. 228-38.
181. Gaush, C.R., W.L. Hard, and T.F. Smith, Characterization of an established line of canine kidney cells (MDCK). Proc Soc Exp Biol Med, 1966. **122**(3): p. 931-5.
182. Nielsen, S., et al., Cellular and subcellular immunolocalization of vasopressin-regulated water channel in rat kidney. Proc Natl Acad Sci U S A, 1993. **90**(24): p. 11663-7.
183. Brown, D., et al., Sensing, signaling and sorting events in kidney epithelial cell physiology. Traffic, 2009. **10**(3): p. 275-84.
184. Liu, Y., Cellular and molecular mechanisms of renal fibrosis. Nat Rev Nephrol, 2011. **7**(12): p. 684-96.

185. Marschall, H.U., et al., Fxr(-/-) mice adapt to biliary obstruction by enhanced phase I detoxification and renal elimination of bile acids. J Lipid Res, 2006. **47**(3): p. 582-92.
186. Krones, E., et al., NorUrsodeoxycholic acid ameliorates cholemic nephropathy in bile duct ligated mice. J Hepatol, 2017.
187. Fickert, P., et al., Differential effects of norUDCA and UDCA in obstructive cholestasis in mice. J Hepatol, 2013. **58**(6): p. 1201-8.
188. Velez, J.C.Q., G. Therapondos, and L.A. Juncos, Reappraising the spectrum of AKI and hepatorenal syndrome in patients with cirrhosis. Nat Rev Nephrol, 2020. **16**(3): p. 137-155.
189. Lee, J., et al., Adaptive regulation of bile salt transporters in kidney and liver in obstructive cholestasis in the rat. Gastroenterology, 2001. **121**(6): p. 1473-84.
190. Masumoto, T. and S. Masuoka, Kidney function in the severely jaundiced dog. Am J Surg, 1980. **140**(3): p. 426-30.
191. Schlattjan, J.H., C. Winter, and J. Greven, Regulation of renal tubular bile acid transport in the early phase of an obstructive cholestasis in the rat. Nephron Physiol, 2003. **95**(3): p. p49-56.
192. Gregus, Z. and C.D. Klaassen, Comparison of Biliary excretion of organic anions in mice and rats. Toxicol Appl Pharmacol, 1982. **63**(1): p. 13-20.
193. Altamirano, J., et al., Acute kidney injury is an early predictor of mortality for patients with alcoholic hepatitis. Clin Gastroenterol Hepatol, 2012. **10**(1): p. 65-71 e3.
194. Elias, M.M., et al., Possible mechanism of unconjugated bilirubin toxicity on renal tissue. Comp Biochem Physiol A Comp Physiol, 1987. **87**(4): p. 1003-7.
195. Vasavan, T., et al., Heart and bile acids - Clinical consequences of altered bile acid metabolism. Biochim Biophys Acta Mol Basis Dis, 2018. **1864**(4 Pt B): p. 1345-1355.
196. Pak, J.M. and S.S. Lee, Vasoactive effects of bile salts in cirrhotic rats: in vivo and in vitro studies. Hepatology, 1993. **18**(5): p. 1175-81.
197. Elias, M.M., et al., Evidence for a secretory component in the handling of unconjugated bilirubin by the isolated perfused rat kidney. Can J Physiol Pharmacol, 1985. **63**(12): p. 1581-5.
198. Ozawa, K., et al., The mechanism of suppression of renal function in patients and rabbits with jaundice. Surg Gynecol Obstet, 1979. **149**(1): p. 54-60.
199. Leung, N., et al., Acute cholestatic liver disease protects against glycerol-induced acute renal failure in the rat. Kidney Int, 2001. **60**(3): p. 1047-57.
200. Bolisetty, S., A. Zarjou, and A. Agarwal, Heme Oxygenase 1 as a Therapeutic Target in Acute Kidney Injury. Am J Kidney Dis, 2017. **69**(4): p. 531-545.
201. Adin, C.A., B.P. Croker, and A. Agarwal, Protective effects of exogenous bilirubin on ischemia-reperfusion injury in the isolated, perfused rat kidney. Am J Physiol Renal Physiol, 2005. **288**(4): p. F778-84.
202. Lanone, S., et al., Bilirubin decreases nos2 expression via inhibition of NAD(P)H oxidase: implications for protection against endotoxic shock in rats. FASEB J, 2005. **19**(13): p. 1890-2.
203. Oh, S.W., et al., Bilirubin attenuates the renal tubular injury by inhibition of oxidative stress and apoptosis. BMC Nephrol, 2013. **14**: p. 105.
204. Deetman, P.E., et al., Plasma bilirubin and late graft failure in renal transplant recipients. Transpl Int, 2012. **25**(8): p. 876-81.
205. Biggins, S.W., et al., Diagnosis, Evaluation, and Management of Ascites, Spontaneous Bacterial Peritonitis and Hepatorenal Syndrome: 2021 Practice

Guidance by the American Association for the Study of Liver Diseases. Hepatology, 2021. **74**(2): p. 1014-1048.
206. Diamond, J.R. and D.C. Yoburn, Nonoliguric acute renal failure associated with a low fractional excretion of sodium. Ann Intern Med, 1982. **96**(5): p. 597-600.
207. Nazar, A., et al., Predictors of response to therapy with terlipressin and albumin in patients with cirrhosis and type 1 hepatorenal syndrome. Hepatology, 2010. **51**(1): p. 219-26.
208. Lopez-Ruiz, A. and L.A. Juncos, Bile Acids are Important Contributors of AKI Associated with Liver Disease: COMMENTARY. Kidney360, 2022. **3**(1): p. 25-27.
209. Allegretti, A.S. and J.M. Belcher, Bile Acids Are Important Contributors to AKI Associated with Liver Disease: CON. Kidney360, 2022. **3**(1): p. 21-24.